Femtosecond Vibrational Spectroscopy – Influence of Base Stacking and Base Pairing on the Excited-State Deactivation of DNA

Dissertation

an der Fakultät für Physik

der Ludwig-Maximilians-Universität München

vorgelegt von

Dominik Benjamin Bucher

aus Dachau

München, den 31. Oktober 2014

Erstgutachter: Prof. Dr. W. Zinth
Zweitgutachter: Prof. Dr. T. Carell
Tag der Prüfung: 19. Januar 2015

Zusammenfassung:

Die Photostabilität der DNA ist von grundliegender Bedeutung für den Schutz des genetischen Codes. DNA-Monomere wandeln die absorbierte UV-Energie ultraschnell in Wärme um und vermeiden somit schädliche photochemische Reaktionen. Dieser effiziente Deaktivierungskanal wird durch die Basenstapelung in DNA-Strängen beeinflusst. Die dabei ablaufenden Prozesse werden aber in der Literatur kontrovers diskutiert. Die Auswirkung der Basenpaarung, der zweiten wichtigen Wechselwirkung in der normalerweise vorliegenden DNA-Doppelhelix, auf die photophysikalischen Deaktivierungskanäle ist weitgehend unbekannt. Aus diesem Grund wurde in dieser Arbeit der Einfluss dieser zwei wichtigsten Wechselwirkungen in der DNA – Basenstapelung und Basenpaarung – auf den Zerfall des angeregten Zustands mit Femtosekunden UV-Anregungs IR-Abfrage Spektroskopie untersucht. Aufgrund der charakteristischen Absorption der DNA-Basen ermöglich IR-Spektroskopie die Dynamik des angeregten Zustrands jeder einzelnen Base in der natürlichen Umgebung – Einzelstrang und Doppelstrang – zu untersuchen.

Der Einfluss der Basenstapelung auf die DNA-Photophysik wurde in dem ersten Teil der Arbeit anhand von einzelsträngigen Oligonukleotiden untersucht. Speziell ausgewählte Sequenzen ermöglichten dabei die Anregung einer einzelnen definierten Base in diesen Strängen. IR-Spektroskopie erlaubte hierbei nicht nur die angeregte Base zu untersuchen, sondern auch die Beiträge benachbarter, ursprünglich nicht angeregter Basen zu beobachten. Mit diesem experimentellen Ansatz konnte gezeigt werden, dass die Basenstapelung langlebige angeregte Zustände auf einer Zeitskala von 100 ps verursacht, wobei neben der angeregten Base auch benachbarte Basen beteiligt sind. Das dazugehörige charakteristische IR-Spektrum konnte einem ladungsgetrennten Zustand zwischen Basen zugeordnet werden. Für diese Zuordnung wurde in unabhängigen Experimenten ein IR-Spektrum des 5-Methyl-2′-desoxycytidin Radikalkations aufgenommen, welches durch einen Zwei-Photonen-Ionisationsprozess erzeugt wurde. Die Richtung der Ladungstrennung wird durch das Redoxpotential der beteiligten Basen bestimmt. Zusätzliche Experimente konnten zeigen, dass die Ladungen in basengestapelten Domänen über 3-4 Basen delokalisiert sind. Das Auftreten von geladenen, reaktiven Radikalen nach der Absorption von UV-Licht in der DNA könnte oxidative wie auch reduktive chemische Reaktionen verursachen, welche bisher nicht in Zusammenhang mit der DNA-Photochemie gebracht worden sind.

Der Einfluss der Basenpaarung auf die DNA-Photophysik wurde in natürlicher Kalbsthymus-DNA im zweiten Teil der Arbeit untersucht. Ultraschnelle IR-Spektroskopie wurde verwendet, um den Zerfall des angeregten Zustands aller vier Basen in der natürlichen DNA zu beobachten. Dabei wurde ein unerwartetes einfaches Zerfallsmuster für diese komplexe Probe entdeckt: Guanin und Cytosin relaxieren gemeinsam in 40 ps, Adenine und Thymine gemeinsam in 210 ps zurück in den Grundzustand. Dieses Ergebnis zeigt, dass der angeregte Zustand über die Watson-Crick-Basen Paarung zerfällt, welches der gängigen Lehrmeinung widerspricht. Bisher wurde angenommen, dass die Basenstapelung den Zerfall des angeregten Zustands bestimmt. In diesem Zusammenhang zeigten weitere Experimente an einzel- und doppelsträngigen Oligonukleotide, dass die Basenpaarung die reaktiven, ladungsgetrennten Zustände der Einzelsträngen löscht. Die Watson-Crick-Wasserstoffbrücken eröffnen somit einen neuen Zerfallskanal, möglicherweise über einen Protonentransfer, welcher die DNA vor der Bildung von reaktiven Zuständen schützt.

Abstract:

Photostability of DNA is essential to ensure the integrity of the genetic code against UV-induced damage. DNA monomers dissipate the absorbed UV energy ultrafast to heat, thereby reducing the probability of UV-induced lesion formation. It is known that this efficient deactivation channel is strongly modulated by base stacking in DNA strands, but a general scientific consensus about the underlying processes has not been reached. In addition, the photophysical deactivation processes occurring in DNA double strands are further complicated by a second interaction – the base pairing – and are largely unknown. For that reason the influence of the two major interactions in DNA – base pairing and base stacking – on the excited state decay has been investigated in this thesis. Femtosecond UV-pump IR-probe spectroscopy has been used to monitor the excited state dynamics of nucleobases. Each nucleobase exhibits characteristic absorbance bands in the mid-IR, which enables to probe the excited-state dynamics of all four nucleobases individually in their naturally stranded and double-stranded environment for the first time.

The influence of base stacking on the excited-state dynamics has been investigated in single stranded oligonucleotides in the first part of the thesis. Specially designed sequences allowed selective excitation of one defined base in the DNA strands. Probing in the mid-IR enabled not only to probe the excited state decay of the excited bases, but also of all other bases in the strand, which were not involved in the initial excitation process. With this approach it could be shown that base stacking causes a long-living excited state on the 100 ps time scale which is not only localized on the excited base, but also involves adjacent bases. The characteristic fingerprint spectrum in the mid-IR allowed to assign this state to a charge separated state between neighboring bases. For the identification of this state, the mid-IR spectrum of the radical cation of 5-methyl-2′-deoxycytidine was recorded upon a two-photon ionization process in independent experiments. The direction of charge transfer is governed by the redox potential of the involved nucleobases. Additional experiments have shown that these charges are delocalized in stacked domains of about three to four bases. The presence of reactive charged radicals in base stacked single-stranded DNA after UV-light excitation may result in oxidative or reductive chemical reactions which have not been considered in DNA photochemistry so far.

The influence of base pairing on the excited-state dynamics has been investigated in natural calf thymus DNA in the second part of the thesis. Ultrafast IR-spectroscopy has been used to monitor the excited-state decay of the four nucleobases individually in natural calf thymus DNA. An unexpectedly simple decay scheme has been discovered for this complex system where guanine and cytosine jointly decay within 40 ps and adenine and thymine within 210 ps to the ground state. This result implies that the excited-states decay concerted via the Watson-Crick base pairs by a joint mechanism. This is in strong contrast to the scientific consensus stating that base stacking controls the excited-state. Further investigation of single- and double-stranded oligonucleotides showed directly that the base pairing quenches the reactive charge transfer states in single-stranded DNA. Thus, the Watson-Crick hydrogen bonds open up a new deactivation channel, possibly by the involvement of a proton transfer, which protects DNA from the formation of reactive states.

Contents

1 Introduction and Aim of the Thesis

Life on earth is based on the interplay of diverse biomolecules. The information flow in these complex molecular systems follows a relatively simple rule. It states – strongly simplified – that deoxyribonucleic acid (DNA) acts as an information storage molecule and encodes the blueprint for proteins – the molecular machines – in genes [1]. Proteins are the workhorses of the cell and are involved in all vital molecular biological processes like metabolism, catalysis, transport, signaling, immune response and many more [2]. All of these processes are only possible, if the genetic information encoded in DNA has not been damaged and the proteins have been assembled correctly. Changes in the molecular composition of DNA – also called mutations – can have severe consequences for the organism, since they alter the genetic code. These changes in the blueprint can lead to the synthesis of nonfunctional or even toxic proteins which may lead to cell cycle arrest, cell death or cell senescence. Mutations in genes associated with cell growth control may cause cancer [3]. The alterations in the genetic code may be caused by DNA lesions induced by chemicals, cell metabolism or radiation [4]. In particular, the energetic UV radiation emitted by the sun is omnipresent on the Earth's surface. Absorption of a UV-photon excites an electron into a high-energetic reactive state. It might induce photochemical reactions, resulting in bond breakage or bond formation, modifying the molecular structure of DNA. Fortunately, most of these lesions are repaired by a sophisticated maintenance machinery in cells [5, 6, 7]. However, if these lesions are not repaired fast enough or are not recognized by the repair system, mutations may result in skin cancer in the worst case [8, 9, 10, 11, 12, 13]. In the U.S., 3.5 million new cases of skin cancer are reported every year which are mainly caused by exposure of skin to the UV-radiation of the sun [14, 15]. Thus, the number of new skin cancer cases each year exceeds by far the number of all other new cancer incidences combined (Fig. 1.1). Recent investigations directly link UV-light-driven mutations to melanoma pathogenesis [16, 17, 18, 19], the type of skin cancer with the highest mortality rate. Although melanoma accounts for less than 2% of all skin cancer cases, it will cause estimated 9,710 deaths in 2014 in the U.S. [20]. These horrifying numbers are the reason for an issue published in September 2014 by the U.S. Department of Health and Human Service to prevent skin cancer. In this report, the authors call skin cancer "a major public health problem" which points out the importance and currentness of UV-induced DNA damage [21].

Although these numbers are enormous, the yield of photolesions (there are 10^5 photoproducts per day and per cell in bright light [22]) and hence the number of cancer cases could be far higher, if its repair and protection mechanisms [23] were less efficient. The DNA molecule itself possesses extraordinary photophysical and photochemical properties in comparison to other organic molecules, which makes it extremely photostable and strongly reduces the probability to undergo UV-induced lesion formation [24]. Generally,

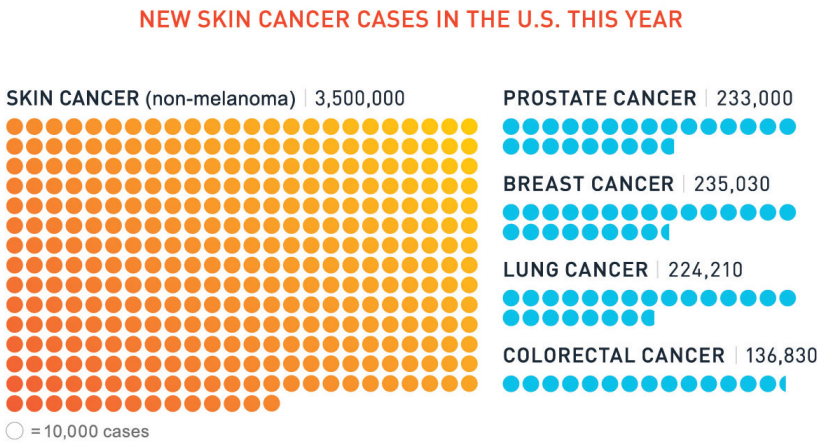

Figure 1.1 – New skin cancer cases in the U.S. (Reprinted from [15])

the photoreactivity of an excited molecule correlates with the excited state lifetime. That simple rule is based on the assumption, that a long-living excited state has a higher probability to undergo a photochemical reaction than an excited state with a short lifetime. The excited state lifetime of aromatic hydrocarbons is in the nanosecond time regime [25]. In contrast, the lifetime of the excited state of all monomeric units of DNA – the nucleobases – is over three to four orders of magnitudes shorter. Experiments and simulations have shown that the energy of the absorbed light is dissipated ultrafast into heat, thereby reducing the rate of lesion formation [26]. This extraordinary photostability is important to ensure the integrity of the genetic code and enables life under UV-light irradiance on earth. This protective deactivation channel is characteristic for the natural DNA bases. Small structural modifications lead to an increase in the excited state lifetime and to a reduction of the photostability. Therefore, it is assumed that the structure of DNA monomers is evolutionarily selected to reduce the rate of damage formation and to obtain maximal photostability [27, 28]. This molecular evolution might have taken place in the prebiotic world. At that time, the Earth's surface was exposed to an extremely high UV flux due to a missing ozone layer [29]. Only molecules with high photostability (the natural DNA bases) have survived those harsh conditions, whereas more photoreactive molecules have been decomposed.

In summary, the interest in investigating DNA photophysics and photochemistry comes from different directions. On the one hand, the motivation is to elucidate the mechanisms leading to the extraordinary photostability of DNA and to correlate this property to the fascinating DNA structure. On the other hand, the elucidation of damaging photochemical processes in excited DNA – despite its photostability – could lead to a molecular understanding of the formation of skin cancer. All of these photophysical and photochemical processes, the dissipation of light energy to heat or the formation of DNA photolesions occur predominantly on the femtosecond to nanosecond timescale. These ultrafast processes in the excited state can be directly monitored by pump-probe spectroscopy. In this method, a short femtosecond light pulse is used to excite DNA. A second delayed light

pulse probes the excited state dynamics. This enables the observation of the ultrafast photophysical processes in excited DNA. For the thesis, UV-pump IR-probe spectroscopy is used to investigate the DNA photophysics. IR-spectroscopy has the advantage that the observed molecular vibrations contain structural information and also report about changes in the electronic states. Thus, it is the ideal method to investigate the excited state dynamics and structural changes leading to damage.

Aim of the Thesis The processes responsible for the photostability of single nucleobases are well understood. However, the genetic information is not encoded in single nucleobases but in their sequence in DNA strands. The photophysical processes and decay channels occurring in these biologically important DNA single and double strands are barely understood. Especially the influence of the two major interactions which stabilize the famous double helical DNA structure – base stacking and base pairing – on the DNA photophysics and photostability is largely unknown until today. Therefore the influence of base stacking and base pairing on the excited state dynamics of the nucleobases shall be investigated with time-resolved IR-spectroscopy in this thesis. The photophysical processes taking place in these strands shall be correlated to photostability. In addition, possible reaction channels leading to DNA damage shall be identified.

DNA single strand: Time-resolved spectroscopic experiments have shown that base stacking in single strands strongly modifies the photophysical processes occurring in single nucleobases. However, the characterization of the modifications remained insufficient. The underlying molecular mechanisms are not answered yet and are highly debated in literature. For that reason, the photophysical processes induced by base stacking shall be characterized in single-stranded oligonucleotides in the first part of this thesis (chapter 4.2).

DNA double strand: An understanding of the photophysical deactivation processes occurring in nucleobases in their natural environment – the DNA double helix – is lacking completely. In the second part of this thesis (chapter 4.3), the excited state deactivation mechanisms in a natural model system – the calf thymus DNA – shall be investigated. The focus of this study lies on the interplay of base stacking and base pairing regarding the DNA photophysics and photochemistry.

2 Theoretical Background

In this chapter a theoretical background for this thesis will be presented. It will start with a brief description of the DNA structure, which is essential to understand the photophysical and photochemical processes occurring after photoexcitation. In the second part DNA photophysics and photochemistry will be reviewed. The major focus of that section is on the excited state decay of single bases, single strands and double strands. Different mechanisms and conflicting models are discussed. In the last part, the basics of photoinduced charge transfer and transport in DNA will be treated.

2.1 DNA Structure

The polymer DNA is made up of four different organic, aromatic bases, connected via a sugar and a phosphate group. The four different nucleobases in DNA are grouped according to their basic ring structure: the pyrimidines thymine (T) and cytosine (C) and the purines adenine (A) and guanine (G) (Fig. 2.1). The monomeric unit of the DNA assembly is called nucleotide, consisting of one of the four nucleobases, the sugar 2′-deoxyribose and a phosphate group. A nucleoside consists only of the nucleobase and the 2′-deoxyribose, lacking the phosphate group. The nucleobase is linked via a N-glycosidic bond to the 2′-deoxyribose. The phosphate group is attached to the 5′-OH group of the 2′-deoxyribose. In the related ribonucleic acid (RNA), 2′-deoxyribose is replaced by ribose, which has

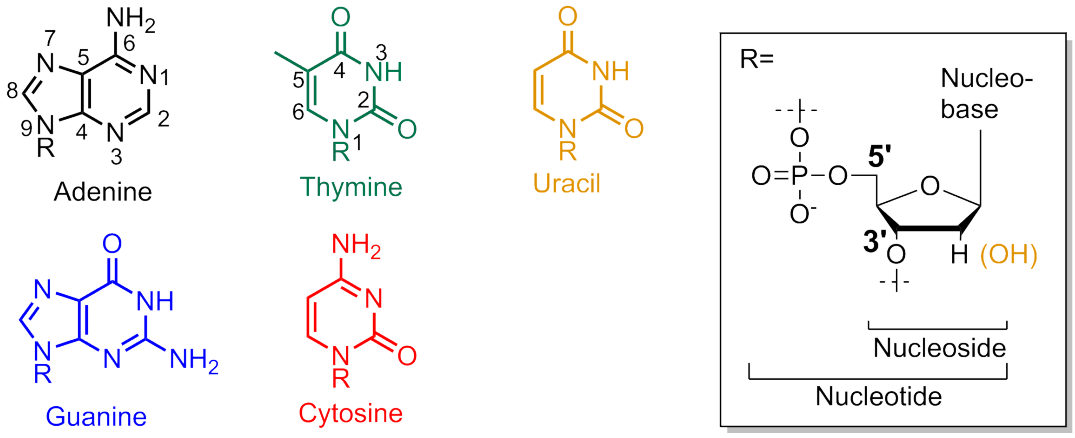

Figure 2.1 – In DNA the four nucleobases thymine (T), adenine (A), cytosine (C) and guanine (G) act as information bits. The monomeric units of the DNA polymer are the nucleotides which are composed of a nucleobase, 2′-deoxyribose and a phosphate group. The nucleoside lacks the phosphate group. In RNA the thymine is replaced by uracil (U) and the 2′-deoxyribose by ribose.

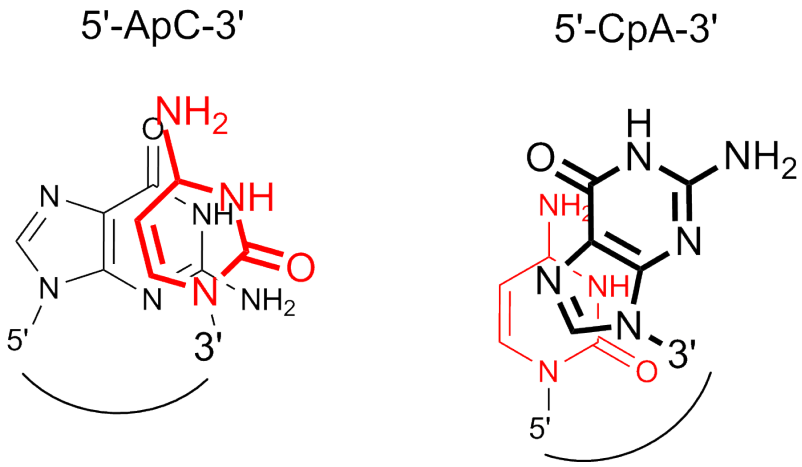

Figure 2.2 – Base stacking in dinucleotides: Schematic picture of the base stacking conformation in AC and CA. The structure shows directly that the interaction is strongly sequence dependent. Drawn according to [34].

an additional hydroxy group at its 3′-position. In addition, thymine is substituted by uracil (U) (Fig. 2.1), where the methyl group is removed [3]. In the following, only the DNA structure will be discussed.

The monomeric residues form the DNA upon polymerization. The 3′-OH group of a sugar is linked via a phosphodiester group to the 5′-OH group of an adjacent one. By definition the sequence is always written beginning with the 5′-end. In solution DNA single strands are not random coils but have a significant structure [30]. This structural stabilization is caused by interacting π-systems of adjacent (planar) aromatic nucleobases. The energetically favorable interaction is called base stacking and is based on several noncovalent forces [31, 32, 33]. Solvation effects, like the hydrophobic interaction, certainly play a role. However, the importance of these entropy driven interactions in base stacking is not clear. Electrostatic forces between the static dipole moments of the bases also contribute to the stacking interaction. The polarizability of the flat π-systems of the nucleobases causes a third interaction – the van der Waals forces. The arrangement for two stacked nucleobases in a dinucleotide is shown in Figure 2.2 [34]. The two dinucleotides AC and CA with an identical base composition stack differently and result in different structures. This shows directly that the sequence has structural implications, resulting in different interactions between adjacent nucleobases.

DNA single strands play only a minor role in biology, but they play an important role as model systems for understanding base stacking between adjacent bases. In nature DNA nearly exclusively occurs in combination with a second complementary strand, forming the famous double helical structure, which was discovered over 50 years ago by Watson and Crick [35] (Fig. 2.3). The second strand is always aligned in an antiparallel fashion and is bound by electrostatic hydrogen bonds between one purine and one pyrimidine base on opposing strands. Each base possesses polar N-H bonds acting as hydrogen bond donors and nonbonding electron pairs acting as hydrogen bond acceptors, the prerequisite for

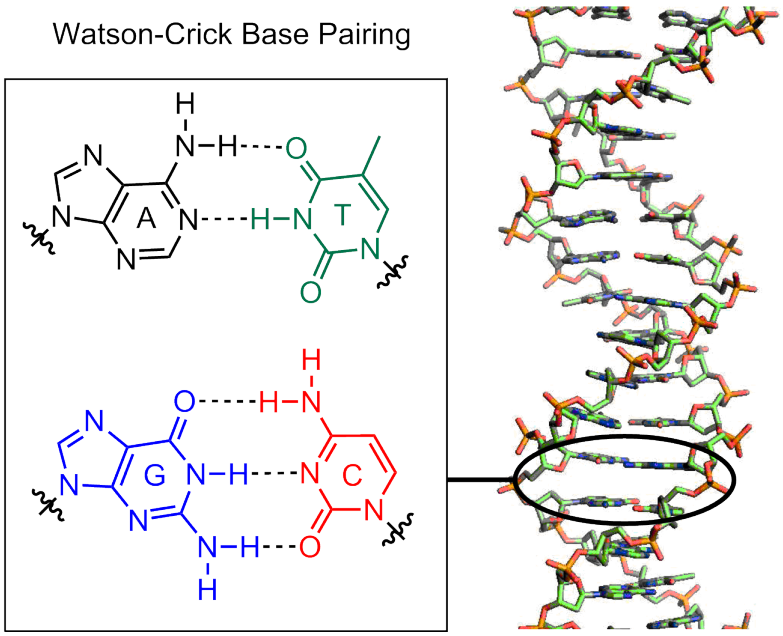

Figure 2.3 – Watson-Crick base pairing between A (black) and T (green) as well as G (blue) and C (red) and the crystal structure of B-DNA (prepared from Protein Data Bank entry 3BSE [38] using Pymol [39]).

hydrogen bonds. Guanine pairs cytosine with three hydrogen bonds, whereas two hydrogen bonds are involved in the adenine-thymine base pair – also called the Watson-Crick base pairs (Fig. 2.3). This base pairing scheme is of fundamental importance for the three basic processes in molecular biology – replication, transcription and translation [36]. It further causes the formation of a double helical structure by two complementary strands. Although base pairing is often in the center of attention due to its importance in molecular recognition, it is not the main stabilization force of the double helix. New investigations suggest that base stacking is mainly responsible for the thermal stability of the DNA double helical structure [37].

Thus, the structure of DNA can be divided into three layers of complexity: (1) the isolated monomers, (2) the single strands stabilized by base stacking and (3) the double helix, where two strands interact by base pairing. It can also be assumed that these different complexity layers have an impact on the DNA photophysics. Therefore the distinction between monomers, single strands and double strands will frame the layout of this thesis to understand the photophysics of DNA, which is described in the following chapter.

2.2 DNA Photophysics and Photochemistry

2.2.1 DNA Excited State Dynamics

The excited state dynamics of DNA are of fundamental interest to understand its inherent photostability and the photochemical processes which lead to UV induced lesion formation. DNA photophysics and photochemistry have been investigated with diverse time-resolved spectroscopic methods. This overview will mainly focus on time-resolved fluorescence, UV/Vis and mid-IR absorption experiments in solution, whereas gas phase experiments will not be discussed in detail. Interested readers should refer to the reviews of de Vries [40] and Saigusa [41]. Due to the complex structure of DNA, the chapter is subdivided: At first, the relatively well understood photophysics of single nucleobases will be treated. Subsequently, the influence of base stacking and base pairing on the excited state decay will be discussed in detail, addressing single- and double-stranded DNA.

2.2.1.1 Single Nucleobase Excited State Dynamics

In order to understand the photophysics of the complex biomolecule DNA, it is essential to understand the excited state dynamics of the single nucleobases adenine, guanine, thymine and cytosine (Fig. 2.1). Linkage of these bases to a deoxyribose and a phosphate group leads to the biologically important nucleosides or nucleotides (see section 2.1). These substitutions modify the photophysics [42, 43, 44, 45], but the fundamental processes are similar for all of these derivatives since the excitation is located on the nucleobase itself. For that reason, nucleobases, nucleosides and nucleotides will be regarded in common in the following and the term "base monomer" will be used for all three species. Each base monomer has distinct properties which cannot be discussed here in detail [26, 46]. However, all bases exhibit a common main decay channel, which will be explained in the subsequent part [47].

In Figure 2.4 the UV/Vis absorbance spectra of the four base monomers are shown. They exhibit strong absorbance bands in the UV-C (200-280 nm) which extend to the UV-B (280-315 nm) regime [48], with only a minor overlap with the solar spectrum on the Earth's surface. The bands are caused by several allowed $\pi\pi^*$ transitions. Additional $n\pi^*$ transitions caused by the lone pairs of the heteroatoms, are hardly observable due to their forbidden character [49]. Thus the photophysics starts from the bright $\pi\pi^*$ state:

ππ* state The extraordinary photophysical properties of the base monomers become evident by the investigation of the fluorescence properties. Excitation of the strong $\pi\pi^*$ transitions results in a very low fluorescence emission, which is in strong contrast to other aromatic hydrocarbons [25]. In 1971 the first fluorescence quantum yield ϕ_f has been published and is found to be of the order of 10^{-4} [51]. The radiative lifetime τ_0 of molecules can be assessed from its oscillator strength according to the Strickler-Berg equation [52]. For the strong oscillator strength of the nucleobases the estimation yields typically a radiative lifetime τ_0 in the nanoseconds time regime [53]. The fluorescence lifetime τ_f can

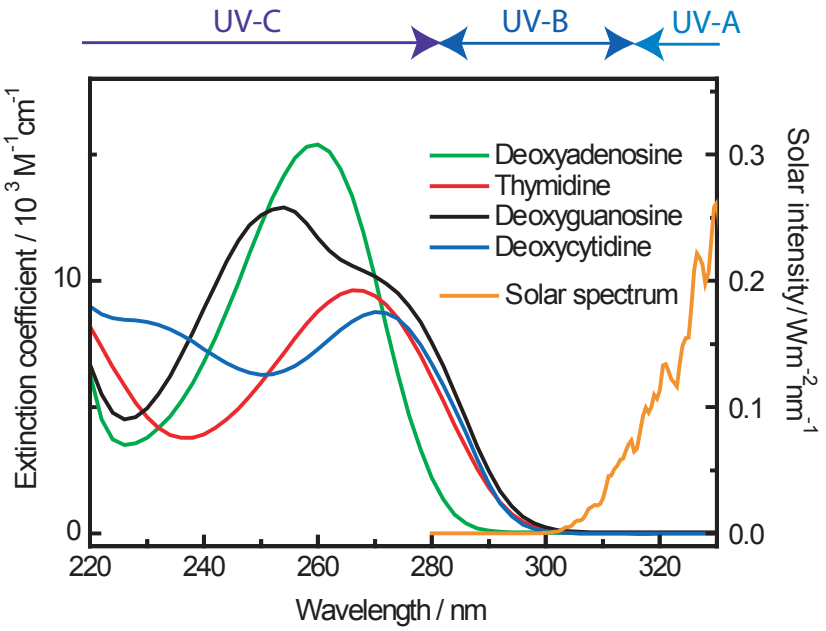

Figure 2.4 – UV absorbance spectra for all four nucleosides. Characteristic is the strong absorbance band with a maximum around 260 nm. The solar spectrum on the Earth's surface [50] has hardly spectral overlap with the nucleobases' absorption bands.

be calculated from the fluorescence quantum yield ϕ_f and the radiative lifetime τ_0 by means of [54]:

$$\tau_f = \phi_f \tau_0 \tag{2.1}$$

This simple estimation gives an ultrashort excited state lifetime below 1 ps, indicating the presence of ultrafast nonradiative deactivation channels. Further evidence for the ultrafast excited state decay of single bases was deduced from polarized emission experiments [55]. At room temperature the fluorescence of nucleobases is polarized, which shows that the emission is faster than the rotational dynamics of the molecule in solution which gives an upper limit of the excited state lifetime in the lower ps time regime. The first time-resolved absorbance and emission measurements could not resolve the excited state lifetime, since the instrumental time resolution was similar to the excited state decay [56, 57]. Only in the year 2000 Pecourt et al. [58] were able to measure the lifetimes of the excited states for all four nucleosides with a femtosecond UV-pump UV/Vis-probe setup directly. They have determined excited state lifetimes on the subpicosecond timescale. Time-resolved emission experiments with an adequate time resolution followed soon after this publication and confirmed the ultrashort excited state lifetimes [59, 42]. The coincidence of the results of both experimental techniques shows that both monitor the decay of the fluorescent state.

In the following the results of a transient absorption experiment of 9-methyladenine will be discussed in more detail [47, 60] (Fig. 2.5). The nucleobase is excited at 267 nm and

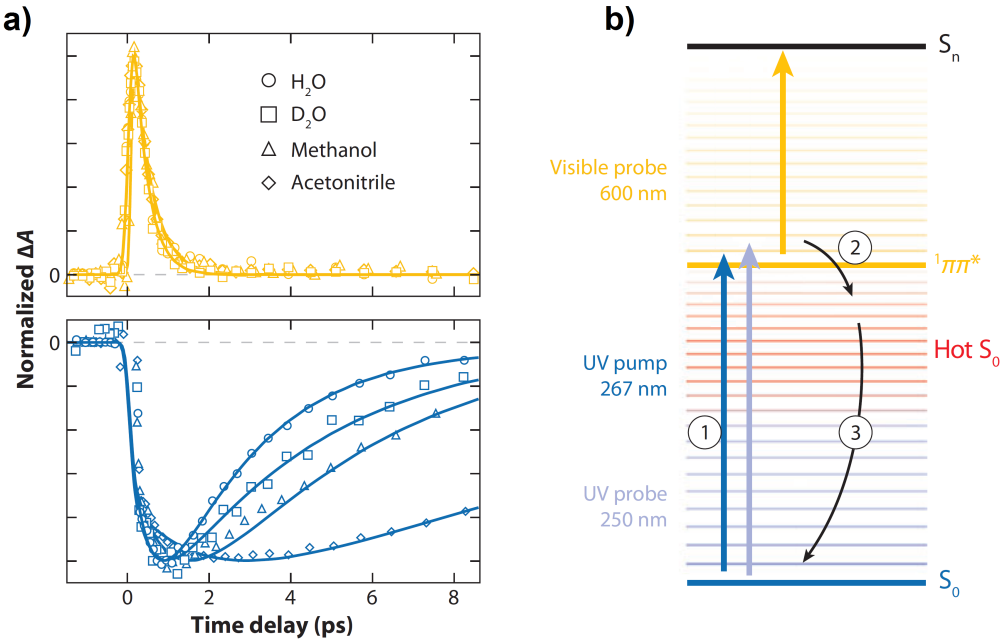

Figure 2.5 – a) Transient absorption at 600 nm (top) and 250 nm (bottom) after excitation of 9-methyladenine at 250 nm. b) Involved energy levels for the excitation of a nucleobase. The yellow and pale blue arrows indicate the transitions probed in Figure a). Step 1 corresponds to the excitation process, step 2 to the ultrafast internal conversion process and step 3 to the vibrational cooling process of the hot ground state. Figure adapted with permission from Middleton et al. [47].

the excited state dynamics are observed in the UV at 250 nm (blue) and in the visible at 600 nm (yellow). At 250 nm the repopulation of the ground state is observed by the ground state bleach recovery since the absorbance bands of the nucleobase are located at this position. At 600 nm a transient signal is detected which can be assigned to the absorbance of the excited state. Thus, at this visible wavelength the excited state decay can be directly monitored and yields a time constant of 300 fs. In contrast, the ground state bleach recovers more slowly than the excited state decay and it is strongly dependent on the solvent. The recovery of the ground state bleach comprises all processes which are involved in the excited state relaxation to the ground state. The ground state bleach recovers completely, which shows that no long-living states are formed, for example photolesions or long-living triplet states. Therefore, ultrafast internal conversion is the major deactivation channel. Since this nonradiative decay is an isoenergetic process, more than 4 eV are deposited in a highly vibrationally excited ground state (Fig. 2.5b), with an initial temperature of around 1000 K [61]. This energy is readily exchanged with the surrounding solvent molecules on a time scale of several picoseconds [62]. This intermolecular vibrational energy transfer is the rate determining step. It controls the ground state bleach recovery which is consequently slower than the excited state decay. Fragmentation of vibrational hot molecules after UV excitation in the gas phase occurs on the μs timescale [63]. This shows that the ultrafast vibrational cooling in solution is fast enough to avoid

damaging reactions. Interestingly, the aqueous solution exhibits the fastest cooling rate [64]. Thus, water enables efficient intermolecular energy transfer, accentuating once more the importance of water in biological systems [65].

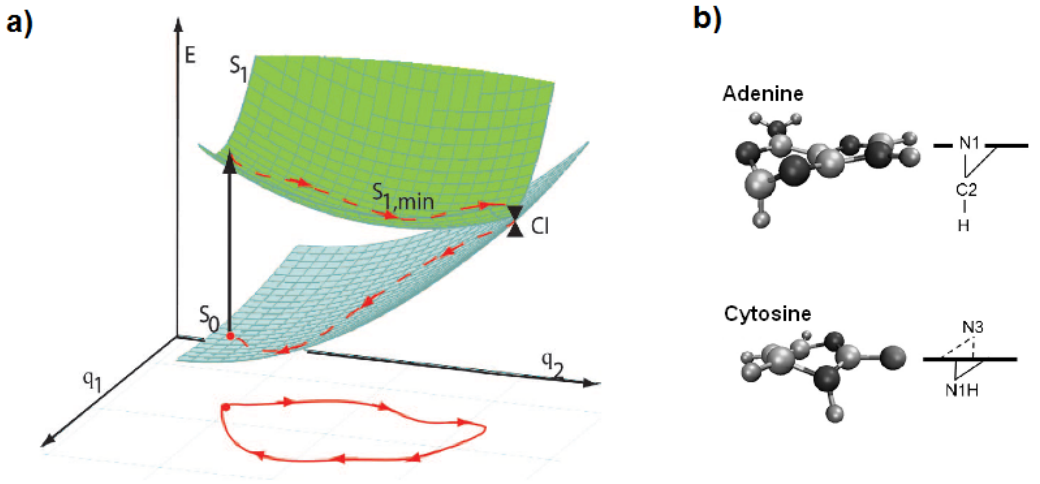

Figure 2.6 – a) Schematic energy landscape with a conical intersection: Due to the strong bending of the ground state energy surface along the coordinate q_2 an intersection with the excited state occurs. At this point – the conical intersection (CI) – an ultrafast transition from the excited to the ground state is possible (adapted with permission from Hare et al. [44] (Copyright (2007) National Academy of Sciences, U.S.A.). b) Excited state conformations at the conical intersection for adenine and cytosine. Figure reprinted with permission from Barbatti et al. [66].

The ultrafast nature of the internal conversion in nucleobases can be explained by the presence of a conical intersection. A conical intersection is a region on a multidimensional molecular nuclear coordinate space, where two potential surfaces intersect [67, 68]. This enables ultrafast transfer from one energy surface to another, in this case from the excited state to the ground state. This mechanism was proposed in 2000 for DNA monomers [58] and subsequently described by a computational study [69]. Conical intersections have now been found for all four nucleobases and are a fundamental part of DNA photophysics [70]. The principle is depicted in a simplified way in Figure 2.6a. Excitation of a nucleobase brings the molecule to the $\pi\pi^*$ state. The excited state energy is relatively insensitive to ring deformation (for example the reaction coordinate q_2), which results in a shallow excited state energy surface. In contrast, the ground state geometry is strongly destabilized by ring puckering, since the aromaticity of the nucleobase is disrupted. As a consequence, the ground state energy surface rises along the ring puckering coordinate and intersects the shallow excited state surface. At this point the Born-Oppenheimer approximation is violated by a strong coupling of nuclear and electron motion and an ultrafast internal conversion to the ground state is enabled. The region on the energy surface of the conical intersection can only be reached by molecular deformation. Calculations have shown that pyrimidines reach the conical intersection via a pyrimidalization of C(5) and C(6). The reaction path for the purines involves an out of plane bending of the C(2)H group [71, 66]

(Fig. 2.6b). Experimental evidence for a deformation has been obtained from ultrafast resonance Raman experiments [72, 73] and recently from ultrafast X-ray Auger probing [74]. Recent quantum chemical simulations for base monomers indicate additional conical intersections induced by the involvement of the surrounding. They are accessed via charge or proton transfer with the environment [75, 76].

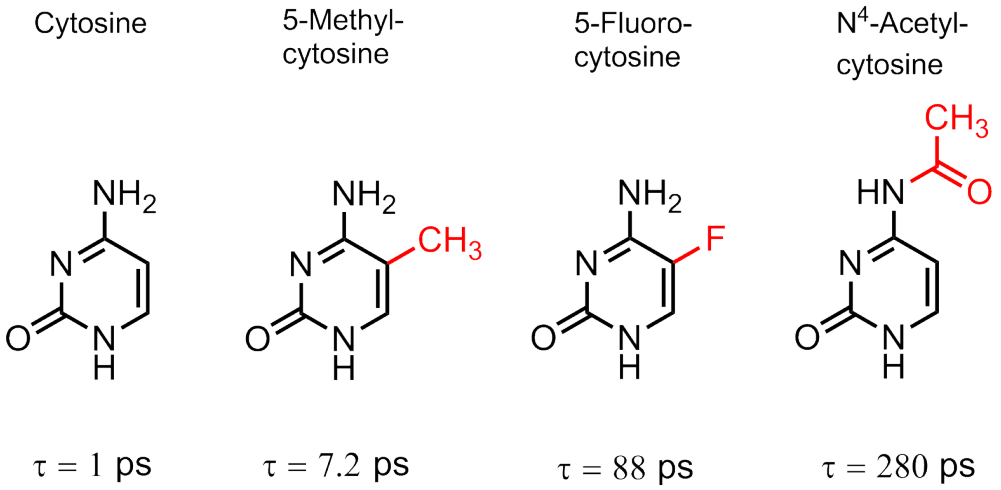

Figure 2.7 – Excited state lifetimes τ for several cytosine derivatives [77].

From the necessity of a structural deformation to reach the conical intersection, it is clear that structural modifications of nucleobases have a strong impact on the excited state lifetimes. In contrast to adenine with its sub-picosecond excited state lifetime, the isomer 2-aminopurine is strongly fluorescent and has an excited state lifetime of more than 1 ns [25]. One possible interpretation is that the 2-amino group restricts the bending of the C(2)H group which is necessary to reach the conical intersection. The effect of structural changes on the excited state lifetime has been investigated for cytosine in more detail by Malone et al. [77] (Fig. 2.7). This data shows unambiguously the sensitivity of the covalent modifications on the excited state dynamics. The natural DNA base cytosine has the shortest excited state lifetime in comparison to the corresponding derivatives. The minor natural nucleobase 5-methylcytosine (5mCyt) plays an important role in epigenetics and is responsible for gene silencing [78, 79]. Its excited state lifetime τ of about 7 ps is much longer in comparison to non-modified cytosine. The increased lifetime of the reactive excited state causes a higher probability to undergo photochemical reaction and damage formation. Indeed, photolesions are preferentially formed at 5mCyt in DNA causing UV-induced mutational hot spots at this position [80, 81]. The artificial bases 5-fluorocytosine and N^4-acetylcytosine exhibit one to two orders of magnitude longer lifetimes than the natural structure. Computations have shown that artificial bases possess energy barriers on the path towards the conical intersection which increase the excited state lifetime. In contrast, all natural bases have a barrierless path from the Franck-Condon region to the conical intersection, which enables ultrafast excited state deactivation which minimizes damaging photochemical reactions [28, 82]. This inherent photophysical property of DNA

bases suggests a possible natural selection of the nucleobase structure according to their photostability in the prebiotic world under harsh UV-conditions. Only adenine, guanine, cytosine and thymine bases have survived those conditions, whereas their derivatives have been decomposed by the UV-light.

The bright $\pi\pi^*$ state decays mainly via internal conversion to the ground state. However, further minor decay channels occur in base monomers. These states are difficult to investigate and their discovery and characterization has just started in recent years [43, 83, 84, 44]. Two further excited states – the $n\pi^*$ state and the triplet state – will be explained in the following:

nπ* state Direct excitation of the nonbonding orbitals of the nucleobase's nitrogen and oxygen atoms is extremely improbable since these transitions are symmetry-forbidden. However, the $n\pi^*$ state can in principle be populated by internal conversion from the energetically higher lying bright $\pi\pi^*$ state. Indeed, there is an ongoing discussion about the contribution of an intermediate $n\pi^*$ state to the deactivation mechanism of photoexcited nucleobases [85, 86, 87]. In addition to this debate based on theory, transient absorption spectroscopy experiments have detected additional longer living states in base monomers in solution, which have been assigned to dark $n\pi^*$ states [44, 88]. The lifetimes of these states are between 10 and 150 ps depending on the pyrimidine bases and are populated in up to 50% of the excited bases. These long-living states are only observed in pyrimidine bases and have not been detected in purine bases in considerable amounts. Whereas the properties of the $\pi\pi^*$ state depend only modestly on the solvent, the energetics and the lifetime of the $n\pi^*$ state are strongly solvent dependent [83]. This solvent dependence might cause difficulties when comparing experiments in water with gas phase calculations. The $n\pi^*$ state has been much less investigated in comparison to the $\pi\pi^*$ state due to its dark nature. However, its possible involvement in the ultrafast deactivation mechanism or in photolesion formation requires future investigations.

Triplet state The triplet state of nucleobases is a matter of special interest since triplet states are generally thought to be the main precursors in photochemical reactions due to their long lifetimes [89]. However, the investigation by transient spectroscopy has been hampered for a long time due to the low triplet quantum yield of only a few percent for the base monomers [24]. Kohler et al. suggest an ultrafast intersystem crossing which leads to a rapid formation of the $^3\pi\pi^*$ state in several picoseconds [84]. One possible precursor is the $^1n\pi^*$ which would lead to the $^3\pi\pi^*$ state according to El-Sayed's rule [90]. Beside this direct population mechanism, the triplet state can also be populated by an indirect bimolecular process. In this process the triplet energy is transferred from an excited molecule upon sensitizing to the base monomer (triplet-triplet energy transfer) [91]. In spite of its incomplete understanding, the triplet state is of fundamental interest, since its long-living nature probably enables DNA damage.

2.2.1.2 Influence of Base Stacking on the Excited State Dynamics

In the previous chapter, the strong influence of the molecular structure on the photophysics and photostability of the base monomers has been reviewed. However, the genetic information of the DNA is stored in the sequence of the nucleobases in DNA strands. In these strands, DNA bases are stacked and in spatial proximity which causes coupling between these aromatic molecules and complicates the photophysics. In this chapter, only single strands and thus the influence of base stacking on the DNA photophysics will be discussed. Single-stranded DNA has a relatively similar structure as in the corresponding double helix [92]. However, the lack of base pairing causes a higher structural heterogeneity in comparison to the well defined DNA double strands.

Only shortly after the determination of excited state lifetime of base monomers, single-stranded DNA has been investigated with transient absorption spectroscopy. In these experiments new, long-living states were detected [93]. These long-living states are a general feature observed in DNA single strands. Here, they will be discussed on the basis of one example. Figure 2.8 shows the recovery of the ground state of the adenosine monophosphate monomer (dAMP) in comparison to the corresponding polyadenosine $(dA)_{18}$ oligomer. Whereas dAMP decays ultrafast to the ground state, the oligomer $(dA)_{18}$ exhibits an additional long-living excited state on the 100 ps timescale.

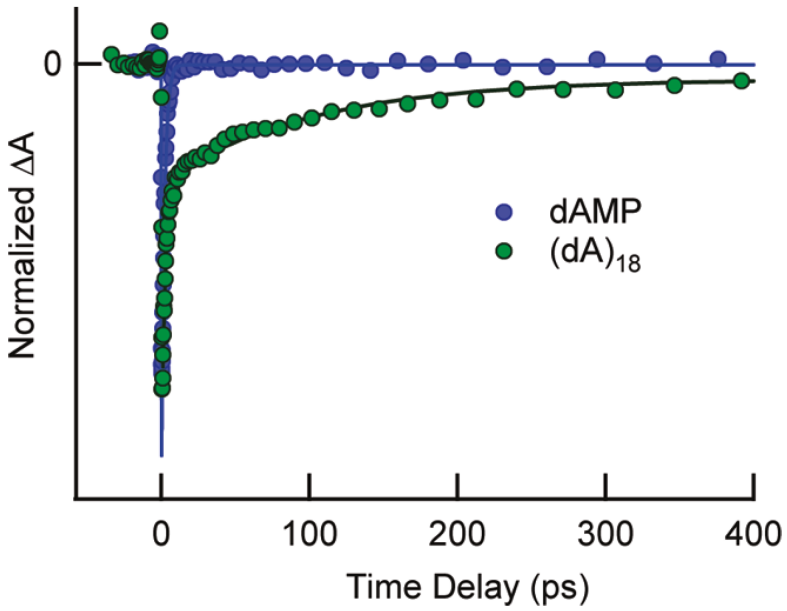

Figure 2.8 – Comparison of the ground state bleach recovery for the monomeric adenosine monophosphate (dAMP, blue dots) and for the corresponding polydeoxyadenosine ($(dA)_{18}$, green dots) monitored at 250 nm. Figure reprinted with permission from Kohler et al. [94]. Copyright (2010) American Chemical Society.

Emission experiments could also show that the organization of nucleobases in a strand slows down the fluorescence decay [95, 96]. Thus, it is evident that new photophysical pro-

cesses occur in single-stranded DNA due to the interaction of neighboring bases. However, the molecular nature of this state and possible delocalization processes have led to conflicting interpretations and are under current debate. Three different excited state decay mechanisms are discussed in the following and one possible, unifying model is presented in the end:

Single Base Decay As mentioned in section 2.2.1.1, the conical intersection causing the ultrafast internal conversion can only be reached by ring puckering. One conceivable idea is, that the DNA strand constrains the conformational space. Thus, the out-of-plane deformations are hampered and the conical intersection cannot be accessed. Indeed, calculations [97] have shown that steric and electrostatic interactions of neighboring bases inhibit the ring puckering which could be responsible for the long-living state. In contrast, other calculations indicate that base stacking is not restraining the out-of-plane deformation [98]. Furthermore, the strong sequence dependence observed in many time-resolved experiments excludes a pure monomer-like state as proposed in this model. Therefore, two other models, based on delocalized states – excitons and excimers – are discussed in the following. Since several definitions are published in literature, mainly caused by different scientific backgrounds from solid state physics to spectroscopy, the following discussion will be referred to the definitions by Kohler et al. [47].

Delocalized Excitons (Frenkel Exciton)

Definition Frenkel Exciton:

"an excited state of a multichromophoric system produced by dipolar coupling of the neutral excited states of individual molecules" [47]. The excited state of this system can be described by a linear combination of the excited states of the monomeric chromophores, which explains its delocalized nature. The dipolar interaction causes a splitting of the excited states, which can be observed with spectroscopic techniques [99].

Due to the similarity of the absorption spectra between single bases and DNA and the lack of any exciton splitting has led to the conclusion that light is absorbed by single bases [100]. However, the group of D. Markovitsi has published an exciton theory where the excited state is delocalized over a few bases without a strong shift of the absorbance bands [101, 102, 103, 104]. The same group has pioneered time-resolved fluorescence spectroscopy to investigate DNA photophysics. Although the group observed a slowdown of the emission upon base stacking with fluorescence upconversion techniques, the decay constants are no more than a few picoseconds [105, 95], in contrast to the transient absorption data mentioned before (Fig. 2.8). This fast (a few picoseconds) decay has been assigned to delocalized Frenkel excitons, formed by coupling of neighboring excited states. Different subensembles of coupling bases give rise to an excitonic band. Fluorescence anisotropy

measurements showed a strong change of the polarization properties during the first picoseconds, which was explained by an ultrafast energy transfer process occurring between these different excitonic states [105, 106]. This energy transfer has been described as an ultrafast internal conversion to the lower part of the excitonic band (also called intraband scattering) in the first 100 fs, which is combined with a shrinking of the exciton size. From this part of the band fluorescence occurs. Conformational fluctuations of the strands alter the electronic coupling between the bases giving rise to several fluorescent states, which explains the complex emission data [107, 108]. Interesting is the question of the spatial size of the excitons. Theory proposes a delocalization size over 3 bases [109]. Fiebig et al. proposed a delocalization size of 3-4 bases according to transient absorption experiments performed on polyadenine [110]. However, this result was recently challenged by the Kohler research group. They could show that the delocalization size is probably a misinterpretation due to the experimental approach [111].

In addition, Kohler et al. argued that the long-living state observed in their transient absorption spectroscopy experiments is not an exciton. In contrast, they proposed a model which is based on excimer/exciplex states, which is discussed in the following. These different models describing the results of transient fluorescence or transient absorption experiments have led to conflicting publications [112, 113, 104].

Excimer/Exciplex

Definition Excimer/Exciplex:

"an excited electronic state with substantial charge transfer character involving two identical (excimer) or different (exciplex) molecules" [47]. In the case of DNA photophysics, the exciplex state is synonymous with an interbase charge-transfer state. Both expressions will be used in the following. However, the exciplex definition does not define the degree of charge separation, which might lead from partial charge transfer states to radical ionic states. One important characteristic property of an exciplex state is the red-shifted emission [114].

Measurements in the 1960s observed a red shifted emission of polynucleotides in cryogenic glasses, which has been assigned to originate from excimers [115]. Recent systematic investigations of different dinucleotides with ultrafast transient spectroscopy have given additional evidence for an exciplex state in photoexcited DNA [116]. In these dinucleotides circa 30 % of the molecules decay via a long-living state, which shows, that this is a major decay channel. In [116], the amplitude of the long-living state could directly be related to the stacking probability between two bases in dinucleotides. Based on this fact the authors proposed, that unstacked bases decay like monomers via ultrafast deactivation through a conical intersection. In stacked bases, neighboring bases interact and lead to the long-living states. It could further be shown that the long-living state is located on two bases, since

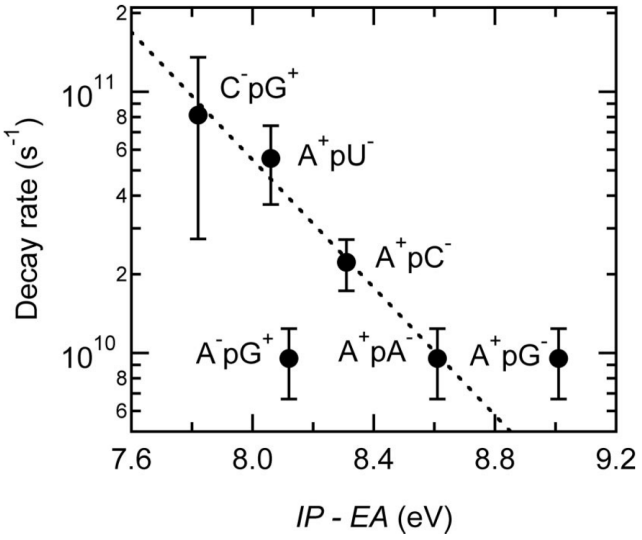

Figure 2.9 – Charge recombination decay rates for dinucleotides plotted against the driving force (ionization potential (IP) – electron affinity (EA)). Figure reprinted with permission from Takaya et al. [116] (Copyright (2008) National Academy of Sciences, U.S.A.).

it makes no difference, which base is excited in a dinucleotide. The involvement of two bases in the excited state indicates the occurrence of charge transfer states. For this reason the authors correlated the lifetime with the driving force of the charge separated state by subtracting the electron affinity of the electron acceptor from the ionization potential of the charge donor. Figure 2.9 shows the decay rate of the long-living component of different dinucleotides plotted against the difference between the ionization potential and the electron affinity. The decay rate of the long-living state decreases logarithmically with the increasing driving force of the charge separated states (except of ApG, where secondary effects might play a role). This behavior is typical for the recombination of diverse radical ion pairs [117]. The data can be interpreted according to the Marcus theory (see section 2.3 and equation 2.2). Highly exothermic electron transfer reactions fall in the inverted Marcus regime. In this regime the electron transfer rate is decreasing with increasing driving force, which is in accordance with the experimental data of the dinucleotides (Fig. 2.9). In addition, the authors showed identical lifetimes for the adenine dimer and longer adenine oligonucleotides. They concluded, that the excimer is located only on two adjacent bases. Other publications argue that the excimer state may be localized on more than two bases [118]. Beside the "charge-transfer" excimers, theoreticians have further proposed the occurrence of "neutral" excimers [119]. However, this relatively simple excimer/exciplex model could not explain the complex emission data, which has led to the conflicting publications mentioned before [112, 113, 104]. A combination of the exciton and exciplex theory provides a unifying picture of excited state decay in DNA single strands, discussed in the following.

A Unifying Model Proposed for the Excited State Decay of Stacked Bases As described above, fluorescence is only able to detect bright states, whereas transient absorption measures all states which are involved in the recovery of the ground state. Charge transfer states are assumed to have extremely low fluorescence quantum yields and cannot be detected by emission experiments. The model depicted in Figure 2.10 combines the observations of both techniques and their interpretations [47]. After the excitation the decay channel depends on the geometry of the stacking. In the case of unstacked bases, monomer-like decay is observed (section 2.2.1.1).

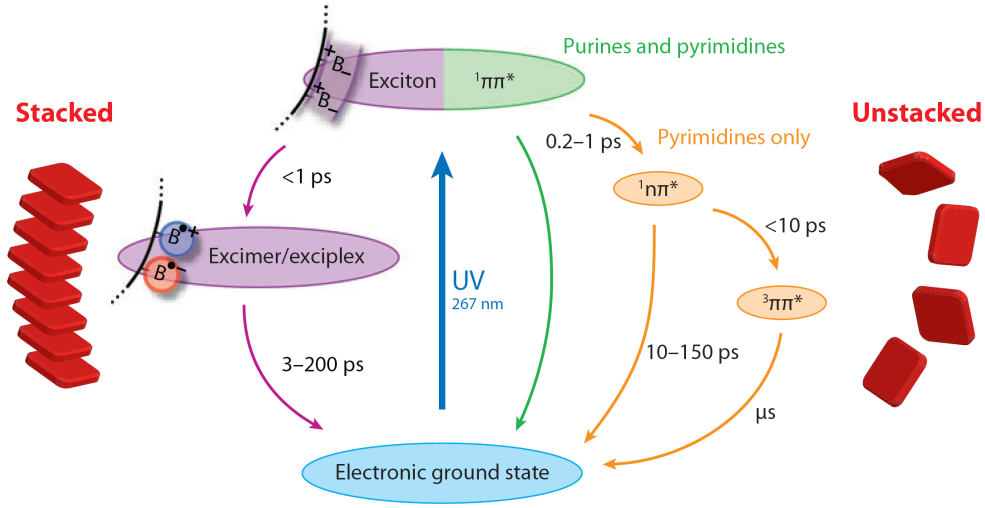

Figure 2.10 – The excited state decay is governed by the stacking interactions in single-stranded DNA. Excitation of stacked bases leads to an excitonic state which decays during 1 ps to an exciplex state. This charge transfer state recombines on the 100 ps time scale back to the ground state. Unstacked bases behave like monomeric bases and relax ultrafast via a conical intersection to the ground state. In pyrimidine bases, the $^1n\pi^*$state provides an additional decay channel. Figure reprinted with permission from Middleton et al. [47].

However, in stacked DNA strands delocalized Frenkel excitons are initially populated. The excitons can be localized by conformational fluctuations or relax by intraband scattering, which causes prompt fluorescence from the $\pi\pi^*$ state, observed by the emission experiments. This Frenkel exciton decays on the subpicosecond timescale to a dark excimer/exciplex state, which cannot be detected in fluorescence experiments. These charge separated states recombine to the ground state on the 100 ps time scale and are detected in the transient absorption experiments. Furthermore, a small part of charge recombination leads to delayed fluorescence, which explains the weak emission observed over several timescales [120, 121, 122]. Calculations have further supported the interplay of excitonic and charge transfer states [123, 124, 125, 126]. However, direct spectroscopic evidence is lacking for the excimer as well as for the exciton state and the model has not been proved experimentally yet. Thus, the mechanism is still under discussion and the timescale of the different processes lead to controversial interpretations in recent publications [127, 128, 129].

2.2.1.3 Influence of Base Pairing on the Excited State Dynamics

In nature DNA occurs predominantly double-stranded, where two single strands are linked via the hydrogen bonds of the Watson-Crick base pairing. Whereas a crude picture of the excited state decay mechanism of single strands exists, the influence of the Watson-Crick base pairing is controversially discussed and no final model can be presented here. The major problem is that both interactions – base stacking and base pairing – are present in DNA double helices and will interfere. Thus, the influence of base pairing without base stacking is difficult to analyze in the duplex. This complicates the data interpretation. For that reason, isolated base pairs in artificial environments and model systems, imitating isolated Watson-Crick base pairs, have been designed [130, 131]. In these systems the effect of base pairing can be investigated exclusively and their small size enables quantum chemical simulations. Two possible decay mechanisms have been postulated for these model systems: "The Excited State Tautomerization" and "The Interstrand Electron Driven Proton Transfer". Both have been concluded from spectroscopic and theoretical calculations.

However, these small artificial systems are not relevant to biology and the mechanisms might be different in duplex DNA. Transient absorption experiments on double-stranded DNA in solution did not show the ultrafast decay of the excited state as found for isolated base pairs. On the contrary, long-living states similar to those in single strands, have been detected [112]. The authors draw the conclusion that base stacking is thus the crucial interaction for the excited state decay and that exciplex states also occur in double-stranded DNA. In recent experiments they modified their model and proposed that the exciplex state causes a proton transfer in special sequences, which will be called "Intrastrand Electron Induced Proton Transfer". The different models will be discussed in the following, starting with mechanisms proposed for isolated base pairs:

Excited State Tautomerization in a Model Base Pair The hydrogen bonds in duplex DNA are in the keto-amino tautomeric form and define the Watson-Crick base pairing A-T and G-C. However, a second minor tautomeric form (enol, imino) is conceivable, which has different base pairing properties. Therefore, Watson, Crick [132] and Loewdin [133] pointed out that changes in the hydrogen bonding pattern might enable spontaneous mutations, which has recently gained some experimental evidence [134]. Calculations have shown, that the minor tautomers are strongly disfavored in the ground state [135, 136]. However, the energetics in the excited state are strongly changed and might enable proton transfer. To investigate such a photo-tautomerization reaction in the excited state, 7-azaindol has been used as one possible model system. This molecule forms hydrogen bonded dimers via two hydrogen bridges, which were used as model base pairs for the adenine-thymine pair [131]. Excitation of this dimer causes an exchange of two protons (Fig. 2.11). One 7-azaindol molecule donates its N–H proton and receives a proton at the pyridinic site from the counter molecule [137, 138]. The driving force for those reactions is the altered charge distribution in the excited state which causes a change in acidity and in basicity. A similar mechanism is conceivable in DNA and has been investigated theoretically for the A-T and G-C base pairs. It could be shown that the tautomerization in the excited state becomes more favorable than in the ground state, but it is still endothermic and has

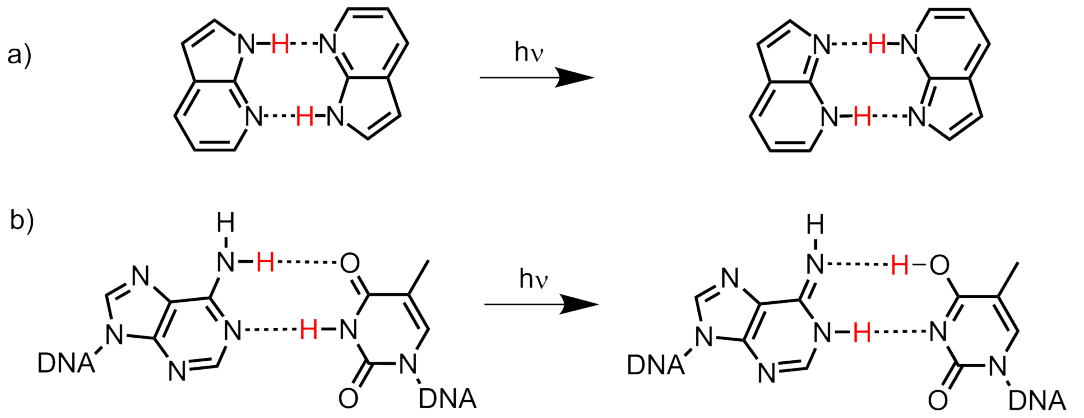

Figure 2.11 – a) The 7-azaindol dimer has been used as an A-T model base pair. Photon absorption causes an excited state tautomerization in this dimer. b) A similar excited state tautomerization can be proposed for the A-T base pair (and also for the G-C, not shown here).

to overcome significant barriers [139]. This and other studies showed further that beside the double proton transfer also a charge transfer state between the bases of the pair with lower energy can be populated, which is strongly stabilized by a single proton transfer [140, 141]. This leads to the next proposed mechanism, the "Interstrand Electron Driven Proton Transfer".

Interstrand Electron Driven Proton Transfer A similar charge transfer state has also been found in excited state calculations of the 2-aminopyridine dimer model base pair by Domcke et al. [142]. The authors proposed further, that this excited state crosses the ground state enabling fast internal conversion. Indeed, a combination of experiments and theory has shown that the excited state lifetime of the 2-aminopyridine dimer is significantly shorter than of the corresponding monomers [130, 143]. Domcke et al. have extended this decay mechanism to the natural G-C and A-T base pairs by quantum chemical calculations [144, 145]. The proposed mechanism is shown in Figure 2.12a for the A-T base pair. The mechanism proposed for the G-C base pair is analogous. The potential energy profiles for the ground state S_0, $\pi\pi^*$, $n\pi^*$ and the charge transfer state between A and T are plotted against the $N(6)-H$ distance in adenine. After excitation, a charge transfer state can be populated via nonadiabatic coupling with the initially excited bright $\pi\pi^*$ state, which gives rise to a positively charged adenine and a negatively charged thymine. This charge transfer state is strongly stabilized by elongation of the $N(6)-H$ bond, which corresponds to a charge neutralizing proton transfer from A to T. In contrast, the ground state is strongly destabilized along this proton transfer coordinate. This strongly curved energy function intersects with the excited state energy function at a $N(6)-H$ distance of 2.8 Å. This conical intersection was assumed to lead to an ultrafast deactivation of base pairs back to the ground state, even faster than in the corresponding monomers. The proton is transferred back in the ground state giving the original A-T base pair. This mechanism has been proposed to be important for the photostability of DNA. Figure 2.12b depicts

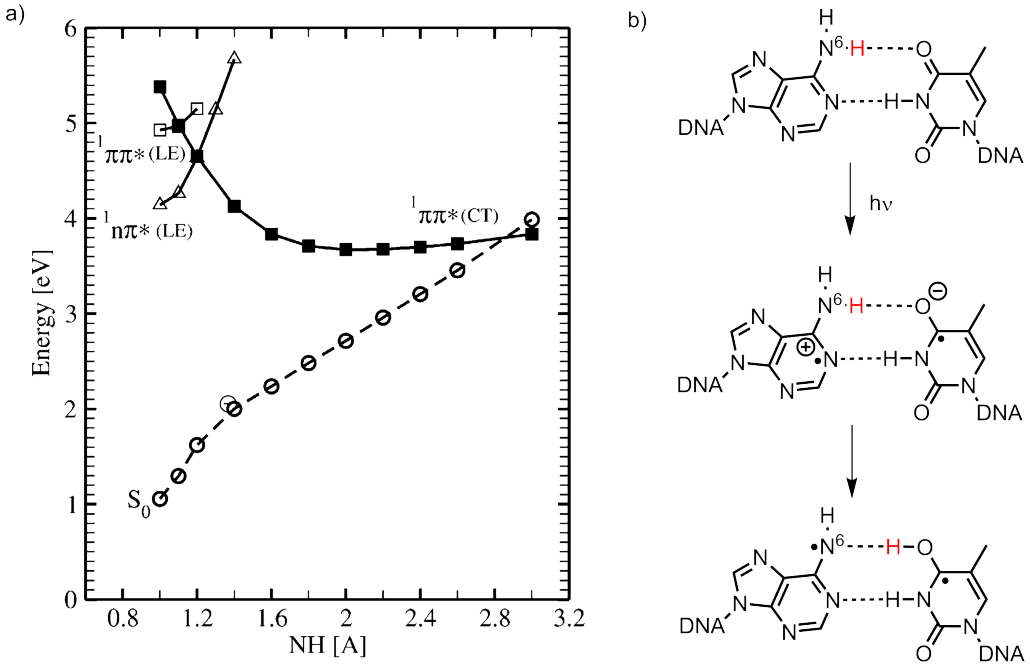

Figure 2.12 – a) Minimum energy profiles of the excited $\pi\pi^*$, $n\pi^*$, charge transfer ($A^{\bullet+}$ $T^{\bullet-}$) and the ground state as function of the $N(6)-H$ distance of adenine for the Watson-Crick structure. The charge transfer state can be populated by nonadiabatic coupling of the bright $\pi\pi^*$ and $n\pi^*$ state. The extension of the $N(6)-H$ distance causes a stabilization of the charge transfer state and a destabilization of the ground state, which leads to conical intersection. This proton transfer enables an ultrafast excited state deactivation for Watson-Crick base pairs. Figure reprinted with permission from Perun et al. [145] (Copyright (2006) American Chemical Society). An analogous mechanism is proposed for G-C base pairs. b) Attempt to display the mechanism by structural formulae. Photon absorption causes a charge transfer state between A and T ($A^{\bullet+}$ $T^{\bullet-}$). The transfer of the N(6) proton of adenine compensates the charge and brings the molecule back to the ground state.

the proton transfer reaction in chemical structures. This simple picture has to be taken with caution, since excited electronic states cannot be represented correctly by chemical formulae.

Experimental evidence for this ultrafast deactivation mechanism has been drawn from several experiments. Abo-Riziq et al. [146] prepared different hydrogen bonded structures of guanine and cytosine in the gas phase. Interestingly, the G-C Watson-Crick base pairing structure exhibits the shortest excited state lifetime of all investigated base pairing schemes. These results were confirmed by calculations which showed, that the ultrafast deactivation via the intrastrand electron induced proton transfer is only possible in Watson-Crick base pairs [147]. The ultrafast decay of the Watson-Crick base pairs was interpreted as the product of natural selection according to photochemical stability [146]. Beside the gas phase experiments, further evidence for the decay mechanism could be found in the liquid phase. Schwalb et al. prepared isolated G-C base pairs in chloroform solutions and investigated the excited state decay with fluorescence upconversion [148, 149]. They ob-

served a faster excited state decay in the G-C base pairs compared to the single monomers. A quenching of the emission upon base pairing was also observed for double-stranded GC-helices in aqueous solution [107].

However, an accelerated repopulation of the ground state, as postulated by the theory, has not been observed by transient absorption spectroscopy in GC-helices in solution [112, 150, 151]. Further theoretical investigations have shown that environmental effects like base stacking and polarity can modify the energy landscape and strongly influence the interstrand electron driven proton transfer [152, 153]. As a consequence, the interstrand electron driven proton transfer has not been assumed to play a role in natural systems [47].

Intrastrand Electron Induced Proton Transfer Crespo-Hernández et al. have shown with ultrafast transient spectroscopy that the excited state of base paired G-C strands decays slower than of the corresponding mononucleotides [150, 154]. The same authors presented further evidence, that the excited state lifetime of double-stranded $(dA)_{18} \cdot (dT)_{18}$ is nearly identical with the corresponding single strands [112]. From that result they concluded that base stacking controls the excited state decay and that base pairing has only minor influence on the excited state dynamics. Due to these experimental results the interstrand electron driven proton transfer model of Domcke et al. (see above) has been regarded as not relevant in base stacked DNA in solution [47].

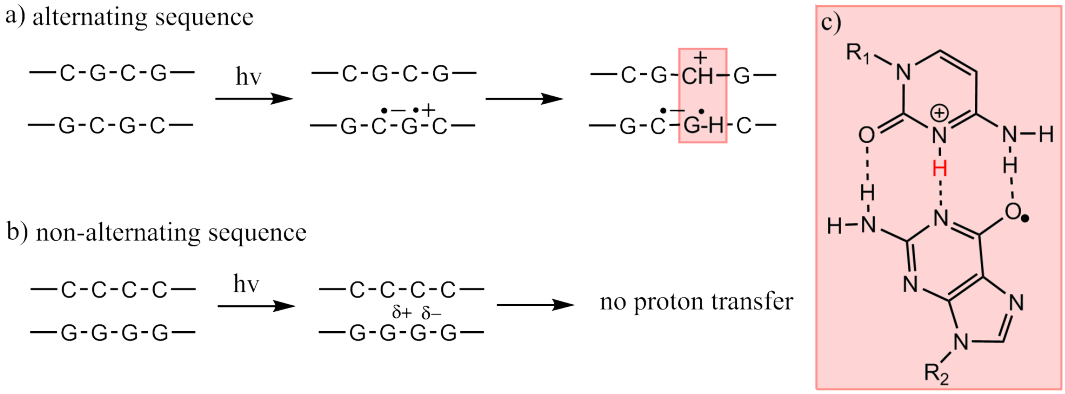

Figure 2.13 – Model explaining the isotope effect observed in transient absorption experiments of DNA double strands [155]. a) Alternating sequence: the redox potential difference between two adjacent bases (G and C) enables charge transfer states after UV-excitation. The guanine radical cation protonates the base paired cytosine, due to its enhanced acidity. b) Non-alternating sequence: in pure G and C strands a complete charge transfer is not possible due to the missing driving force. This partial charge transfer does not enable proton transfer. An analogous mechanism is proposed for A-T base pairs and sequences. c) Molecular structure shown for the proton transferred G-C base pair.

However, recent experimental results of the Kohler group indicate that the excited state decay is possibly modified by base pairing [156, 129]. In these studies, the authors observe an isotope effect on the excited state dynamics [155]. The excited state lifetime of DNA double strands depends on the used solvent: the excited state lifetime in H_2O is

shorter than in D_2O. In deuterated water, all exchangeable protons of the nucleobases are exchanged with deuterons. This isotope effect shows a contribution of the hydrogen/deuterium on the excited state decay which hints to a proton transfer. To prove that, the authors substituted the proton at the C(3) position of cytosine with a methyl group, giving 3-methylcytidine, which cannot form hydrogen bonds. In this sample, no isotope effect was observed, which was taken as a strong evidence that the proton is involved in the excited state deactivation [155]. Furthermore, the isotope effect is only observed in alternating sequences, whereas a deuterium effect could not be detected in non-alternating sequences [155, 112]. De La Harpe et al. [155] propose the following model explaining their experimental results (Fig. 2.13):

In an alternating sequence, charge separated states between adjacent bases are formed due to the redox potential difference between neighboring bases (see section 2.2.1.3). These charge transfer states form radical cations and radical anions. It is known that these species have strongly changed acidities and basicities in comparison to their parent nucleobases. For example, the guanine base gets more acidic upon one electron oxidation which decreases the pK_a-value from 9.5 to 3.9 [157]. The radical anion of cytosine is much more alkaline than the cytosine itself. This change in the pK_a-values is able to shift the proton equilibrium in the Watson-Crick base pairs. Therefore, the proton from N(1) of guanine is transferred to the N(3) atom of cytosine [158, 159]. The kinetics of the proton transfer depend on the isotope and is slowed down by deuteration of the DNA bases. In contrast, UV-excitation of non-alternating sequences leads only to a partial charge transfer, which is not strong enough to cause a proton transfer and no isotope effect can be observed. Thus, this model explains the experimental findings. Although recent calculations [160] could support the model, direct evidence is lacking and many open questions remain. This model is in strong contrast to the previous ones, since the driving force for the proton transfer is the intrastrand charge transfer caused by base stacking.

All three models described in this section have a proton transfer step in common. However, the timescale, the involvement of intra- and interstrand effects and the repopulation mechanism of the ground state are different. Improved quantum chemical approaches might enable to simulate these processes in DNA strands satisfactorily in future, which could reconcile the different models. In summary, the photostability of base monomers is well understood, whereas many open questions remain for the excited state decay in single-stranded DNA. The processes induced by base pairing in double-stranded DNA are not understood.

2.2.2 DNA Photolesions

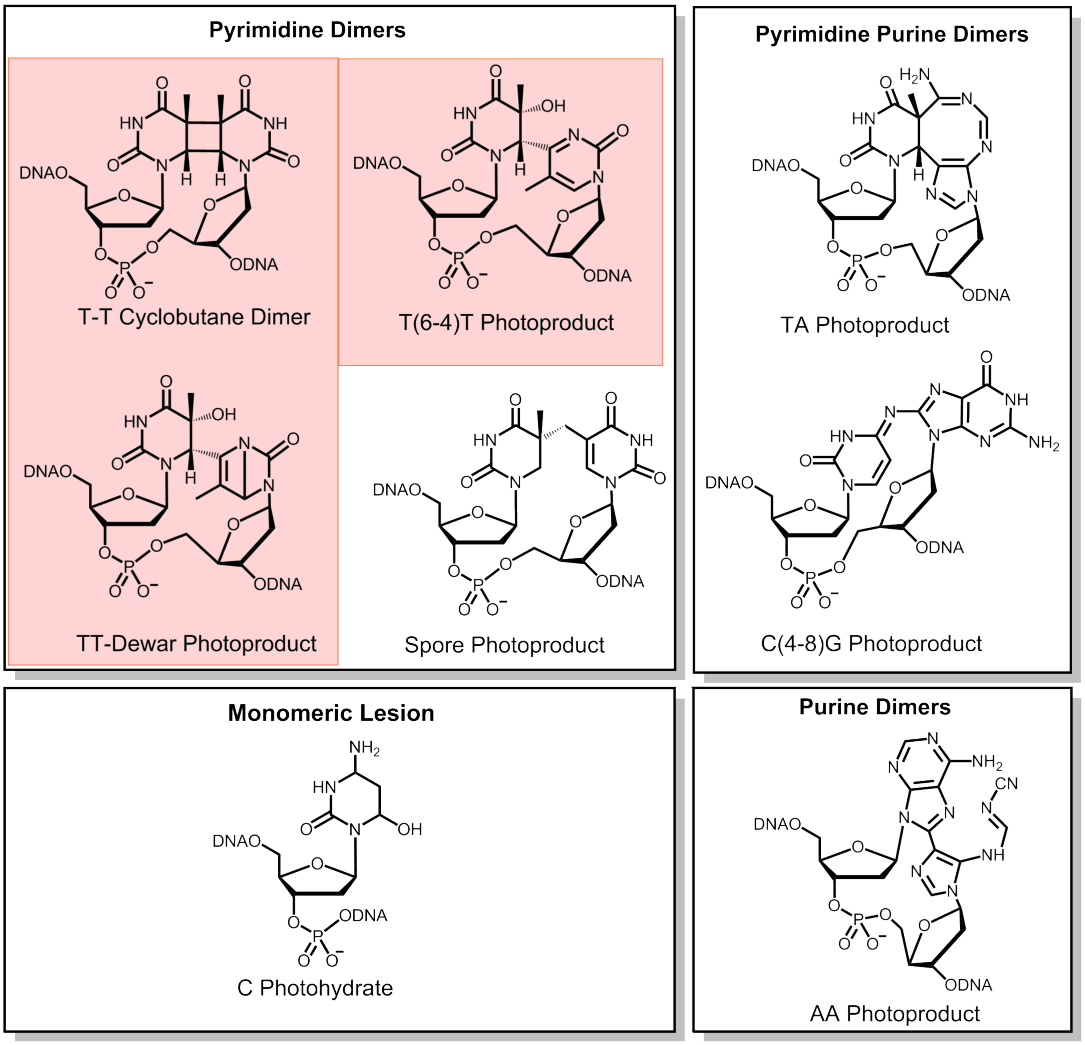

Figure 2.14 – Overview of DNA photolesions. The lesions can be divided into pyrimidine dimers, pyrimidine purine dimers, a purine dimer and a monomeric lesion. The lesions shaded in red are discussed in detail in the text.

In the previous chapter some efficient excited state deactivation processes causing the high photostability of DNA have been described. Nevertheless, there is a small probability that some excited states undergo photochemical transformations. Any change in the molecular structure of the DNA double helix has an impact on the underlying genetic information and may lead to severe biological consequences like cell death or cancer [8, 9]. The reaction quantum yield, i.e. the probability of damage formation after photon absorption is fortunately extremely low for all of these photoreactions ($\leq$1%) [24]. These processes induced by direct excitation of a nucleobase are called direct induced photolesions and will be treated in the following. Photolesions can also be generated by secondary photochemical

reactions, like photosensitizing or oxidation processes for example by singlet oxygen ($^1O_2$), which will not be discussed in this thesis (further information can be found in [161]).

An overview on direct induced photolesions is given in Figure 2.14 [161, 162, 163]. These lesions can further be subdivided in four different groups: (1) Dimerization reactions between two pyrimidines: This group contains the most frequently occurring lesions (CPD), (6-4) photoproduct and its Dewar isomer. All of these lesions can be formed between each type of pyrimidine. 75% and 25% of all photolesions are CPDs and (6-4) lesions, respectively [164]. These main photolesions and their photochemistry will be discussed in detail in the next paragraph. An additional special dimeric pyrimidine photolesion has been discovered in DNA, which is packed in spores, the spore photoproduct. In this case, two thymines are linked via a methylene bridge between the two C(5) atoms [165, 166]. (2) Dimerization products between pyrimidines and purine bases cause the TA photoproduct [167, 168] and the recently discovered C(4-8)G photoproduct [169]. (3) Dimerization reaction between two purines leads to the adenine dimerization photoproduct [170, 171]. The yield of this purine containing lesions is about two orders of magnitude lower than the pyrimidine based dimers [172, 173]. (4) Monomeric lesions: UV-light absorption causes water addition to the C(5)C(6) double bonds of pyrimidine bases and yields the photohydrate [174, 175]. The three most frequently occurring photolesions and their formation mechanism are explained in detail in the following:

Cyclobutane Pyrimidine Dimer

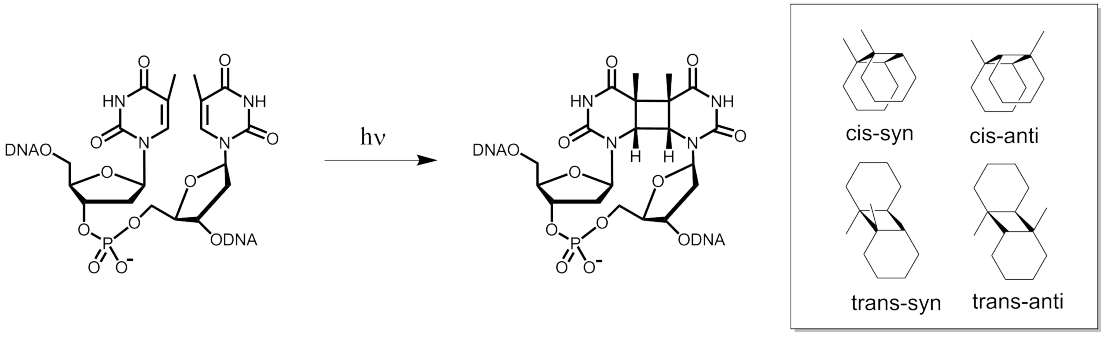

Figure 2.15 – Cyclobutane pyrimidine dimer formation by a [2π+2π] cycloaddition of two adjacent thymines. The inset depicts four possible diastereomers.

The CPD is the most frequently occurring photolesion in DNA [176, 177]. It is formed between two adjacent pyrimidines via a [2π+2π] cycloaddition of the two C(5)C(6) double bonds (Fig. 2.15). The formed cyclobutane causes an intrastrand crosslink. Several stereoisomers can be formed and can be distinguished according to the relative position of the two methyl groups (*syn/anti*) and according to the arrangement of the pyrimidine moieties with respect to the cyclobutane ring *(cis/trans)* [178]. Due to the constraints imposed by the DNA backbone only *syn* isomers are formed in the double strand. The *trans-syn* isomer is formed in flexible single strands with lower yields than the *cis-syn* iso-

mer, which represents the major isomer [161]. It has been assumed for a long time, that the precursor of this lesion is the triplet state of the pyrimidine base [179, 180, 181]. However, our group has shown via ultrafast vibrational spectroscopy that the CPD is formed within 1 ps after excitation [182, 183]. The ultrafast reaction clearly indicates a direct formation of the CPD from the singlet $\pi\pi^*$. On this timescale only prearranged nucleobases are able to react, and thus the ground state conformation controls the photoreaction [184, 185]. The reactivity is higher for thymine than for cytosine and follows the series 5′-TT-3′ > 5′-TC-3′ > 5′-CT-3′ > 5′-CC-3′ [186]. The difference in reactivity can be explained by electronic as well as by steric reasons [187, 188]. Although CPDs with cytosines are less frequently formed, they are more mutagenic than their thymine derivatives. This is caused by an enhanced deamination rate for the cytosine involved in a CPD in comparison to the undamaged cytosine. In this reaction the amino-group of the cytosine is attacked by water and replaced by a carbonyl group, resulting in a T(CPD)C→T(CPD)U transition. Subsequent replication causes a C-T mutation [189]. Beside this direct formation, the CPD is also formed indirectly via triplet sensitizing [190].

(6-4) Photoproduct

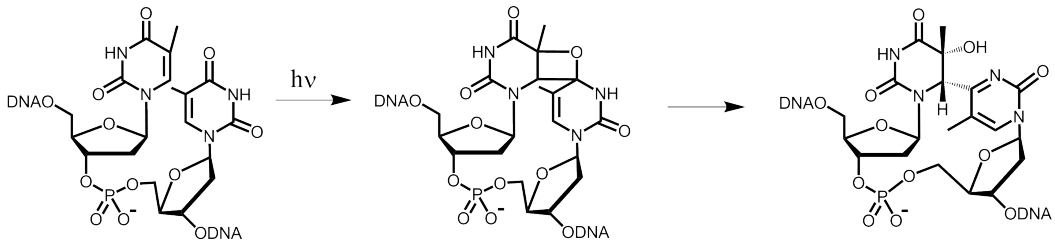

Figure 2.16 – Proposed mechanism for the (6-4) lesion formation between two thymines. A [2π+2π] cycloaddition between the C(5)C(6) double bond and C(4)O carbonyl group of an adjacent thymine forms the unstable oxetane, which rearranges to the (6-4) photoproduct.

The second major photolesion is the (6-4) lesion whose formation mechanism is more complicated than for the CPD lesion. In the first step the C(5)C(6) double bond of the 5′-end pyrimidine is reacting with the C(4)O carbonyl group of the adjacent 3′-thymine (Fig. 2.16). In the case of a cytosine at that position the double bond of the tautomeric imine form is reacting. This photochemical process is called Paterno-Buechi reaction [191]. The formed oxetane or azetidine ring is only stable at low temperatures and rearranges thermally to the final (6-4) product. The name (6-4) originates from the covalent linkage of the C(6) at the 5′-end base to the C(4) at the 3′-end base. The proposed mechanism is based on mainly two experimental results. Firstly, a cyclic intermediate has been isolated in model systems which supports the oxetane/azetidine intermediate [192]. Secondly, time-resolved spectroscopy showed that the final (6-4) product is formed within 4 ms via an intermediate [193]. Direct evidence for that molecular mechanism is still missing. A recent joint experimental-theoretical investigation proposes, that (6-4) lesions are formed via

charge transfer states, whereas excitonic states act as precursors for the CPD lesions [194]. This links the lesion formation directly to the photophysical processes discussed in the previous chapter.

The (6-4) lesion has peculiar spectroscopic properties due to the presence of a substituted pyrimidone ring at the 3′-end [195]. Due to its two conjugated double bonds it absorbs in the UV-A regime at 325 nm and is the only fluorophore formed naturally in DNA. Upon excitation in the UV-A a secondary photoreaction forms the Dewar lesion. Furthermore, a recent study has proposed that the triplet state of the pyrimidone moiety might sensitize the formation of CPD lesions in DNA [196, 197]. This would drastically broaden the harmfulness of the (6-4) lesion.

Dewar lesion

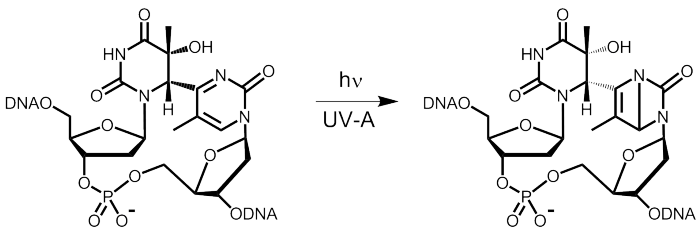

Figure 2.17 – The Dewar lesion is formed by a 4π electrocyclic ring closure reaction after excitation of the (6-4) pyrimidone moiety in the UV-A.

The Dewar lesion is a secondary photoproduct of the 6-4 lesion. It is formed by a 4π-electrocyclic ring closure reaction of the (6-4) pyrimidone ring after excitation around 325 nm (Fig. 2.17). This rearrangement leads to a covalent bond between the N(3) and C(6) atom of the pyrimidone, yielding a similar structure to that proposed for the benzene by James Dewar in 1867 [198]. Fs-IR spectroscopy in combination with quantum chemical calculations have shown that the Dewar product is formed from the singlet state within 100-200 ps [199, 200]. The linkage of the backbone is necessary for the efficient formation of the highly strained Dewar photoproduct, which is stable within the DNA double helix. The Dewar formation has special properties that are strongly different from other photoreactions in DNA. It is the only photoreaction which is triggered directly in the UV-A. This spectral regime overlaps strongly with the emitted spectrum of the sun at the Earth's surface (Fig. 2.4). Furthermore, the reaction quantum yield is high in dinucleotides (~ 8%) [200, 201] in comparison to other photolesions. These properties make the Dewar lesion especially dangerous.

In summary, UV-excitation of DNA bases can lead to photochemical reactions, which cause mainly intrastrand crosslinks between two adjacent bases. The connected bases tilt DNA [202], change the structure locally and destabilize the duplex DNA [203]. These structural changes might interfere with DNA's transcription and replication. Polymerases may be stalled at those positions or wrong complementary bases might be incorporated

due to an undefined or altered base pairing scheme [204, 205]. This causes cell death or mutations, which may cause cancer. Therefore, the repair of these lesions is of fundamental importance to ensure the genetic code integrity. Three main repair mechanisms shall be mentioned briefly here. The perhaps simplest and oldest repair system is based on photoactive enzymes, the photolyases [206]. These enzymes bind the lesion (CPD, (6-4) or Dewar lesion) and repair it by a photoinduced electron transfer, also called photoreactivation [207, 208, 209]. However, photolyases are either absent or non-functional in humans, but play an important role for example in plants and bacteria [210].

In humans, there exist dark and much more complex repair mechanisms. These systems excise the damaged DNA and rebuild the strand with intact nucleotides, instead of directly reversing the damage, like photolyases. There are two major "excision repair" pathways [211, 212, 213]: The base excision repair (BER) removes single nucleotides and plays consequently a minor role for dimeric photolesions. For this kind of lesions, the nucleotide excision repair (NER) is important. It excises the dimer from the strand and resynthesizes the missing sequence. This mechanism is extremely complex and comprises the involvement of about 30 genes. Thus, the interplay of the subtle repair mechanisms and of the photostability enable the protection of DNA from damage and life under UV irradiance.

2.3 Photoinduced Charge Transport in DNA

In section 2.2.1.3 the influence of base stacking on the excited state dynamics has been discussed. It has been proposed that the interaction of planar heterocyclic aromatic systems causes charge transfer states in DNA after photoexcitation. A related process is charge transport along DNA strands which is also mediated by base stacking. The results of this thesis will combine these two different research topics. Therefore, a short overview over photoinduced charge transfer in DNA will be given.

The array of the stacked aromatic nucleobases resembles that of a one-dimensional aromatic crystal, which implicates the possibility of charge transport or even conductivity along the DNA helix which was proposed over 50 years ago [214]. The interest in DNA mediated charge transfer in the 1990s came from the application in nanotechnology or bioelectronics [215] but also from the biological relevance of damage formation by oxidation [216, 217].

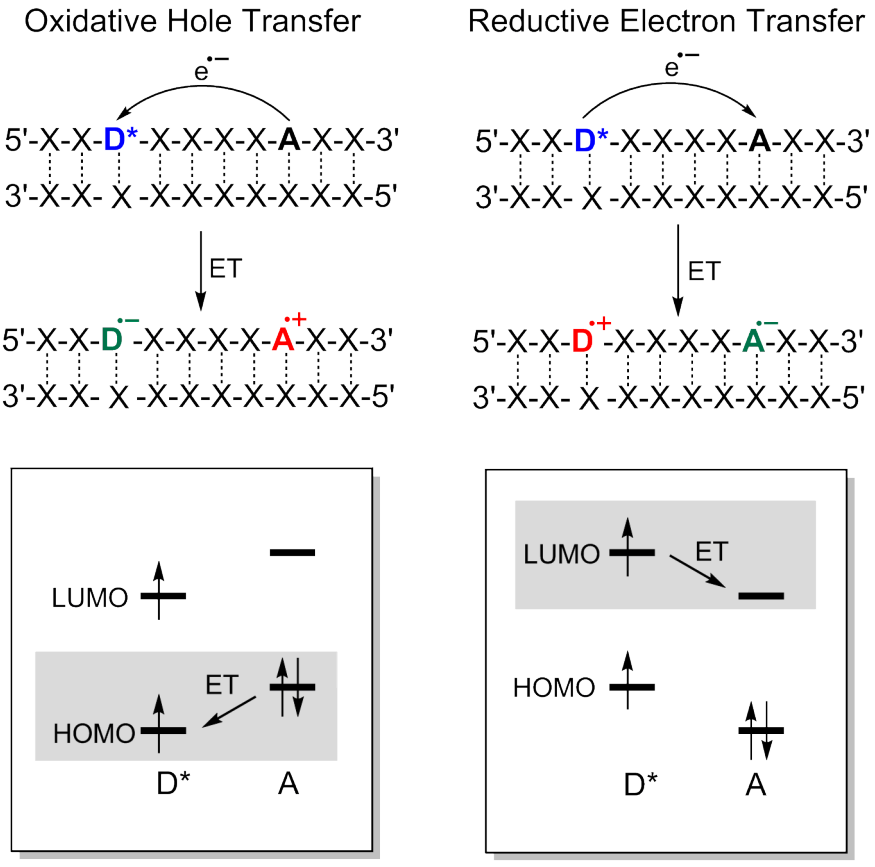

Figure 2.18 – Comparison of oxidative hole and reductive electron transfer. Excitation of the donor (D) promotes an electron in its excited state, causing a hole in the HOMO. If the energy of this HOMO is lower than the energy of the acceptor (A), an electron transfer between these HOMOs occurs (HOMO controlled). If the donor energies of the HOMO and LUMO are higher than those of the acceptor, the excited electron of the LUMO is transferred to the LUMO of the adjacent acceptor (LUMO controlled) [218].

Photoinjection of charges is one main technique to investigate charge transport in DNA, which was pioneered by the Barton group [219]. In this case, a charge donor and an acceptor are incorporated into DNA strands. Many different systems have been developed for this purpose, for example modified or artificial DNA bases, intercalators or capping hairpins which donate electrons or holes into the DNA strand upon photoexcitation [218]. A second molecule in the strand (a nucleobase or modified nucleobase) is used as a charge acceptor (A). The DNA strand in between the donor and acceptor is called bridge. The charge transport is mainly detected either by a charge triggered chemical reaction (e.g. [220, 221, 222, 223]) of the acceptor molecule or is directly monitored by time-resolved spectroscopy (e.g. [224, 225, 226]). Photoexcitation of the donor brings the molecule into its excited state with strongly changed redox properties, causing charge transfer with the acceptor. That is exactly the same process assumed to occur between adjacent DNA bases in single strands (see section 2.2.1.2). Depending on the redox properties, either an electron or a hole can be transferred to the acceptor, also called reductive electron or oxidative hole transfer, respectively. Both of these processes can be described as electron transfer reactions in different directions. However, the categorization of these processes is not just a formalism since the involved molecular orbitals are different (Fig. 2.18). If the energies of the HOMO (Highest Occupied Molecular Orbital) and LUMO (Lowest Unoccupied Molecular Orbital) of the excited molecule are lower than those of the acceptor, an electron in the HOMO of the acceptor is transferred to the HOMO of the donor. Thus, this reaction is HOMO controlled. If the energies of the HOMO and LUMO of the donor are higher than of the acceptor, the excited electron in the LUMO of the donor is transferred to the LUMO of the acceptor, also called LUMO controlled.

All charge transfer mechanisms depend on the involved HOMO-LUMO energies and thus on the redox properties of the involved molecules. The oxidation-potentials for the four base monomers have been established in the following series [227, 228]:

$$G < A < C \approx T$$

This shows that the easily oxidizable purine bases G and A act as hole conductors [229]. The pyrimidine bases T and C are involved in excess electron transfer due to their high reduction potentials [230]. In the following, hole and electron transfer will not be distinguished any further, since the underlying mechanisms are similar to each other.

Charge transport in DNA can be generally described according to the Marcus theory of nonadiabatic electron transfer. The rate of electron transfer k_{ET} can be described by the following equation [231]:

$$k_{ET} = \frac{4\pi^2 \mid V_{el} \mid^2}{h} \cdot \sqrt{\frac{1}{4\pi\lambda k_b T}} \cdot exp\left(\frac{-(\Delta G_{ET} + \lambda)^2}{4\lambda k_b T}\right) \tag{2.2}$$

The equation shows three important quantities which influence the rate of charge transfer [232, 233]: (1) Electronic coupling V_{el} between the donor and the acceptor. The coupling and thus the rate of charge transfer decreases with increasing distance and energy gap between the donor and the bridge. (2) The driving force $\triangle G_{ET}$ of the electron trans-

fer process. Increasing $\triangle G_{ET}$ (the difference in redox potential) in photoinduced charge transport in DNA has shown to increase also the charge separation and transfer rate. Thus, these systems operate in the "normal" Marcus regime ($\triangle G_{ET} + \lambda > 0$) [234]. In contrast, the charge recombination in these systems is in the inverted regime, as for the excimer states in dinucleotides, as discussed before [116] (Fig. 2.9). In this regime, the electron transfer rate is decreasing with increasing driving force ($\triangle G_{ET} + \lambda < 0$). (3) The reorganization energy λ, which is associated with changes in internal geometry and in polarization of the environment during the charge transfer process.

In most cases, the rate constant has been investigated as a function of the distance between the charge donor and acceptor. That has been done by varying the bridge length. For that case, mainly two mechanisms have been proposed:

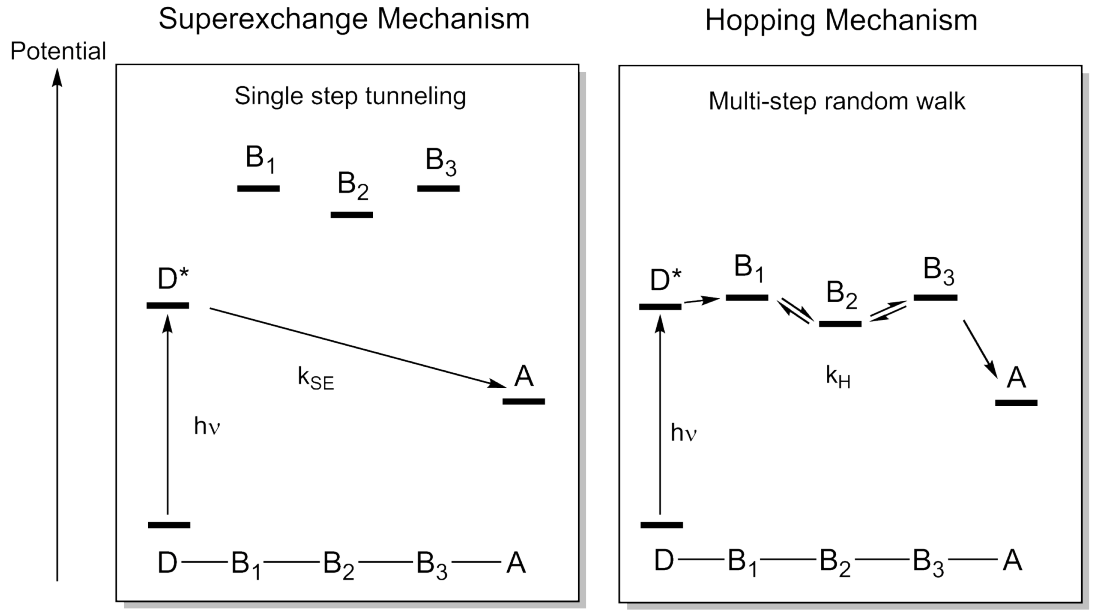

Figure 2.19 – Comparison of the superexchange mechanism and the hopping mechanism. If the bridging molecules B are higher in energy than the excited donor (D), tunneling occurs (superexchange mechanism). If the bridging molecules are similar in energy and thermally accessible, charge hopping between these sides may occur [218].

Superexchange Mechanism The superexchange mechanism occurs when the donor and the acceptor are separated by energetically high lying bridging molecules, which are not thermally accessible (Fig. 2.19). In this case the charge tunnels in a coherent step from the donor to the acceptor and is not populating the bridging molecules. The rate of charge transport for the superexchange mechanism k_{SE} can be described by the simplified Marcus-Levich-Jortner equation [235]:

$$k_{SE} \propto e^{-\beta \cdot R} \tag{2.3}$$

with the distance R between donor and acceptor and β describing the distance depen-

dence of the electronic coupling. β is strongly modulated by the mediating bases of the bridge. For short DNA hairpins a value of 0.6-0.7 $Å^{-1}$ has been obtained [236, 237]. This value is much larger than for π-conjugated oligomers ($\beta < 0.1$ $Å^{-1}$) and smaller than for proteins with their hydrocarbon framework ($\beta <$ 1.0-1.4 $Å^{-1}$) [238]. Thus, the charge transport process in DNA is not molecular-wire-like, but is much more effective than in proteins. The charge transport is mediated by stacked π-conjugated molecules with relatively weak electronic coupling. The strong distance dependence shows that charge transfer by the superexchange mechanism is limited to short distances of one to three base pairs. Nevertheless, long range hole transfer has been observed over 100-200 Å [239, 240]. This discrepancy has led to the description of an alternative mechanism – the hopping mechanism [241].

Hopping Mechanism If the bridging molecules and donor molecules have similar energies, charge hopping might occur (Fig. 2.19). In this case, the charge is injected into the bridge and is hopping between neighboring bases of similar and thermally accessible energies. It does not require a significant coupling between the bridging sides. The rate of charge transport k_{HM} for the hopping mechanism can be described as diffusive or random walk-like and can be modeled with the equation [235]:

$$k_{HM} \propto N^{-\eta} \tag{2.4}$$

where N is the number of equidistant hopping steps and η is a value between 1 and 2, representing the influence of the medium [242]. In the ideal case of a random walk η has a value of 2 [220]. Each hopping step itself can be described by the superexchange mechanism. Therefore, the multistep transfer reduces the exponential distance dependence of the tunneling. The shallow distance dependence for the hopping enables charge transport over long distances. Mostly discussed in this case are $G^{\bullet+}$ to G and $A^{\bullet+}$ to A hole hoppings [243]. When G is not present as an intermediate hole carrier, an endothermic thermally activated hole hopping from $G^{\bullet+}$ to A has been postulated [223].

The different distance dependences of these two mechanisms have been directly observed in several experiments [223, 244, 245]. In one example, the hole arrival rates as a function of A-T bridge length have been investigated in capped hairpins (Fig. 2.20). The hole was injected by photoexcitation of the hole donor (Sa) and the arrival at the acceptor (Sd) was monitored by time-resolved transient spectroscopy. For short distances between the donor and the acceptor (1-4 A-T base pairs), the rate constants decrease rapidly with an increasing number of A-T base pairs in accordance with the superexchange mechanism. For longer distances (5-7 A-T base pairs), a shallow distance dependence has been observed, characteristic for the hopping mechanism. Therefore, both transfer mechanisms play a role in DNA charge transport.

The processes mentioned above describe charge transport in DNA by localized charges on single bases. However, there are some indications that charges are possibly delocalized along the strand. Barton et al. have published experimental data, which indicate that charges are transported via conformationally gated stacked domains [246, 247, 222, 248].

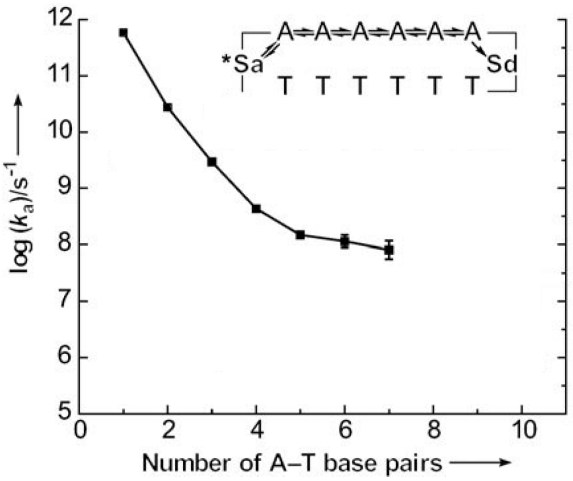

Figure 2.20 – Rate constants for the hole arrival at the acceptor (Sd) after photoexcitation of the donor (Sa). The strong distance dependence for short bridge lengths is attributed to the superexchange mechanism, whereas the shallow distance dependence for longer oligonucleotides is assigned to the hopping mechanism. Figure adapted with permission from Lewis et al. [244].

The charge is delocalized in these domains of about 4-5 bases where strong orbital mixing occurs. Others propose a model of phonon assisted polaron hopping. In this model the charge causes a polaron-like distortion in the DNA which is migrating along the helix by thermal activation [249, 250]. Recently, calculations suggest an intermediate mechanism between superexchange and hopping with a strong delocalization of the charge along the strand [251, 252]. This year, a further model of charge transfer via flickering resonance has been published [253]. In this case, fluctuations bring multiple bases into transient conformations with electronic degeneracy. The charge is transported along the DNA in this degenerate state.

The recent appearance of advanced models for charge transport in DNA shows that the mechanism has not been fully elucidated yet. Especially the question on charge delocalization is still open. These models may also play a role in DNA photophysics, when charge transfer states are formed after photoexcitation. Therefore DNA charge transport and DNA photophysics mechanisms have to be combined for future research.

3 Experimental Methods

The thesis is based on a collaboration project between a physical and a chemical research group. Thus, diverse methods from chemistry and physics have been used to characterize DNA samples and to investigate the excited state dynamics of DNA. While the analytical methods used in chemistry are all standard techniques (see section 3.2), the laser-spectroscopic experiment in the physics department is home-built and is the central method of this thesis. The experimental setup has been described recently in detail in several theses [254, 255, 256]. Therefore, only a short overview of the fs-pump-probe setup will be given in the following.

3.1 Pump-Probe Spectroscopy and Experimental Setup

Concept

For the investigation of the excited state dynamics fs-pump-probe spectroscopy is used to monitor processes on the femtosecond to nanosecond timescale. In 1999 the Nobel prize was awarded in the context of this spectroscopic method [257]. Figure 3.1 depicts the basic idea of this technique. A fs-laser system is used to provide fs-light pulses. These light pulses are split in two parts – the pump pulses and the probe pulses. The pump pulses are used to excite the sample in order to initiate photophysical reactions or photochemical processes. The evolution of these excited state processes are probed with a delayed light pulse – the probe pulse – whose transmittance is recorded on a detector. A defined delay between the pump and the probe pulse is simply achieved by elongation of the pathway of the light of one of the two pulses. Two moveable mirrors change the path length for example of the probe light pulses with respect to the pump light pulses. The time delay between the pump and probe pulses can simply be calculated by dividing the additional distance which the light has to travel by the speed of light. Each position of the mirrors equals one time point after the excitation. This procedure enables to resolve dynamics on the femtosecond to nanosecond time scale.

Upon absorption of the pump pulse, the sample is excited from the ground state to the excited state. Due to the new electronic configuration, the absorbance properties are typically different from those in the ground state. The differences in absorption between the ground state and the excited state are sampled with the probe beam, as a transmittance change. It is simply determined by recording the transmittance of the probe pulses with excitation and without excitation of the sample. The transmittance change is typically converted to the absorbance change, which is plotted against the time delay. These transient absorbance changes are used to analyze the excited state dynamics (Fig. 3.1b).

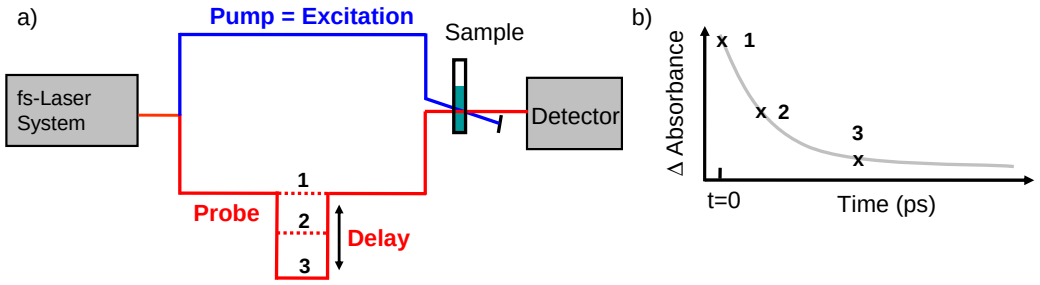

Figure 3.1 – Principle of fs-pump-probe spectroscopy. The light pulses of a fs-laser system are split into two parts – pump and probe pulses. a) The pump beam excites the sample. The evolution of the excited state is probed by delayed pulses of the probe beam. The delay is achieved by changing the pathway of the light by moveable mirrors. Each mirror position (1, 2, 3) equals one time point after excitation. The recorded absorbance change on the detector for each of these mirror positions gives the transient signal plotted in b).

Experimental Setup

Although the basic concept of fs-pump-probe spectroscopy is quite simple, the experimental setup used in this thesis is relatively complicated. The complexity is mainly caused by many nonlinear optical processes which generate different wavelengths for the pump pulses and the probe pulses. A commercially available Ti:Sapphire-Amplifier system (pump laser: Spectra Physics, Tsunami; amplifier: Spectra Physics, Spitfire Pro) is used to provide light pulses with a duration of about 100 fs at 800 nm and a repetition rate of 1 kHz (details in [254]). On the one hand, the output light pulses at 800 nm have to be converted into the UV to excite DNA bases (pump pulses). On the other hand, mid-IR pulses have to be generated from the 800 nm pulses to probe the absorbance change after excitation. The frequency conversion processes are explained in the following.

Pump Pulse The pump pulse wavelength has to be adjusted between 250-300 nm to match the absorbance bands of the nucleobases (Fig. 2.4). In most experiments of this thesis, light pulses at 295 nm were used to excite the sample. This wavelength enabled the selective excitation of 5-methyl-2′-deoxycytidine in specially designed oligonucleotides (chapter 4.2). The 295 nm light pulses were generated by a frequency-doubled two stage non-collinear optical parametric amplifier (NOPA) [258]. First, the light pulses in the pump branch are split into two parts (Fig. 3.2). One part with 4% of the light intensity is used to produce white light (WL) in a sapphire crystal. The other part, with the main intensity, is frequency doubled in a beta barium borate (BBO) crystal (Type I) to 400 nm. 30% of these 400 nm pulses are temporally and spatially superimposed with the generated white-light in a further BBO crystal (Type I). In this NOPA process, a spectral part of the white-light is selected and amplified in a $\chi^{(2)}$ parametric process. The output wavelength can be controlled by the phase matching condition (that means the angle of the BBO crystal) and the temporal superposition of both pulses. Adjusting these two parameters allows to tune the output wavelength in the visible part of the spectrum. Due to the conservation of energy, a second pulse is generated in the near IR (Idler), which is emitted

at an angle to the visible light and is directly blocked after generation. To generate pump pulses at 295 nm, the output wavelength of the NOPA was adjusted to 590 nm. The pulses are further amplified by superimposing the 590 nm pulses of the first stage with the remaining 400 nm pulses in a second NOPA stage (NOPA II). Subsequently, the light is passing through the movable mirrors stage, where the pump pulses are delayed versus the probe pulses. It allows to delay the pulses up to 3 ns. In the final step the 590 nm pulses are frequency doubled in a BBO crystal (Type I) (SHG) to generate pulses at the desired excitation wavelength of 295 nm. The energy of these pulses was about 0.8 μJ to 1 μJ. The light is focused on the sample (ca. 150 μm) and excites the DNA molecules.

In some experiments pump pulses at 266 nm have been used (chapter 4.1 and 4.3). The generation of this wavelength is described in detail in [256]. In brief, 400 nm pulses are generated by frequency doubling the laser output pulses at 800 nm in a BBO crystal (Typ I) in the first step. The efficiency of this process is around 30 %. In the second step, the pulses at 400 nm and 800 nm, which have not been converted in the first step, are frequency mixed (sum frequency generation, SFG) in a BBO crystal (Typ I) to yield 266 nm pulses.

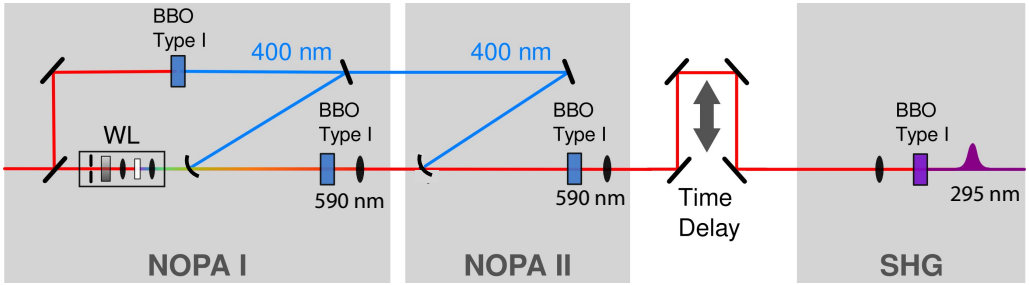

Figure 3.2 – Setup of the pump pulse generation in the UV. Visible light (590 nm) is generated in a two stage non-collinear optical parametric amplifier (NOPA) which is subsequently frequency doubled to generate light pulses at 295 nm. Figure adapted from K. Haiser [254].

Probe Pulses The conversion of the 800 nm pulses of the laser system to the mid-IR is shown in Figure 3.3. It can be subdivided in three different sections – NOPA, optical parametric amplifier (OPA) and difference frequency mixing (DFM). The first nonlinear optical process is a NOPA, similar to that described in the previous section. However, in this case near-IR (NIR) light is amplified at 1400 nm. The additionally generated idler beam at 560 nm is used to monitor the process. In the next step, the NIR pulses are amplified in an OPA process. The 1400 nm photons act as seed photons and are superimposed collinearly in a BBO crystal (Type II) with pulses of 800 nm. Beside the amplification of pulses at 1400 nm, additional photons with a wavelength of 1800 nm are generated due to the conservation of energy. Both light pulses at 1800 nm and 1400 nm are frequency mixed in an $AgGaS_2$ to obtain light in the mid-IR around 6 μm. The mid-IR pulses have a spectral width of about 150 cm^{-1} which is spectrally dispersed (Chromex 250IS, Bruker)

and detected on a 64-channel MCT array (IR-0144, Infrared Systems Development). The mid-IR pulses can be tuned between 3-10 μm by adjusting the DFM and OPA/NOPA processes. In both cases the phase matching angle and temporal superposition of the pulses are adjusted to give the desired wavelength in the mid-IR.

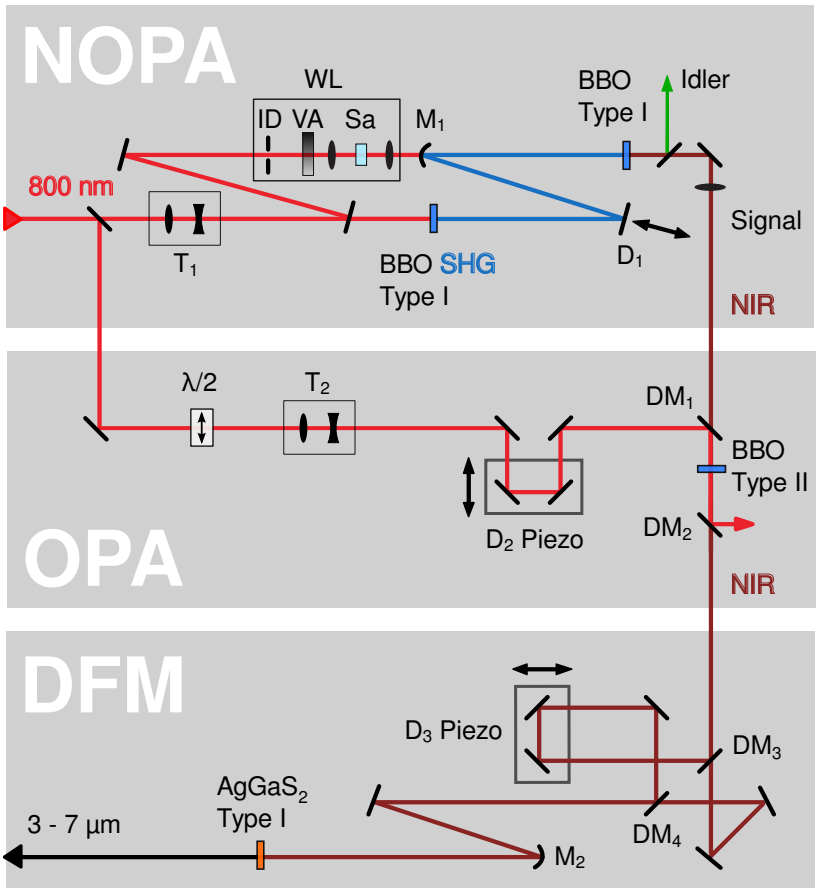

Figure 3.3 – Setup of probe pulse generation in the mid-IR. In the first two steps, 800 nm is converted by a NOPA and ab OPA process to near IR pulses between 1200 nm -1500 nm and 1700 nm - 2200 nm. These pulses are frequency mixed in a third step to generate mid-IR pulses from 3-10 μm. Figure reprinted from K. Haiser [254].

Data acquisition The difference in transmittance is calculated by dividing the signal with excitation (i.e. the energy of the transmitted probe light) by the signal without excitation. That is done by building a chopper wheel into the pump branch which blocks every second pump pulse. Thus, the signal recorded on the detector is alternating between transmitted light with sample excitation ($S_{i,sample,ex}$) and without excitation ($S_{i,sample,nonex}$). To improve the signal-to-noise ratio, the signals are averaged over several thousands of shots.

The averaged transmittance difference $\triangle T_{sample}$ as a function of wavelength λ and time delay τ is calculated according to the following equation [255, 259]:

$$\Delta T_{sample}(\lambda,\tau) = \frac{\sum_{i=1}^{N} S_{i,sample,ex}(\lambda,\tau)}{\sum_{i=1}^{N} S_{i,sample,nonex}(\lambda,\tau)} \tag{3.1}$$

To reduce the noise caused by variations in the light pulse energy, the probe pulses are split before transmitting the sample into two branches – sample and reference branch. The sample pulse is spatially superimposed with the pump pulse and is thus transmitting the excited sample as described before ($\Delta T_{sample}(\lambda,\tau)$). The reference pulse transmits the sample at a position without an excitation. For this reference light beam the transmittance difference $\triangle T_{ref}$ is calculated according to equation 3.1 [255, 259]:

$$\Delta T_{ref}(\lambda,\tau) = \frac{\sum_{i=1}^{N} S_{i,ref,ex}(\lambda,\tau)}{\sum_{i=1}^{N} S_{i,ref,nonex}(\lambda,\tau)} \tag{3.2}$$

Dividing the transmittance of the sample branch $\triangle T_{sample}$ by the reference branch $\triangle T_{ref}$ reduces the noise induced by the laser significantly [255]. The absorbance change ΔA, used for the data analysis is calculated according to [255, 259]:

$$\Delta A = -log(\Delta T(\lambda,\tau)) = -log\left(\frac{\Delta T_{sample}(\lambda,\tau)}{\Delta T_{ref}(\lambda,\tau)}\right) \tag{3.3}$$

The sample is exchanged between two consecutive light pulses in a flow cuvette (BaF_2 windows, 100 μm path length) to avoid artifacts caused by damaged sample. The polarization of the pump and the probe beam is adjusted according to the magic angle conditions to avoid any contribution of rotational diffusion. All experiments have been performed under room temperature.

3.2 Additional Chemical, Spectroscopic and Computational Methods

For characterizing oligonucleotides and the calf thymus DNA several chemical and spectroscopic methods have been used in this thesis. All the different analytical methods like HPLC-MS, gel-electrophoresis, melting curve determination, CD-, UV/Vis- and IR-spectroscopy are described in detail in the corresponding publications and will not be presented here. The details for quantum chemical calculations of vibrational spectra with Gaussian [260] can also be found in the corresponding publications.

4 Results

In this chapter, the results of the thesis which have been published in scientific peer reviewed journals are presented. Three publications are attached combined with a short summary. The publications are reprinted with the permissions of the publishers.

4.1 The IR-Spectrum of the Radical Cation of 5-Methyl-2′-Deoxycytidine

The communication "Fingerprinting DNA Oxidation Processes: IR Characterization of the 5-Methyl-2′-Deoxycytidine Radical Cation" published in *ChemPhysChem* [261] provides the basis for identifying charge transfer states in photoexcited DNA for the subsequent part of this thesis. In addition, the results will enable the characterization of oxidative damage processes of 5-methyl-2′-deoxycytidine (mC) in DNA.

The naturally modified nucleobase mC occurs about 4-5% in the human genome [262] and plays an important role in gene regulation [79]. It is furthermore a mutational hot spot [263] and undergoes oxidative lesion formation [264]. The UV absorbance band of mC is red shifted relative to the bands of other nucleobases which enables selective excitation of mC in special designed sequences with light at 295 nm (chapter 4.2) [265]. For the identification of charge transfer states in these DNA strands and to investigate oxidative lesion formation, the infrared spectrum of the mC radical cation is reported here. The radical cation of mC was prepared by a two-photon/two-step ionization process upon excitation with fs-light pulses at 266 nm. A transient spectrum of this species is recorded with fs-IR spectroscopy at delay times of 800 ps to 1000 ps. Density functional theory simulations of the IR-spectrum of the mC radical cation supported the assignment. The radical cation is stable on the picosecond timescale but undergoes secondary chemical reactions on the ns - μs time scale. Its final oxidation products in water were identified with ultra high performance liquid chromatography coupled with electrospray ionization tandem mass spectrometry.

The combination of laser-spectroscopic, computational and chemical methods has allowed to identify IR-marker bands of the mC radical cation. These marker bands will be of fundamental importance to characterize the long-living states in photoexcited single-stranded DNA in the next chapter.

ChemPubSoc Europe

DOI: 10.1002/cphc.201300954

Fingerprinting DNA Oxidation Processes: IR Characterization of the 5-Methyl-2′-Deoxycytidine Radical Cation

Dominik B. Bucher,[a, b] Bert M. Pilles,[a] Toni Pfaffeneder,[b] Thomas Carell,[b] and Wolfgang Zinth*[a]

Methylated cytidine plays an important role as an epigenetic signal in gene regulation. Its oxidation products are assumed to be involved in active demethylation processes but also in damaging DNA. Here, we report the photochemical production of the 5-methyl-2′-deoxycytidine radical cation via a two-photon ionization process. The radical cation is detected by time-resolved IR spectroscopy and identified by band assignment using density functional theory calculations. Two final oxidation products are characterized with liquid chromatography coupled to mass spectrometry.

In the human genome about 4–5% of all cytosines that are mainly located in CpG sites are methylated at the 5-position.[1] This modification is associated with gene silencing.[2] Genomic methylation patterns are dynamic, and their controlled (re)-programming is crucial during cellular differentiation.[3] Active demethylation by stepwise oxidation of 5-methyl-2′-deoxycytidine (5mdC) to 5-hydroxymethyl-2′-deoxycytidine (5hmdC), 5-formyl-2′-deoxycytidine (5fdC), and finally 5-carboxy-2′-deoxycytidine (5cadC) has been proposed.[4–8] Furthermore, 5hmdC and 5fdC are also known to be oxidatively generated lesions of 5mdC,[9–11] and the mCpG sequence is known to be a mutational hot spot.[12,13] These lesions are formed via hydroxyl-radical-mediated hydrogen-atom abstraction from the methyl group of 5mdC or by one-electron oxidation and the formation of the 5mdC radical cation.[9,14] Here we report the photochemical production of the 5mdC radical cation and its identification by time-resolved vibrational spectroscopy. The cationic species was formed after two-photon ionization with femtosecond light pulses at 266 nm and identified by a combination of time-resolved IR spectroscopy and density functional theory (DFT) calculations. Two reaction products were characterized by ultra-high performance liquid chromatography coupled with electrospray ionization tandem mass spectrometry (UHPLC-ESI-MS/MS) measurements.

[a] D. B. Bucher, B. M. Pilles, Prof. W. Zinth
BioMolecular Optics and Center for Integrated Protein Science
Ludwig-Maximilians-Universität
Oettingenstr. 67, 80538 München (Germany)
Fax: (+49) 89-2180-9202
E-mail: wolfgang.zinth@physik.uni-muenchen.de

[b] D. B. Bucher, T. Pfaffeneder, Prof. Dr. T. Carell
Center for Integrated Protein Science
Department für Chemie, Ludwig-Maximilians-Universität
Butenandtstr. 5–13, 81377 München (Germany)

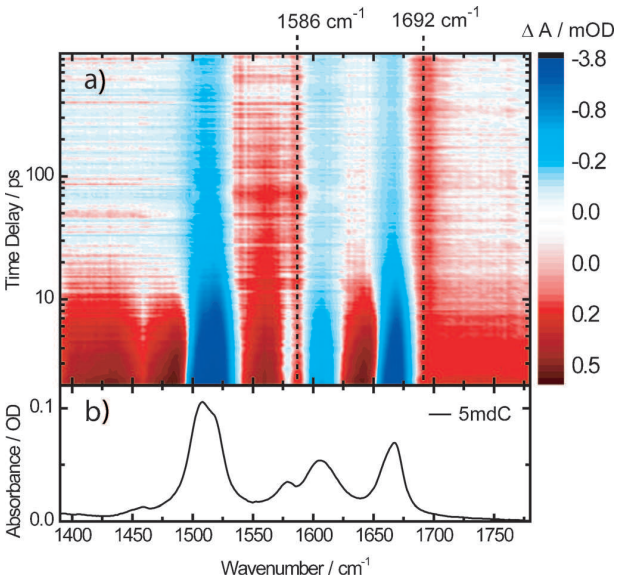

Figure 1. a) Absorption difference (color coded) plotted versus wavenumber and delay time for 5mdC after excitation with a femtosecond laser pulse at 266 nm. Background of heated water is subtracted.[18] Characteristic positive bands are marked with a dashed line. b) Absorption spectrum of 5mdC.

The results from a femto/picosecond transient absorption experiment of 5mdC after excitation at 266 nm is shown in Figure 1a. Negative bands are observable at the position of the ground-state absorbance (Figure 1b). Positive absorbance changes are caused by excited-state absorption or photoproducts. The data are globally fitted with three exponentials. Two fast ones ($\tau_0 = 1.3$ ps and $\tau_1 = 5$ ps) describe the decay of the first excited state (S_1) and the cooling of the hot ground state. The third time constant with $\tau_2 = 48$ ps is tentatively assigned to the nπ^* decay, which is similar to the nπ^* in 2′-deoxycytidine.[15–17]

After these initial transients a long-lasting absorption change persists. The ground-state bleach is not recovering completely and characteristic positive bands are observable (Figure 1, dashed lines). These features do not change in the investigated time window of 1 ns. The signature of this spectrum also contains some contributions from water heated by the excitation process. The spectrum of the 5mdC reaction product can be obtained by subtracting the spectrum of the heated water (Figure 2a), which has been obtained by temperature-depended steady-state measurements.[18] The resulting difference spectrum (Figure 2b) shows the bleach of the origi-

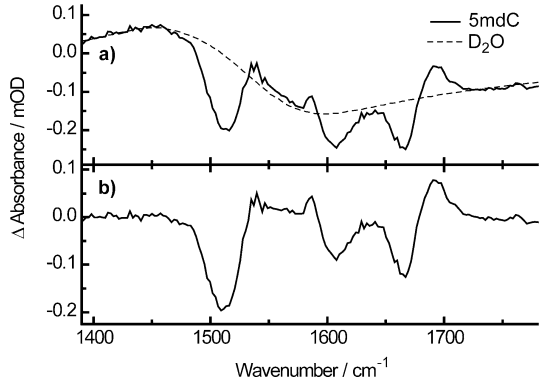

Figure 2. a) Transient absorbance spectrum averaged over late delay times of 5mdC and steady-state difference absorbance spectra of heated D_2O.[18] b) Subtracting the contribution of the heated D_2O from the transient 5mdC spectrum gives the difference spectrum of the reaction product.

nal 5mdC and two characteristic positive bands at 1586 and 1692 cm^{-1}.

In order to obtain further information about this species, we performed an experiment with a ns-pulse excitation with the same excitation energy. Surprisingly in this measurement no long-living species was observed (data not shown).

The only difference between the fs and the ns experiment was the peak intensity of the excitation pulse. This result points to a multi-photon process in the generation of the 5mdC reaction product, which is only formed at high peak intensities. For that reason, we varied the excitation energy in the fs experiment. Figure 3 shows the difference spectra recorded (500–1000 ps averaged) for different excitation energies. It can be seen that the growth of the amplitude is nonlinear. For a more quantitative analysis the amplitude of the 1692 cm^{-1} marker band is plotted versus the excitation energy. Here a clear quadratic dependence is found (Figure 3, inset) indicating that the formation occurs presumably via a two-photon process.

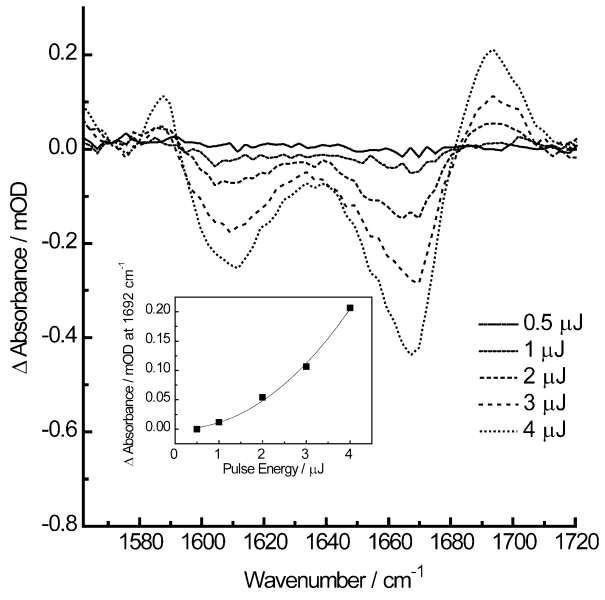

Figure 3. Transient spectra (averaged over the 500–1000 ps range) for different excitation energies. Inset: Absorbance change at 1692 cm^{-1} (marker band) plotted versus excitation energy. The pulse energy of 1 μJ corresponds to circa 20 GW cm^{-2}.

Information about the molecular composition of the product was obtained by UHPLC-ESI-MS/MS with quantitative isotope dilution[19] of an illuminated 5mdC sample with intense fs pulses at 266 nm. The analysis revealed 5hmdC and 5fdC as final reaction products (Figure 4). These species are known to

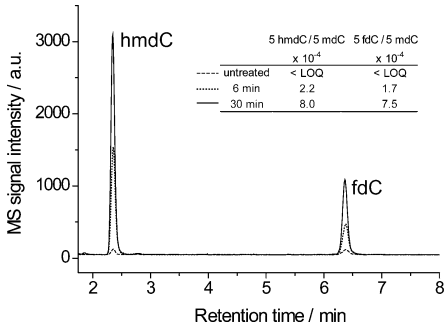

Figure 4. Illumination of an aqueous 5mdC solution with fs laser pulses yields 5hmdC and 5fdC in equal amounts. Analysis was performed by quantitative UHPLC-ESI-MS/MS. Depicted are the overlaid ion chromatograms of the MS/MS transitions for the protonated ions ($[M+H]^+$) of 5hmdC (258.1→142.1) and 5fdC (256.1→140.1). The selected ion chromatograms of the isotope-labeled internal standards [D_2,$^{15}N_2$]-5hmdC and [$^{15}N_2$]-5fdC were omitted for clarity. The inset compiles the quantified 5hmdC and 5fdC amounts relative to 5mdC depending on illumination time. LOQ = limit of quantification.

be the oxidation products of 5mdC among others.[9–11] As a consequence, these species are apparently formed in the reaction chain initiated by a two-photon ionization process of 5mdC. A possible reaction mechanism is shown in Scheme 1. 5mdC is ionized by absorbing two photons, which leads to the 5mdC radical cation ($5mdC^{\cdot+}$). This cation is acidic and may lose a proton at the 5-methyl-group. Further reactions including molecular oxygen attack give 5hmdC and 5fdC as products.[10] The observed radical species in our case is at the beginning of the reaction chain. It could be either $5mdC^{\cdot+}$ or the corresponding deprotonated species ($5mdC-H^{\cdot}$). The subsequent reactions are diffusion limited and occur on a much longer time scale well above the picosecond range. Similar photoionization experiments have been performed recently with guanine (G), in which the guanine radical cation ($G^{\cdot+}$) and not the deprotonated species ($G-H^{\cdot}$) was observed after excitation at 200 nm in a one-photon process on a similar time scale.[20,21] Pulse radiolysis experiments gave a time constant of 55 ns for the deprotonation of $G^{\cdot+}$.[22] We assume a similar timescale for the deprotonation of $5mdC^{\cdot+}$.

To confirm this assignment, the infrared spectra of 5mdC, $5mdC^{\cdot+}$, and $5mdC-H^{\cdot}$ were calculated by DFT (Figure 5). The $5mdC^{\cdot+}$ spectrum (Figure 5b) shows a similar signature with

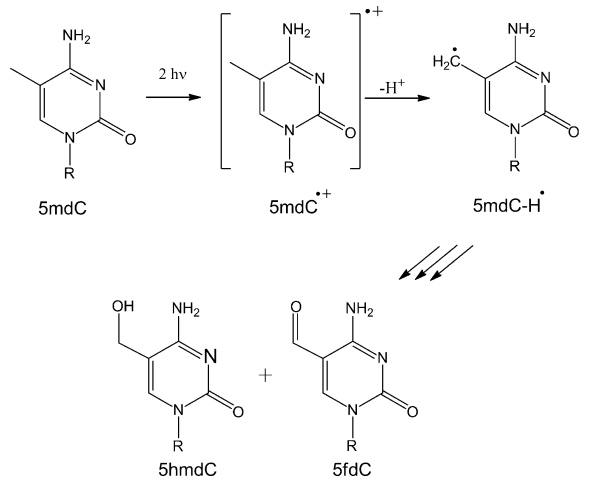

Scheme 1. Mechanism of 5hmdC and 5fdC formation after one-electron oxidation of 5mdC[10].

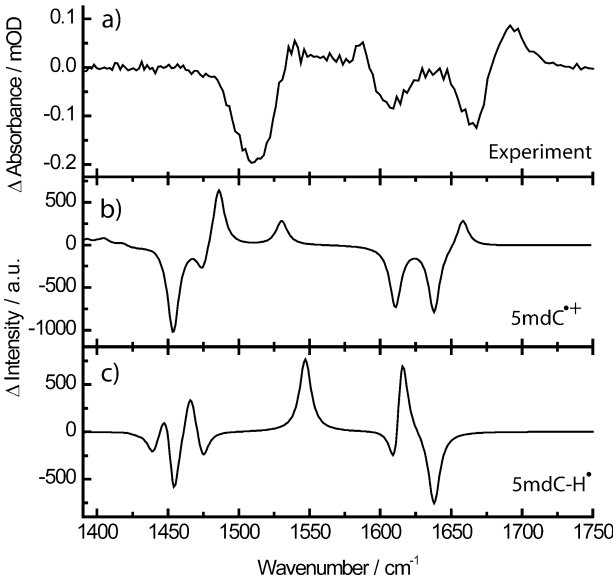

Figure 5. a) Averaged (500–1000 ps) transient spectra of 5mdC (hot water subtracted). Calculated difference spectra (reaction product 5mdC) of $5mdC^{\cdot+}$ (b) and $5mdC–H^{\cdot}$ (c).

two positive bands in the region of the marker bands of the observed difference spectrum. A further positive band at 1486 cm^{-1} is not observed in our experiment, since it is probably overlaid by the ground-state bleach at 1510 cm^{-1}. In contrast, the $5mdC–H^{\cdot}$ spectrum (see Figure 5c) shows a completely different spectral signature. As a consequence we assign the product generated in the two-photon process to $5mdC^{\cdot+}$.

In summary we report that two-photon excitation of 5mdC gives an intermediate reaction product with a characteristic difference spectrum. The associated species is formed ultrafast (< 5 ps) and shows no spectral evolution during the first nanosecond. Because it is known that nucleobase cations deprotonate on a nanosecond time scale, we assign the spectroscopic signature to $5mdC^{\cdot+}$. This assignment is further supported by DFT calculations. The spectrum of $5mdC^{\cdot+}$ is expected to give valuable information for future investigations of oxidative damage and charge-transfer processes in DNA.

Experimental Section

5-Methyl-2′-deoxycytidine was purchased from Sigma-Aldrich and used without any further purification. All time-resolved measurements were performed in a phosphate buffer D_2O solution (50 mM) to reduce IR background absorption with a solute concentration of 10 mM. This equals an absorbance of approximately 0.6 optical density (OD) at 266 nm in a flow cell with a path length of 100 μm.

The fs/ps time-resolved experimental setup is based on a Ti-sapphire laser-amplifier system (Spitfire Pro, SpectraPhysics) with 100 fs pulses at 800 nm and a repetition rate of 1 kHz. The third harmonic (266 nm) of the laser fundamental was used for excitation. The excitation energy was varied depending on the experiment (0.5 –4 μJ) with a beam diameter at the sample position of 150 μm and a pulse duration of circa 300 fs. The probe light in the mid IR was obtained by a combination of a non-collinear and a collinear optical parametric amplifier and a following difference frequency mixing in a $AgGaS_2$ crystal. The transmitted probe pulse was spectrally dispersed (Brucker, Chromex 250 IS) and detected on a 64 Channel MCT array (Infrared Systems Development, IR-0144). Pump- and probe-pulse polarization were orientated in the magic-angle configuration to avoid molecular rotational diffusion artefacts. For all measurements a flow cell (100 μm, BaF_2) was used, in which the sample volume was exchanged between two consecutive excitation pulses. All experiments were performed at room temperature.

For the ns experiment a setup with the third harmonic of an externally triggered Q-switched Nd:YVO laser (AOT) electronically synchronized to the IR probe pulses was used under the same conditions.

The steady-state experiments in the IR were done with a Fourier transform infrared (FTIR) spectrometer (Model IFS 66, Bruker). UV/Vis spectra were recorded using a PerkinElmer Lambda 750 spectrophotometer.

The reaction products of the two photon ionization were analyzed with UHPLC-ESI-MS/MS. A solution of 5mdC (0.8 mL, 10 mM) was irradiated with fs-laser pulses at 266 nm (2 μJ, beam diameter 150 μm, 300 fs pulse duration) for 6 and 30 min. As reference a non-illuminated sample was analyzed. Aliquots of the samples, which initially contained 100 pmol 5mdC, were spiked with a specific amount of [D_3]-5mdC, [D_2,$^{15}N_2$]-5hmdC and [$^{15}N_2$]-5fdC. The samples were then filtered with 0.45 μm Supor® (Pall Life Sciences). The UHPLC-ESI-MS/MS analysis of the reaction products was performed by an Agilent 1290 UHPLC system and an Agilent 6490 triple quadrupole mass spectrometer with quantitative isotope dilution according to our earlier published method.[19] Briefly, the compounds were separated using a Poroshell 120 SB-C8 column from Agilent (2.7 μm, 2.1 mm × 150 mm) by a gradient using water and MeCN, each containing 0.0075% (v/v) formic acid: 0→5 min; 0→3.5% (v/v) MeCN; 5→6.9 min; 3.5→5% (v/v) MeCN: 6.9→7.2 min; 5→80% (v/v) MeCN: 7.2→10.5 min; 80% (v/v) MeCN: 10.5→11.3 min; 80→0% (v/v) MeCN: 11.3→13 min; 0% MeCN. The column temperature was maintained at 30 °C; the flow rate was 0.35 mL min^{-1}.

The nucleosides were detected in the positive ion selected reaction monitoring mode (SRM). For a more detailed description including source- and compound-dependent parameters (MS/MS transitions) as well as calibration curves see ref. [19].

The DFT calculations were performed with the Gaussian 03 software.[23] Becke3Lyp 6–311G** was used with the PCM solvent model to calculate the theoretical spectra of 5mdC, $5mdC^{\cdot+}$, and $5mdC-H^{\cdot}$. For each harmonic frequency calculation the geometry was optimized. All exchangeable hydrogen atoms were exchanged with deuterium in the molecular structure. The frequency was adjusted with a correction factor of 0.9669.[24]

Acknowledgements

This work was supported by the Deutsche Forschungsgemeinschaft (DFG) through the Sonderforschungsbereich 'Dynamics and Intermediates of Molecular Transformations' (SFB 749, TP A4 and A5), the Clusters of Excellence 'Center for Integrated Protein Science Munich (CIPS^{M})' and the 'Munich-Center for Advanced Photonics' (MAP). T.P. thanks the Fonds der Chemischen Industrie for a pre-doctoral fellowship.

Keywords: 5-methyl-2′-deoxycytidine · DNA damage · DNA oxidation · time-resolved spectroscopy · vibrational spectroscopy

[1] R. Lister, M. Pelizzola, R. H. Dowen, R. D. Hawkins, G. Hon, J. Tonti-Filippini, J. R. Nery, L. Lee, Z. Ye, Q.-M. Ngo, L. Edsall, J. Antosiewicz-Bourget, R. Stewart, V. Ruotti, A. H. Millar, J. A. Thomson, B. Ren, J. R. Ecker, *Nature* **2009**, *462*, 315 – 322.
[2] Z. D. Smith, A. Meissner, *Nat. Rev. Genet.* **2013**, *14*, 204 – 220.
[3] D.-M. Franchini, K.-M. Schmitz, S. K. Petersen-Mahrt, *Annu. Rev. Genet.* **2012**, *46*, 419 – 441.
[4] S. Kriaucionis, N. Heintz, *Science* **2009**, *324*, 929 – 930.
[5] M. Tahiliani, K. P. Koh, Y. Shen, W. A. Pastor, H. Bandukwala, Y. Brudno, S. Agarwal, L. M. Iyer, D. R. Liu, L. Aravind, A. Rao, *Science* **2009**, *324*, 930 – 935.
[6] Y. F. He, B. Z. Li, Z. Li, P. Liu, Y. Wang, Q. Tang, J. Ding, Y. Jia, Z. Chen, L. Li, Y. Sun, X. Li, Q. Dai, C. X. Song, K. Zhang, C. He, G. L. Xu, *Science* **2011**, *333*, 1303 – 1307.
[7] S. Ito, L. Shen, Q. Dai, S. C. Wu, L. B. Collins, J. A. Swenberg, C. He, Y. Zhang, *Science* **2011**, *333*, 1300 – 1303.
[8] T. Pfaffeneder, B. Hackner, M. Truß, M. Münzel, M. Müller, C. A. Deiml, C. Hagemeier, T. Carell, *Angew. Chem.* **2011**, *123*, 7146 – 7150; *Angew. Chem. Int. Ed.* **2011**, *50*, 7008 – 7012.
[9] J. R. Wagner, J. Cadet, *Acc. Chem. Res.* **2010**, *43*, 564 – 571.
[10] C. Bienvenu, J. R. Wagner, J. Cadet, *J. Am. Chem. Soc.* **1996**, *118*, 11406 – 11411.
[11] H. Cao, Y. Wang, *Nucleic Acids Res.* **2007**, *35*, 4833 – 4844.
[12] W. Rideout, G. Coetzee, A. Olumi, P. Jones, *Science* **1990**, *249*, 1288 – 1290.
[13] M. F. Denissenko, J. X. Chen, M.-s. Tang, G. P. Pfeifer, *Proc. Natl. Acad. Sci. USA* **1997**, *94*, 3893 – 3898.
[14] C.-H. Jie Shao, Balaraman Kalyanaraman, Ben-ZhanZhu, *Free Radical Biol. Med.* **2013**, *60*, 177 – 182.
[15] P. M. Keane, M. Wojdyla, G. W. Doorley, G. W. Watson, I. P. Clark, G. M. Greetham, A. W. Parker, M. Towrie, J. M. Kelly, S. J. Quinn, *J. Am. Chem. Soc.* **2011**, *133*, 4212 – 4215.
[16] S. Quinn, G. W. Doorley, G. W. Watson, A. J. Cowan, M. W. George, A. W. Parker, K. L. Ronayne, M. Towrie, J. M. Kelly, *Chem. Commun.* **2007**, 2130 – 2132.
[17] P. M. Hare, C. E. Crespo-Hernández, B. Kohler, *Proc. Natl. Acad. Sci. USA* **2007**, *104*, 435 – 440.
[18] W. J. Schreier, T. E. Schrader, F. O. Koller, P. Gilch, C. E. Crespo-Hernández, V. N. Swaminathan, T. Carell, W. Zinth, B. Kohler, *Science* **2007**, *315*, 625 – 629.
[19] S. Schiesser, T. Pfaffeneder, K. Sadeghian, B. Hackner, B. Steigenberger, A. S. Schröder, J. Steinbacher, G. Kashiwazaki, G. Höfner, K. T. Wanner, C. Ochsenfeld, T. Carell, *J. Am. Chem. Soc.* **2013**, *135*, 14593 – 14599.
[20] M. K. Kuimova, A. J. Cowan, P. Matousek, A. W. Parker, X. Z. Sun, M. Towrie, M. W. George, *Proc. Natl. Acad. Sci. USA* **2006**, *103*, 2150 – 2153.
[21] A. W. Parker, C. Y. Lin, M. W. George, M. Towrie, M. K. Kuimova, *J. Phys. Chem. B* **2010**, *114*, 3660 – 3667.
[22] K. Kobayashi, S. Tagawa, *J. Am. Chem. Soc.* **2003**, *125*, 10213 – 10218.
[23] Gaussian 03 (Revision D.01), M. J. Frisch, G. W. Trucks, H. B. Schlegel, G. E. Scuseria, M. A. Robb, J. R. Cheeseman, J. A. Montgomery, T. V. Jr, K. N. Kudin, J. C. Burant, J. M. Millam, S. S. Iyengar, J. Tomasi, V. Barone, B. Mennucci, M. Cossi, G. Scalmani, N. Rega, G. A. Petersson, H. Nakatsuji, M. Hada, M. Ehara, K. Toyota, R. Fukuda, J. Hasegawa, M. Ishida, T. Nakajima, Y. Honda, O. Kitao, H. Nakai, M. Klene, X. Li, J. E. Knox, H. P. Hratchian, J. B. Cross, V. Bakken, C. Adamo, J. Jaramillo, R. Gomperts, R. E. Stratmann, O. Yazyev, A. J. Austin, R. Cammi, C. Pomelli, J. W. Ochterski, P. Y. Ayala, K. Morokuma, G. A. Voth, P. Salvador, J. J. Dannenberg, V. G. Zakrzewski, S. Dapprich, A. D. Daniels, M. C. Strain, O. Farkas, D. K. Malick, A. D. Rabuck, K. Raghavachari, J. B. Foresman, J. V. Ortiz, Q. Cui, A. G. Baboul, S. Clifford, J. Cioslowski, B. B. Stefanov, G. Liu, A. Liashenko, P. Piskorz, I. Komaromi, R. L. Martin, D. J. Fox, T. Keith, M. A. Al-Laham, C. Y. Peng, A. Nanayakkara, M. Challacombe, P. M. W. Gill, B. Johnson, W. Chen, M. W. Wong, C. Gonzalez, J. A. Pople, Gaussian, Inc., Wallingford CT, **2003**.
[24] K. K. Irikura, R. D. Johnson, R. N. Kacker, *J. Phys. Chem. A* **2005**, *109*, 8430 – 8437.

Received: October 17, 2013
Published online on January 2, 2014

4.2 Base Stacking in DNA Single Strands Causes Delocalized Charge Transfer States After UV-Light Absorption

In the article "Charge separation and charge delocalization identified in long-living states of photoexcited DNA" published in the *Proceedings of the National Academy of Sciences* [265] the highly debated question (section 2.2.1.2) about the nature of the long-living state in stranded DNA could be solved and the underlying photophysical process could be identified.

The results were obtained by a new experimental approach. First, specially designed sequences were used, which enable selective excitation at 295 nm of 5-methyl-2′-deoxycytidine (mC) in DNA single strands. Second, ultrafast infrared spectroscopy was used to probe the system after the defined excitation of mC. Narrow absorbance bands of the nucleobases in the IR allowed not only to monitor the decay of the originally excited mC but also to detect processes occurring on adjacent bases. With this new approach three main questions could be answered:

1. The long-living state in photoexcited single-stranded DNA is caused by the interaction of stacked nucleobases. Its population depends on the stacking probabilities of the involved bases and reaches up to 40%. Unstacked bases decay via the ultrafast deactivation mechanism, known from single nucleotides.

2. The long-living state could be identified by investigating dinucleotides. Both bases of the dinucleotides are involved in the long-living state and the transient IR-spectrum shows characteristic IR-marker bands. These coincide with experimentally determined absorbance bands of radical cations (mC, previous chapter 4.1, [261] and G [266, 267]). Additional marker bands could be assigned to radical anions of nucleobases, which were simulated with density functional theory. The occurrence of these species shows directly that the long-living state is a charge separated state between neighboring bases. The direction of the charge transfer is governed by the redox potential of the involved nucleobases and is consequently strongly sequence dependent.

3. The charge separation is not only localized on two bases. In longer oligonucleotides a charge transfer over 3-4 bases has been detected. Interestingly, all of these 3-4 bases are involved in the charge transfer process which directly shows that the charges are delocalized along the strand in stacked domains.

The presence of radical cations and anions in DNA after photoexcitation indicates that UV-light can presumably trigger chemical reactions, which have not been considered in DNA photochemistry so far. These experiments have not only identified one major decay channel of photoexcited DNA but they will also have an important impact for the DNA charge transport community. These data demonstrate – for the first time to our knowledge – that charges in DNA are delocalized, which has been proposed, but has not directly been observed. In addition, this publication unifies the research fields of DNA photochemistry and DNA charge transport.

Charge separation and charge delocalization identified in long-living states of photoexcited DNA

Dominik B. Bucher[a,b], Bert M. Pilles[a], Thomas Carell[b,1], and Wolfgang Zinth[a,1]

[a]BioMolecular Optics and Center for Integrated Protein Science, Ludwig-Maximilians-Universität München, 80538 Munich, Germany; and [b]Center for Integrated Protein Science, Department of Chemistry, Ludwig-Maximilians-Universität München, 81377 Munich, Germany

Edited by Mark Ratner, Northwestern University, Evanston, IL, and approved February 19, 2014 (received for review December 20, 2013)

Base stacking in DNA is related to long-living excited states whose molecular nature is still under debate. To elucidate the molecular background we study well-defined oligonucleotides with natural bases, which allow selective UV excitation of one single base in the strand. IR probing in the picosecond regime enables us to dissect the contribution of different single bases to the excited state. All investigated oligonucleotides show long-living states on the 100-ps time scale, which are not observable in a mixture of single bases. The fraction of these states is well correlated with the stacking probabilities and reaches values up to 0.4. The long-living states show characteristic absorbance bands that can be assigned to charge-transfer states by comparing them to marker bands of radical cation and anion spectra. The charge separation is directed by the redox potential of the involved bases and thus controlled by the sequence. The spatial dimension of this charge separation was investigated in longer oligonucleotides, where bridging sequences separate the excited base from a sensor base with a characteristic marker band. After excitation we observe a bleach of all involved bases. The contribution of the sensor base is observable even if the bridge is composed of several bases. This result can be explained by a charge delocalization along a well-stacked domain in the strand. The presence of charged radicals in DNA strands after light absorption may cause reactions—oxidative or reductive damage—currently not considered in DNA photochemistry.

DNA photophysics | DNA damage | DNA electron transfer | ultrafast vibrational spectroscopy

DNA photophysics is crucial for the understanding of light-induced damage of the genetic code (1). The excited state of single DNA bases is known to decay extremely fast on the sub-picosecond time scale, predominantly via internal conversion (2, 3). This ultrafast decay is assumed to suppress destructive decay channels, thereby protecting the DNA from photodamage and avoiding disintegration of the genetic information. In contrast to this ultrafast deactivation of single nucleobases, the biological relevant DNA strands show further long-living states (4, 5). Several explanations for these long-living states and the size of their spatial extent have been discussed in the literature (5–9). Delocalized excitons (9); excitons that decay to charge-separated states or neutral excimer states (10, 11); exciplexes located on two neighboring bases (5, 8, 12, 13); or even excited single bases, where steric interactions in the DNA strand impedes the ultrafast decay (14), have been proposed. Further computations suggest a decay of an initially populated delocalized exciton to localized neutral or charged excimer states (15–17). However, to our knowledge, a final understanding of the nature of these long-living states has not been reached. Related experiments were performed in the last decade to investigate charge transport processes in DNA, motivated by DNA electronics and oxidative damage (18, 19). Charge transport was initiated by photoexcitation of modified DNA bases or chromophores and followed by transient absorption (20–23). The transport mechanism was described by charge-hopping, superexchange, or transfer of charge along delocalized domains in DNA (18).

Until now, most experimental investigations of the long-living state were performed with transient absorption spectroscopy in the UV-visible (UV/Vis) regime (5, 9, 12) or with time-resolved fluorescence (10, 24, 25). Due to the broad, featureless, and overlapping absorption bands of the different DNA bases in this spectral region, it is difficult to investigate the molecular origin of the long-living states using these methods. A further drawback is the unselective and simultaneous excitation of several bases used in most experiments. To circumvent these problems, we used for the present study well-defined oligonucleotides, which enable selective excitation of one single base. Observation of the long-living excited states was performed via time-resolved IR spectroscopy, which can profit from the many "fingerprint" vibrational bands (26, 27). IR spectroscopy is able to distinguish between different DNA bases and their molecular states. It can also reveal changes in the electronic structure and identify charge-separated states.

In this study we used single-stranded DNA, in which π stacking between neighboring bases leads to structured domains, similar to the structure in a double helix (28). This interaction is known to be crucial for the long-living states (5). The investigation of single-stranded DNA enables us to construct special sequences, where only one base can be selectively excited. We used the natural bases 2′-deoxyuridine (U), 2′-deoxyadenosine (A), 5-methyl-2′-deoxycytidine (mC), and 2′-deoxyguanosine (G). The nucleobase U occurs naturally in RNA and is similar to the DNA base thymine but shows a blue-shifted absorbance spectrum. mC occurs with a frequency of 4–5% in mammalian DNA (29) and plays an important role as an epigenetic marker (30). The UV/Vis absorbance of mC and G are red-shifted in comparison with A and U, which allows selective excitation at 295 nm in oligonucleotides

Significance

The high photostability of single nucleobases is related to the rapid disposal of the UV excitation energy from high-lying electronic states into heat, preventing damaging reactions. However, in the biological important DNA strands, further long-living excited states are found. With femtosecond vibrational spectroscopy, these excited states in DNA are now identified as charge-separated states, which are delocalized along the strand. The charge separation is directed by the redox potential of the involved bases and is thus encoded in the DNA sequence. The presence of delocalized charged species in DNA strands for a considerably long time after UV light absorption may lead to reactions—oxidative or reductive damage—currently not considered in DNA photochemistry.

Author contributions: D.B.B. and W.Z. designed research; D.B.B. and B.M.P. performed research; D.B.B., T.C., and W.Z. analyzed data; and D.B.B., T.C., and W.Z. wrote the paper.

The authors declare no conflict of interest.

This article is a PNAS Direct Submission.

[1]To whom correspondence may be addressed. E-mail: wolfgang.zinth@physik.uni-muenchen.de or thomas.carell@cup.uni-muenchen.de.

This article contains supporting information online at www.pnas.org/lookup/suppl/doi:10.1073/pnas.1323700111/-/DCSupplemental.

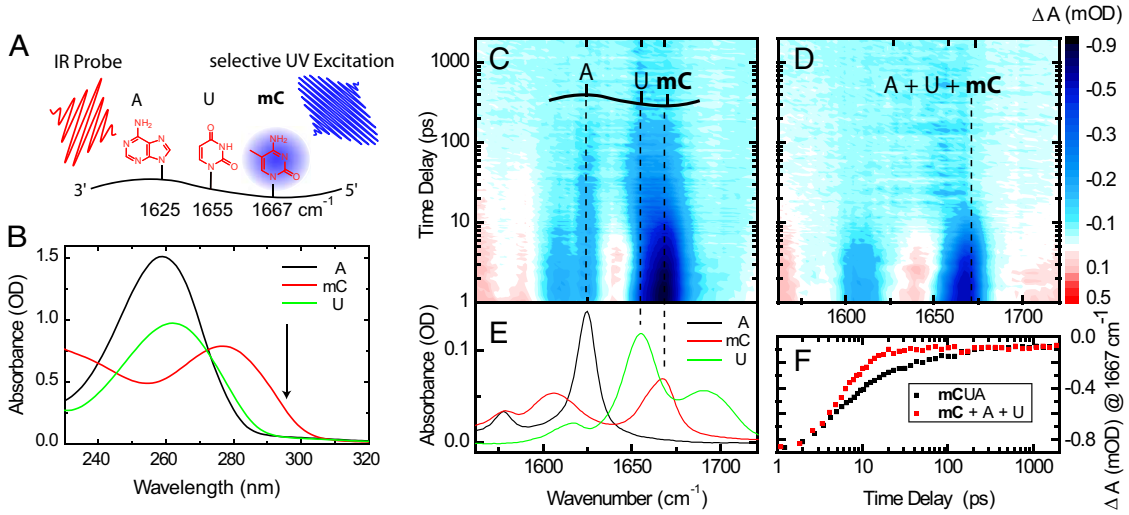

Fig. 1. Selective excitation of mC in mCUA and probing of characteristic A, U, and mC marker bands in the IR. (*A*, *B*, and *E*) Picosecond UV light pulses at 295 nm allow selective excitation of mC (shown in bold) in mixed DNA sequences consisting of mC, U, and A. (*B*) Absorbance spectra of 2′-deoxyadenosine monophosphate (A), 2′-deoxy-5-methylcytidine (mC), and uridine monophosphate (U). (*C*) Time-resolved absorption difference (color-coded) plotted vs. wavenumber and delay time for mCUA and (*D*) for a mixture of the corresponding monomers. (*E*) Probing the individual contribution of each base is possible in the IR at 1,625 cm^{-1} (A), 1,655 cm^{-1} (U), and 1,667 cm^{-1} (mC) (marked by dashed lines). (*F*) Transients at 1,667 cm^{-1} for mCUA and the mixture of monomers.

consisting of mC, A, and U (Fig. 1 *A* and *B*) or G and A. This selectivity can only be obtained in single-stranded DNA because G and its complementary base mC have overlapping absorbance bands in the UV range (Fig. S1). Selectivity in probing is based on the significant differences in the IR-absorption spectra of these bases, which display distinct marker bands for each base (Fig. 1 *A* and *E*).

With the combination of selective excitation and selective probing we are able to elucidate the nature of the long-living states in DNA strands. Investigation of dinucleotides clearly shows that light absorption in DNA leads to charge separation between stacked neighboring bases, which recombine on the 100-ps time scale. In longer oligonucleotides we observe simultaneous bleach of several bases, which points to a delocalization of the charges along the strand. Our results show that charge transfer in DNA is a natural process, induced by UV-light absorption of DNA.

Results and Discussion

In a first example, the trimer mCUA is used to demonstrate the feasibility of the approach. In Fig. 1*C*, the evolution of the absorption transients in the IR is plotted vs. wavenumber and delay time between UV excitation and IR probing pulses. After selective excitation of mC with light at 295 nm, two processes are evident: an ultrafast decay within 10 ps and a much slower process on the 100-ps time scale. The fast process can be assigned to the decay of the excited electronic state (S_1) of mC (31) with concomitant vibrational cooling of the molecule. These fast dynamics resemble those found in a reference measurement of a solution containing the monomers mC, A, and U (Fig. 1 *D* and *F*). In this solution, slower transients are not observed. The slower process is only found in the trimeric sample; its absorption change clearly shows contributions of all three bases, although only the mC has initially been excited. Apparently, the slow component is the consequence of the connection of the bases in the trinucleotide. The time constant in the 100-ps range agrees well with the dynamics found in previous investigations with UV probing (5).

A global fit (*Materials and Methods*) confirms the qualitative view given above. The ultrafast decay of the excited electronic state and the vibrational cooling are represented by the two fast components with time constants in the one picosecond (τ_0) and 5- to 10-ps range (τ_1). Only in the oligonucleotide an additional kinetic process in the 100-ps range ($\tau_2 = 90$ ps) is evident. The decay-associated difference spectrum $D_2(\nu)$ related to τ_2 contains the spectral information on the long-living species; it gives an insight into the molecular nature of the state (see below) and allows us to estimate the fraction F_2 of molecules involved.

Amplitude of the Long-Living State. The fraction F_2 of the long-lived state is shown in Fig. 2 for different DNA oligomers. Values of F_2 from 0.23 to over 0.4 have been found (Table 1). These large numbers show that the long-lived states may play a significant role in the photochemical reactions of DNA oligomers. In detail, the fraction F_2 depends on the specific sequence of the compound. Longer oligonucleotides show larger values of F_2 than shorter ones. Adenine in direct neighborhood of the excited mC results in a higher population of the long-living state in comparison with U

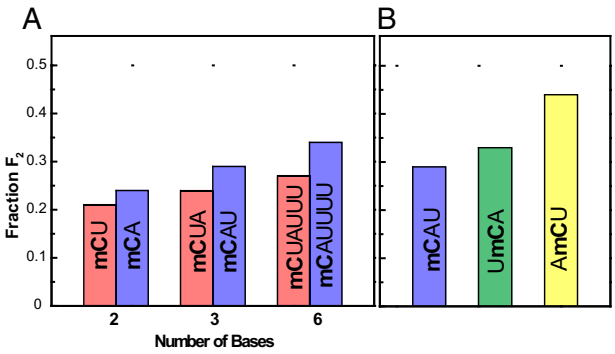

Fig. 2. Comparison of the fraction of the long-living state in different oligonucleotides. Fraction F_2 of molecules involved in the long-living state for different oligonucleotides (mC is excited, shown in bold). The values F_2 are obtained from two independent experiments, which show the same trend. (*A*) Dependency on the type of the base neighboring to the excited mC and on the length of the oligonucleotides. (*B*) Dependency on the sequence of trinucleotides.

Table 1. Fitting parameters and fraction F_2 of the long-living state

Oligonucleotide	τ_0/ps	τ_1/ps	τ_2/ps	Fraction F_2
mC + A + U	1.2	5		
mCA	1.3	6	110	0.25
mCU	1.2	6	50	0.23
mCG	1.5	3	20	
GA	1.7	3	300	
mCAU	0.7	6	120	0.29
mCUA	1.1	6	90	0.24
A**mC**U	1.4	10	150	0.45
U**mC**A	0.7	8	110	0.32
mCAUUUU	1.3	6	170	0.34
mCUAUUU	1.4	8	120	0.27
mCUUAUU	1.6	5	110	0.32
mCUUUAU	2.0	5	90	0.30
mCUUUUA	1.7	6	100	0.28
mCUUUU	1.3	6	80	0.24

All experiments were measured in two independent experiments; time constants are an average of both experiments. Selective excited base is shown in bold. For samples with selective excitation of mC, the fraction F_2 was calculated. The trend of F_2 is reproduced in the two independent experiments.

(Fig. 2*A*). Even inverting the sequence has a major influence: adenine at the 5′ end shows a much higher fraction F_2 than at the 3′ end (Fig. 2*B*). These observations are in line with the assumption that base stacking is the prerequisite for the appearance of the long-living component. Indeed, Kohler and coworkers (12) have shown for dinucleotides that the amplitude of the long-living state detected in UV experiments correlates well with stacking properties. In addition, CD spectroscopy (32) shows that the order of the stacking probability α of dinucleotides follows the trend $\alpha_{CU} < \alpha_{CA} < \alpha_{AC}$, which correlates exactly with the order of F_2 in our study. Furthermore, the stacking probability is rising with the increasing length (8) of the DNA strand, which is also observed in our data. Apparently, the long-living state is only formed between stacked bases, whereas unstacked bases show the reported ultrafast deactivation known from single bases.

Characterization of Marker Bands. From different simple dinucleotides we obtain detailed information on the molecular properties of the long-living state via the individual decay spectra $D_2(\nu)$ (Fig. 3*B*). Negative bands in these spectra represent the decrease of the original absorption of the bases involved in the long-living state; they compare well with the stationary absorption spectra of the corresponding dimers (dashed lines) and show that both bases of the dimer contribute to $D_2(\nu)$. Positive features reflect newly formed absorption bands of the long-living state. For a possible interpretation of the nature of these states we present in Fig. 3*A* experimental difference spectra of G and its radical cation $G^{\bullet+}$ (33, 34) as well as mC and its radical cation $mC^{\bullet+}$ (35). Both spectra were obtained by two photon ionization of the bases (for details, see *Materials and Methods*) and show characteristic marker bands (Fig. 3*A*). $A^{\bullet+}$ does not possess any characteristic absorbance band in this spectral region. The $G^{\bullet+}$ marker bands at 1,608 cm^{-1} and 1,704 cm^{-1} are well recognized in the decay spectra of GA and mCG. The marker bands of the $mC^{\bullet+}$ at 1,586 cm^{-1} and 1,692 cm^{-1} occur only in the long-living state of mCU and are absent in the decay spectra of mCA and mCG.

Anion radical spectra of the involved bases were calculated with density functional theory. Clear marker bands are found for the $mC^{\bullet-}$ and $U^{\bullet-}$; they are shown in Fig. 3*C* with their distinct positive marker bands in the investigated IR range (for additional information and calculated spectra of all cations and anions, see Fig. S2). A comparison of the anion radical marker bands with the positive bands of the long-lived components (Fig. 3*B*) shows that $mC^{\bullet-}$ is formed in the mCG and mCA dinucleotide, whereas the radical anion $U^{\bullet-}$ can be detected in the mCU dinucleotide. Combining the results of the anion and cation radical marker bands leads to the conclusion that the ion pairs $G^{\bullet+}A^{\bullet-}$, $mC^{\bullet}G^{\bullet+}$, $mC^{\bullet+}U^{\bullet-}$, and $mC^{\bullet}A^{\bullet+}$ are present after excitation of the respective dimer. These experimental results are exactly in accordance with the direction of charge separation imposed by the redox potential (36, 37) of the involved DNA bases (Fig. 3*D*). We can conclude that the charge separation is directed by the redox potential, i.e., the positive charge moves toward the molecule with the lower oxidation potential. The subsequent decay of the long-lived charge separated states occurs on the 100-ps (20–300 ps) time scale by charge recombination to the ground state.

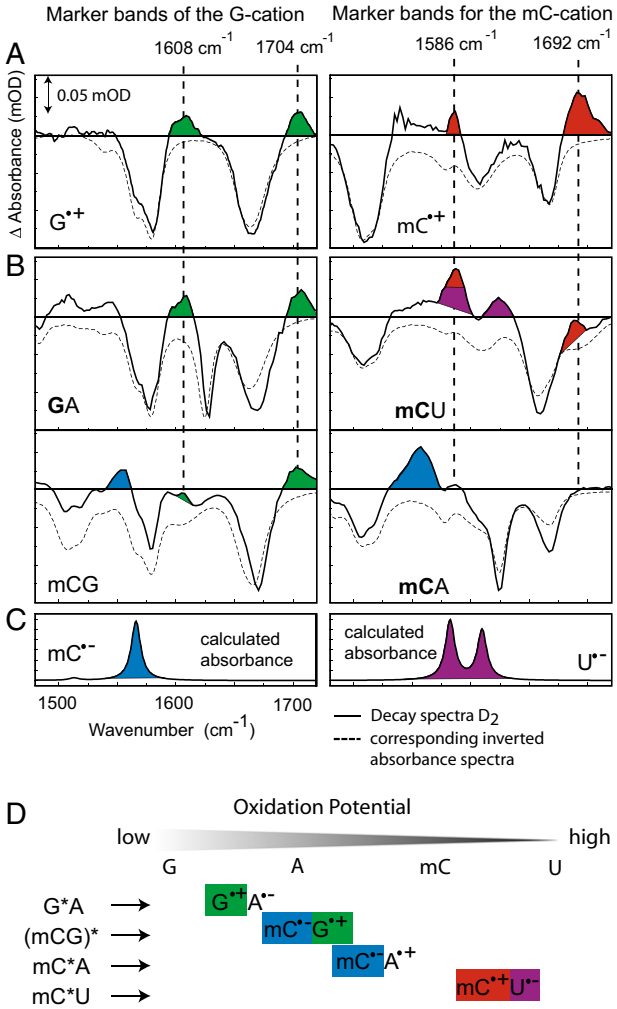

Fig. 3. Identification of cation and anion marker bands in the decay spectra of different dinucleotides. (*A*) Two-photon ionization of G and mC yields the difference spectra of G/$G^{\bullet+}$ and mC/$mC^{\bullet+}$ with the characteristic positive marker bands at 1,608 cm^{-1}, 1,704 cm^{-1} and 1,586 cm^{-1}, 1,692 cm^{-1} for the radical cationic form. The corresponding inverted absorption spectra of the dinucleotides are overlaid (dashed lines). (*B*) Decay spectra $D_2(\nu)$ of **GA**, mCG, **mC**U, and **mC**A [selectively excited base in bold (295 nm), mCG was unselectively excited at 266 nm]. The marker bands are highlighted in color. The position of cation marker bands in the decay spectra is marked by dashed lines. (*C*) $mC^{\bullet-}$ and $U^{\bullet-}$ absorption spectra calculated with density functional theory. (*D*) Oxidation potential of G, A, mC, and U and resulting charge-transfer states of the different dimeric samples. The species assigned in the decay spectra are highlighted by the appropriate color.

Spatial Extension. With longer oligomers we address the question about the spatial extension of the charge transfer. In the trinucleotide mCUA we observe a bleach of all three bases, although mC was solely excited (Fig. 1*C*); this can only be explained by charge migration or delocalization. To obtain further information about this process, longer oligonucleotides of the type $mCU_aAU_{(4-a)}$ with a = 0–4, were investigated (Fig. 4*A*). In this case, mC is excited exclusively and the bleach of the band at 1,625 cm^{-1} (ground state of A) is used to show the participation of A in the charge-separated state. This bleach decreases with the increasing number of U molecules between mC and approaches a constant value for a ≥3. This offset bleach may be assigned to a long-distance charge separation. However, we cannot exclude a small shift of the absorbance band of A upon stacking, which might also lead to the offset signal via direct excitation. In any case, the pronounced bleach after mC excitation, directly observable up to a = 2, reveals that charge separation occurs over a distance of more than 10 Å.

The time dependencies of the bleach at 1,625 cm^{-1}, i.e., the transients at the position of the A band, are shown in Fig. 4*B* for the longer oligomers. The decay of the first excited electronic state (S_1), accompanied by vibrational cooling of the hot ground state, dominates the signal during the first 5 ps. The decay of the charge-transfer state is observable after 5 ps. The normalized transient absorbance at 1,625 cm^{-1} (A) shows the same time dependence for all samples independent of the mC–A distance. In all cases, the absorption features due to the charge-separated state are formed within the first 5 ps. Thus, charge-hopping, which is known to occur on a much longer time scale of 10–100 ps (38, 39), cannot explain the results. In all $mCU_aAU_{(4-a)}$ oligonucleotides, we observe not only the mC and A bleach but also a very strong bleach of the bridging base U. As a consequence, the base U must be involved in the long-living state and a direct tunneling from the excited mC to the A base can be ruled out as the exclusive reaction mechanism. The bleach of all involved bases can only be explained by a charge delocalization over several bases. Such a behavior has been proposed in the literature, but a direct experimental evidence has been missing (40, 41).

The decrease of the bleach signal of A with increasing distance can be modeled using a heterogeneous ensemble of oligomers with stacked and unstacked bases in the strands. Assuming a fixed probability α for the stacking of two neighboring bases, the probability of longer stacked parts rapidly decreases with increasing length. For α = 0.5, the occurrence of longer stacked strands is shown in Fig. 4*C*, red dots. In a model with delocalization of the charges over the stacked parts the bleach of A should reflect the probability of the corresponding stacked parts. Indeed, the integrated bleach signal of the A band at 1,625 cm^{-1} (black triangles) closely follows the behavior expected from stacking; it also shows that the observation of charge delocalization is limited due to the small occurrence of longer stacked domains.

The spectra of Fig. 4*A* display different marker bands of the involved anions and cations. Though it is straightforward to deduce the charge distribution for dinucleotides, the stacking heterogeneity in the longer oligonucleotides prevents a quantitative analysis. Because the experiment averages over the differently stacked subensembles, a ready disentanglement of the heterogeneity with a defined assignment of charge distributions is not possible; this is further complicated by the larger number of involved bases, which leads to an increased overlap of the bands.

Conclusion

Selective UV excitation of DNA multimers combined with femtosecond IR probing has been used to obtain interesting information on the nature of long-living electronic states in DNA strands (Fig. 5). Excitation of unstacked DNA bases by UV light is followed by ultrafast deactivation via internal conversion, which is known to be the dominating deactivation mechanism for single bases in solution. However, DNA single strands contain a considerable amount of

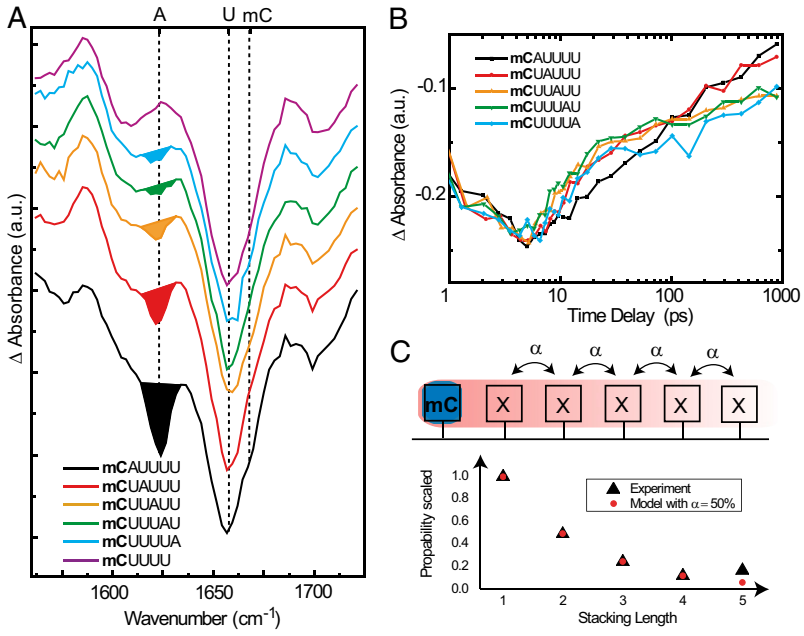

Fig. 4. Distance dependency of the A bleach in $mCU_aAU_{(4-a)}$ oligonucleotides. (*A*) Normalized decay spectra $D_2(\nu)$ of the oligomers $mCU_aAU_{(4-a)}$, (a = 0–4). mC is selectively excited at 295 nm in all cases. Bleach of ground-state absorbance band of A at 1,625 cm^{-1} is highlighted by the colored area. A, mC, and U absorbance bands are marked with dashed lines. (*B*) Scaled transient absorbance at 1,625 cm^{-1} for the $mCU_aAU_{(4-a)}$ oligonucleotides. (*C*) Simple stacking model. The stacking-length probability can be calculated by assuming a noncooperative stacking probability α of 50% (red dots), which reproduces well the experimental bleach signal of A (integrated bleach signal, black triangles).

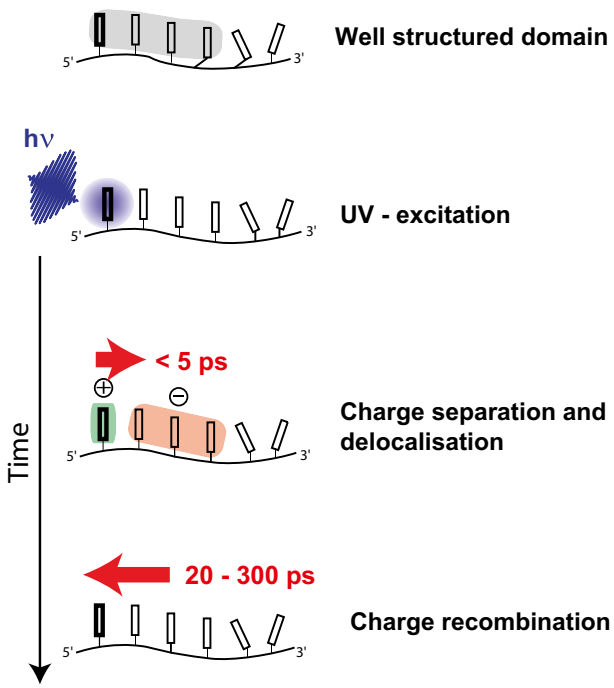

Fig. 5. Reaction model for light absorption in DNA. Model for photoexcitation of DNA: DNA bases are arranged in domains with well-orientated stacked bases (gray background). If a base absorbs light in this domain (in this case the first base), charge separation occurs during the first 5 ps. The direction of charge transfer depends on the redox potential of the involved bases and is delocalized in the domain. Only one possible charge distribution is shown. Charge recombination occurs within 20–300 ps, depending on the sequence.

well-stacked domains. Within a few picoseconds, the excitation of these bases leads to a long-living charge-separated state formed with high probability. This efficient charge transfer requires stacked bases, and the direction of the charge movement is governed by the oxidation potentials and thus by the base sequence. The charges are delocalized in the stacked domains. These long-living ionic states decay by charge recombination to the neutral ground-state on the 100-ps time scale. The mechanism is related to the charge transport observed in DNA double strands after excitation of modified bases (18). However, the present investigation reveals that charge transfer in DNA oligonucleotides is a natural process, occurring to a high probability after absorption of UV light.

The presence of charges along a DNA strand may have severe consequences for the integrity of a DNA strand, because charged base radicals form starting points for oxidative (42) and reductive (43) DNA damage. Thus, the presented observation of charged states with relatively long lifetime adds an important element to the discussion of DNA photolesions and mutational hot spots (44).

Materials and Methods

Oligodeoxyribonucleotides. All oligonucleotides were purchased from Metabion AG. The lyophilized samples were dissolved in 50 mM phosphate buffer in D_2O. The final concentration was ~3–6 mM, depending on the solubility of the sample. The corresponding absorbance in the time-resolved experiments was 0.1–0.2 OD at 295 nm in a cuvette with 100-μm path length.

Femtosecond UV-Pump IR-Probe Measurements. All time-resolved measurements are based on a Ti:Sapphire laser amplifier system (Spitfire Pro; Spectra-Physics) with 100-fs pulses at 800 nm and a repetition rate of 1 kHz. The pump pulses at 295 nm were generated with a frequency-doubled two-stage noncollinear optical parametric amplifier (45). The excitation energy was ~800 nJ with a beam diameter at the sample position of 150 μm.

The mid-IR probe light was generated by a combination of a noncollinear and a collinear optical parametric amplifier and subsequent difference frequency mixing in a $AgGaS_2$ crystal. The transmitted IR pulse was spectrally dispersed (Chromex 250IS; Bruker) and detected on a 64-channel MCT array (IR-0144; Infrared Systems Development). All experiments were performed at room temperature and under magic-angle conditions. The excited sample volume was exchanged between consecutive excitation pulses via a BaF_2 flow cuvette.

Data Handling. The data are collected as an array of absorption changes for different probing frequencies ν and delay times t_D. The absorption changes $\Delta A(\nu, t_D)$ of all investigated oligonucleotides were globally fitted for delay times >1 ps with three exponentials and a constant offset representing long-lasting absorption changes from irreversible processes or triplet states.

$$\Delta A(\nu,t_D) = \sum_{i=0}^{2} D_i(\nu)\cdot \exp\left(-\frac{t_D}{\tau_i}\right) + D_3(\nu)$$

For each exponential component, amplitude spectra $D_i(\nu)$ are determined in the fit, which represent the absorption changes related with this process [decay-associated difference spectra (DADS)]. The time constants determined by the fitting procedure are given in Table 1. For the mixture of single bases (Fig. 1), two exponentials were sufficient to model the data. For the oligonucleotides, three time constants are required. The DADS $D_2(\nu)$ related to the time constant τ_2 in the 20- to 300-ps range contains the information on the charge-separated long-living states. For all oligonucleotides with selective excitation via mC we estimated the fraction F_2 of the molecules in the long-living state by dividing the fitting amplitude D_2 by the initial bleach signal at $t_D = 1$ ps (representing the amount of excited molecules) at the position of the mC absorption band at 1,667 cm^{-1}.

Radical Cation Spectra. The cation difference spectra were obtained by exciting solutions of mC and G at 266 nm with a pulse energy of 2–4 μJ (pulse length 300 fs). This excitation leads to ionization of the base, which is stable in both cases in the observed time window (1 ns). The decay spectra D_∞ yields the difference spectra used in Fig. 3*A*. The G cation difference spectrum has been published previously (33, 34). The ionization conditions and the characterization of the mC cation are in ref. 35.

Stationary Spectroscopy. FTIR measurements were performed with a Bruker IFS 66 FT spectrophotometer in 100-μm CaF_2 cuvettes. The UV/Vis spectra were recorded with a PerkinElmer spectrophotometer (Lambda 750).

Density Functional Theory Calculations. Becke3Lyp 6-311-G** functional with the solvent model PCM was used to calculate the harmonic vibrational frequencies with the Gaussian 03 software (46). For simplicity, all calculations were done for the 1-methyl-substituted nucleobases where all exchangeable hydrogen atoms in the structure were substituted with deuterium. Each vibrational frequency analysis was preceded by a geometry optimization. The frequencies were scaled with a factor of 0.9669 (47).

ACKNOWLEDGMENTS. This work was supported by the Deutsche Forschungsgemeinschaft through the Sonderforschungsbereich Dynamics and Intermediates of Molecular Transformations SFB 749, the Clusters of Excellence Center for Integrated Protein Science Munich, and Munich-Centre for Advanced Photonics.

1. Taylor JS (1994) Unraveling the molecular pathway from sunlight to skin cancer. *Acc Chem Res* 27(3):76–82.
2. Crespo-Hernández CE, Cohen B, Hare PM, Kohler B (2004) Ultrafast excited-state dynamics in nucleic acids. *Chem Rev* 104(4):1977–2019.
3. Pecourt J-ML, Peon J, Kohler B (2001) DNA excited-state dynamics: Ultrafast internal conversion and vibrational cooling in a series of nucleosides. *J Am Chem Soc* 123(42):10370–10378.
4. Middleton CT, et al. (2009) DNA excited-state dynamics: From single bases to the double helix. *Annu Rev Phys Chem* 60(1):217–239.
5. Crespo-Hernández CE, Cohen B, Kohler B (2005) Base stacking controls excited-state dynamics in A.T DNA. *Nature* 436(7054):1141–1144.
6. Kohler B (2010) Nonradiative decay mechanisms in DNA model systems. *J Phys Chem Lett* 1(13):2047–2053.
7. Markovitsi D, et al. (2006) Molecular spectroscopy: Complexity of excited-state dynamics in DNA. *Nature* 441(7094):E7, discussion E8.
8. Su C, Middleton CT, Kohler B (2012) Base-stacking disorder and excited-state dynamics in single-stranded adenine homo-oligonucleotides. *J Phys Chem B* 116(34):10266–10274.

9. Buchvarov I, Wang Q, Raytchev M, Trifonov A, Fiebig T (2007) Electronic energy delocalization and dissipation in single- and double-stranded DNA. *Proc Natl Acad Sci USA* 104(12):4794–4797.
10. Vayá I, Gustavsson T, Douki T, Berlin Y, Markovitsi D (2012) Electronic excitation energy transfer between nucleobases of natural DNA. *J Am Chem Soc* 134(28): 11366–11368.
11. Banyasz A, et al. (2013) Multi-pathway excited state relaxation of adenine oligomers in aqueous solution: A joint theoretical and experimental study. *Chemistry* 19(11): 3762–3774.
12. Takaya T, Su C, de La Harpe K, Crespo-Hernández CE, Kohler B (2008) UV excitation of single DNA and RNA strands produces high yields of exciplex states between two stacked bases. *Proc Natl Acad Sci USA* 105(30):10285–10290.
13. Doorley GW, et al. (2013) Tracking DNA excited states by picosecond-time-resolved infrared spectroscopy: Signature band for a charge-transfer excited state in stacked adenine-thymine systems. *J Phys Chem Lett* 4(16):2739–2744.
14. Conti I, Altoè P, Stenta M, Garavelli M, Orlandi G (2010) Adenine deactivation in DNA resolved at the CASPT2//CASSCF/ AMBER level. *Phys Chem Chem Phys* 12(19): 5016–5023.
15. Improta R, Barone V (2011) Interplay between neutral and charge-transfer- excimers rules the excited state decay in adenine-rich polynucleotides. *Angew Chem Int Ed Engl* 50(50):12016–12019.
16. Santoro F, Barone V, Improta R (2007) Influence of base stacking on excited-state behavior of polyadenine in water, based on time-dependent density functional calculations. *Proc Natl Acad Sci USA* 104(24):9931–9936.
17. Olaso-González G, Merchán M, Serrano-Andrés L (2009) The role of adenine excimers in the photophysics of oligonucleotides. *J Am Chem Soc* 131(12):4368–4377.
18. Genereux JC, Barton JK (2010) Mechanisms for DNA charge transport. *Chem Rev* 110(3):1642–1662.
19. Hall DB, Holmlin RE, Barton JK (1996) Oxidative DNA damage through long-range electron transfer. *Nature* 382(6593):731–735.
20. Wan C, et al. (1999) Femtosecond dynamics of DNA-mediated electron transfer. *Proc Natl Acad Sci USA* 96(11):6014–6019.
21. Wan C, Fiebig T, Schiemann O, Barton JK, Zewail AH (2000) Femtosecond direct observation of charge transfer between bases in DNA. *Proc Natl Acad Sci USA* 97(26): 14052–14055.
22. Lewis FD, et al. (2000) Direct measurement of hole transport dynamics in DNA. *Nature* 406(6791):51–53.
23. O'Neill MA, Becker H-C, Wan C, Barton JK, Zewail AH (2003) Ultrafast dynamics in DNA-mediated electron transfer: Base gating and the role of temperature. *Angew Chem Int Ed Engl* 42(47):5896–5900.
24. Markovitsi D, Gustavsson T, Vayá I (2010) Fluorescence of DNA duplexes: From model helices to natural DNA. *J Phys Chem Lett* 1(22):3271–3276.
25. Schwalb NK, Temps F (2008) Base sequence and higher-order structure induce the complex excited-state dynamics in DNA. *Science* 322(5899):243–245.
26. Schreier WJ, et al. (2007) Thymine dimerization in DNA is an ultrafast photoreaction. *Science* 315(5812):625–629.
27. Harpe KD (2011) Femtosecond UV and infrared time-resolved spectroscopy of DNA: From well-ordered sequences to genomic DNA. PhD dissertation (The Ohio State University, Columbus, Ohio).
28. Saenger W (1984) *Principles of Nucleic Acid Structure* (Springer, Berlin).
29. Lister R, et al. (2009) Human DNA methylomes at base resolution show widespread epigenomic differences. *Nature* 462(7271):315–322.
30. Smith ZD, Meissner A (2013) DNA methylation: Roles in mammalian development. *Nat Rev Genet* 14(3):204–220.
31. Malone RJ, Miller AM, Kohler B (2003) Singlet excited-state lifetimes of cytosine derivatives measured by femtosecond transient absorption. *Photochem Photobiol* 77(2): 158–164.
32. Brahms J, Maurizot JC, Michelson AM (1967) Conformational stability of dinucleotides in solution. *J Mol Biol* 25(3):481–495.
33. Kuimova MK, et al. (2006) Monitoring the direct and indirect damage of DNA bases and polynucleotides by using time-resolved infrared spectroscopy. *Proc Natl Acad Sci USA* 103(7):2150–2153.
34. Parker AW, Lin CY, George MW, Towrie M, Kuimova MK (2010) Infrared characterization of the guanine radical cation: Finger printing DNA damage. *J Phys Chem B* 114(10):3660–3667.
35. Bucher DB, Pilles BM, Pfaffeneder T, Carell T, Zinth W (2014) Fingerprinting DNA oxidation process: IR characterization of the 5-methyl-2′-deoxycytidine radical cation. *ChemPhysChem* 15(3):420–423.
36. Seidel CAM, Schulz A, Sauer MHM (1996) Nucleobase-specific quenching of fluorescent dyes. 1. Nucleobase one-electron redox potentials and their correlation with static and dynamic quenching efficiencies. *J Phys Chem* 100(13):5541–5553.
37. Paukku Y, Hill G (2011) Theoretical determination of one-electron redox potentials for DNA bases, base pairs, and stacks. *J Phys Chem A* 115(18):4804–4810.
38. Park MJ, Fujitsuka M, Kawai K, Majima T (2011) Direct measurement of the dynamics of excess electron transfer through consecutive thymine sequence in DNA. *J Am Chem Soc* 133(39):15320–15323.
39. Takada T, et al. (2004) Charge separation in DNA via consecutive adenine hopping. *J Am Chem Soc* 126(4):1125–1129.
40. Shao F, Augustyn K, Barton JK (2005) Sequence dependence of charge transport through DNA domains. *J Am Chem Soc* 127(49):17445–17452.
41. Renaud N, Berlin YA, Ratner MA (2013) Impact of a single base pair substitution on the charge transfer rate along short DNA hairpins. *Proc Natl Acad Sci USA* 110(37): 14867–14871.
42. Kanvah S, et al. (2010) Oxidation of DNA: Damage to nucleobases. *Acc Chem Res* 43(2):280–287.
43. Wang C-R, Nguyen J, Lu Q-B (2009) Bond breaks of nucleotides by dissociative electron transfer of nonequilibrium prehydrated electrons: A new molecular mechanism for reductive DNA damage. *J Am Chem Soc* 131(32):11320–11322.
44. You Y-H, Szabó PE, Pfeifer GP (2000) Cyclobutane pyrimidine dimers form preferentially at the major p53 mutational hotspot in UVB-induced mouse skin tumors. *Carcinogenesis* 21(11):2113–2117.
45. Riedle E, et al. (2000) Generation of 10 to 50 fs pulses tunable through all of the visible and the NIR. *Appl Phys B* 71(3):457–465.
46. Frisch MJ, et al. (2004) *Gaussian 03*. Revision D.01 (Gaussian, Inc., Wallingford CT).
47. Irikura KK, Johnson RD, 3rd, Kacker RN (2005) Uncertainties in scaling factors for ab initio vibrational frequencies. *J Phys Chem A* 109(37):8430–8437.

Supporting Information

Bucher et al. 10.1073/pnas.1323700111

SI Text

Absorbance spectra of the 10 mM solutions of 2′-deoxyadenosine monophosphate (A), 2′-deoxyguanosine monophosphate (G), 2′-deoxy-5-methylcytidine (mC), and uridine monophosphate (U) in 50 mM D_2O phosphate buffer are shown in Fig. S1. The spectra were recorded with a UV-visible spectrometer (Lambda 750; PerkinElmer) with a path length of 100 μm. The red-shifted absorbance spectra of mC and G allow us to construct oligonucleotides with selective excitation of mC or G at 295 nm (arrow).

Vibrational spectra were simulated for all involved nucleobases and their corresponding radical states with density functional methods (Fig. S2). The Becke3Lyp 6-311G** functional with the solvent model PCM was used to calculate the harmonic vibrational frequencies. Gaussian 03 software (1) was used for calculations. For simplicity, all calculations were done for the 1-methyl–substituted nucleobases, where all exchangeable hydrogen atoms in the structure were substituted with deuterium. Each vibrational frequency analysis was preceded by a geometry optimization. The frequencies were scaled with a factor of 0.9669 (2). The experimental absorbance spectra (Fig. S2, first row of upper and lower graphs) are very well reproduced by the calculation with this method apart from a spectral shift (second row). For all bases, the cation (third row), and anion (fourth row) spectra were calculated. The marker bands used to characterize the charge-transfer states are colored.

1. Frisch MJ, et al. (2004) *Gaussian 03*. Revision D.01 (Gaussian, Inc., Wallingford CT).

2. Irikura KK, Johnson RD, 3rd, Kacker RN (2005) Uncertainties in scaling factors for ab initio vibrational frequencies. *J Phys Chem A* 109(37):8430–8437.

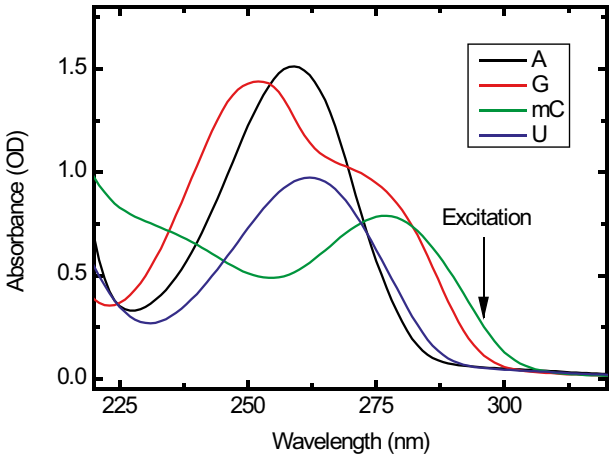

Fig. S1. Absorbance spectra of A, G, mC, and U.

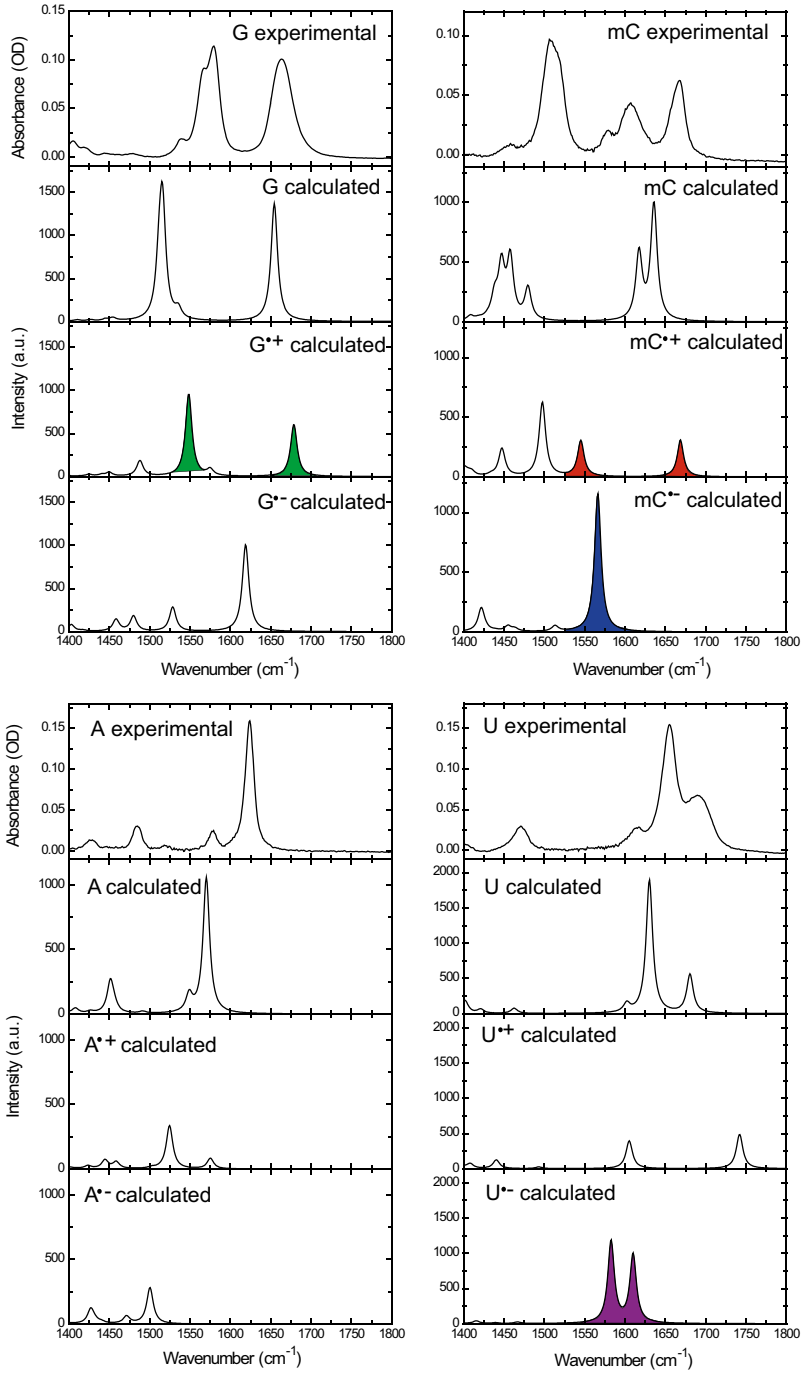

Fig. S2. Theoretical absorbance spectra.

4.3 Watson-Crick Base Pairing Controls Excited State Decay in Natural DNA

In the communication "Watson-Crick Base Pairing Controls Excited-State Decay in Natural DNA" published in the *Angewandte Chemie International Edition* [268, 269] the excited state dynamics of the four nucleobases in natural calf thymus DNA have been investigated. It could be shown that the excited state decay is controlled by the Watson-Crick base pairing, which opens up a new deactivation channel. This contradicts the general scientific consensus, which claims that base stacking governs the excited state decay.

The basic idea behind this publication is to use the characteristic absorbance bands of the four nucleobases in the IR to monitor the excited state decay of each base individually in natural calf thymus DNA. For that reason, marker bands for each of the four nucleobases have been determined by FTIR-spectroscopy and assigned to the absorbance spectrum of the complex calf thymus DNA. These marker bands allowed the determination of the excited state lifetime for each nucleobase in the natural double helix.

Instead of an expected complex excited state decay caused by the heterogeneous sequence, a simple well defined decay scheme has been discovered: The excited states of nucleobases connected via the Watson-Crick hydrogen bonds decay in a concerted way. This interstrand coupling of the excited state has been further investigated in single- and double-stranded model oligonucleotides. Whereas charge transfer states could be detected in single strands, a new excited state decay channel is appearing upon base pairing. Thus, base pairing quenches the charge transfer states caused by base stacking in single strands. The strong influence of the Watson-Crick hydrogen bonds points to the involvement of an interstrand proton transfer which deactivates the formation of reactive charge transfer states. The structural arrangement of the double helix with the Watson-Crick base pairing is presumably responsible for the extraordinary photostability of DNA.

VIP DNA Photochemistry Very Important Paper

DOI: 10.1002/anie.201406286

Watson–Crick Base Pairing Controls Excited-State Decay in Natural DNA**

Dominik B. Bucher, Alexander Schlueter, Thomas Carell, and Wolfgang Zinth**

Abstract: *Excited-state dynamics are essential to understanding the formation of DNA lesions induced by UV light. By using femtosecond IR spectroscopy, it was possible to determine the lifetimes of the excited states of all four bases in the double-stranded environment of natural DNA. After UV excitation of the DNA duplex, we detected a concerted decay of base pairs connected by Watson–Crick hydrogen bonds. A comparison of single- and double-stranded DNA showed that the reactive charge-transfer states formed in the single strands are suppressed by base pairing in the duplex. The strong influence of the Watson–Crick hydrogen bonds indicates that proton transfer opens an efficient decay path in the duplex that prohibits the formation or reduces the lifetime of reactive charge-transfer states.*

Exposure to UV light is a major cause of damage to the genetic information of living organisms. UV radiation populates reactive excited states in the nucleobases. These excited states give rise to photochemical reactions that modify the molecular structure of DNA, thereby leading to mutations and cell death.[1] An understanding of the photophysical primary processes is consequently essential for deciphering the pathways that cause radiation-induced damage of the genetic code. The photophysics of single nucleotides is well understood. The absorbed photon energy is dissipated in an ultrafast internal conversion to heat, a process which minimizes the occupation of reactive excited states that could lead to DNA damage.[2] This deactivation mechanism was of utmost importance during the early stages of evolution when the genetic code developed under extreme ultraviolet irradiation. Today, nucleotides act as information bits in all organisms on earth. They are organized in long DNA double strands with a double helical structure held together by two major interactions—base stacking and base pairing. Both influence the photophysical properties of DNA. π stacking is known to be the reason for the formation of long-lived excited states with high yields after UV excitation. These states do not exist in the monomers.[3] Recently, these long-lived states were characterized in single strands. It was shown that they are formed in response to charge separation and charge delocalization.[4] Neutral excimers are discussed for homogeneous sequences.[5] In double-stranded DNA, base pairing is the second important interaction next to base stacking. It is unknown how interbase hydrogen bonds influence the photophysical behaviour of DNA but theoretical calculations suggest that they may provide an alternative ultrafast deactivation channel for excited states.[6] In this model, a charge-separated state within a base pair is formed, which decays ultrafast to the ground state through proton transfer between the hydrogen-bonded bases. Indeed, model base pairs in the gas phase[7] and isolated GC base pairs dissolved in chloroform[8] decay faster than the corresponding monomers. Interestingly, gas-phase experiments on different GC base pair structures yielded ultrafast excited-state decay only for the Watson–Crick arrangement, which is in agreement with theoretical studies.[9] In GC duplexes in aqueous solution, a quenching of the originally excited ππ* state has been found.[10] However, an accelerated return to the ground-state could not be shown. On the contrary, as in single strands, longer-lived excited states were observed.[11] As a consequence, current models to explain excited-state decay in the duplex argue that base stacking is the controlling interaction.[3a,b,4b,12]

Besides a few measurements on natural systems,[13] previous time resolved experiments were predominantly performed on synthetic oligonucleotides by using UV/Vis or fluorescence spectroscopy.[3a,11d,14] In this spectral range, the overlap of the absorption bands prevents the resolution of the contributions of individual nucleobases in the excited states. To allow the discrimination of the four bases, we used time-resolved IR-spectroscopy.[4a,15] The nucleobases give narrow and characteristic absorption bands in the mid-IR region, which allows the dissection of the individual contributions of the four DNA bases to the excited states of duplex DNA. By using UV excitation and IR probing, we are able to record the decay of the excited states after UV irradiation for each of the four bases in natural calf thymus DNA.

Marker bands for the four individual nucleobases in double-stranded DNA were identified by FTIR on the basis of literature data[16] (Figures S1–3 in the Supporting Information). These marker positions for each nucleobase are displayed in all of the figures as colored bars. The experiments were performed in D_2O buffer solution (see the Supporting

[*] D. B. Bucher, A. Schlueter, Prof. Dr. W. Zinth
BioMolecular Optics and Center for Integrated Protein Science (CIPSM), Ludwig-Maximilians-Universität München
Oettingenstrasse 67, 80538 Munich (Germany)
E-mail: wolfgang.zinth@physik.uni-muenchen.de
D. B. Bucher, Prof. Dr. T. Carell
Center for Integrated Protein Science at the Department of Chemistry, Ludwig-Maximilians-Universität München
Butenandtstrasse 5–13, 81377 Munich (Germany)
E-mail: thomas.carell@cup.uni-muenchen.de

[**] We thank the Deutsche Forschungsgemeinschaft (SFB 749, TP A4 and A5, the Clusters of Excellence "Center for Integrated Protein Science Munich (CIPSM)" and "Munich-Center for Advanced Photonics" (MAP)) for financial support. The authors thank B. Kohler and W. Domcke for helpful discussions.

Supporting information for this article is available on the WWW under http://dx.doi.org/10.1002/anie.201406286.

Information). In the experiment shown in Figure 1, we nonselectively excited the nucleobases of double-stranded calf thymus DNA at 266 nm and monitored the absorption changes in the mid-IR region. Upon excitation, the absorption bands of the original ground state disappear. We used these marker bands to identify the return to the ground state for each nucleobase. Figure 1 a shows the absorbance-difference spectrum at a short delay time (0.25 ps) when the initially excited electronic states of the nucleobases are populated. There is a broad absorption increase known to represent the absorption of the initially excited electronic state. Superimposed are narrow negative bands (bleaching). The bleaching of the signal matches the absorption of the ground state (Figures S1–3) and allows the assignment of the transient bands to the different nucleobases (Figure 1 a). The absorption change because the initially excited electronic state decays within less than one picosecond, thus leading to features of a vibrationally hot ground state. The cooling of this vibrational hot state is finished within the next 10 ps (time constant ca. 6 ps, Figure S4). The contour plot in Figure 1 b shows the evolution of the absorption-difference spectrum after the cooling process ($t > 10$ ps). The absorption-difference spectrum displays spectral features remarkably different to the ones observed directly after UV excitation of the DNA, and importantly, the spectrum changes considerably over time. The kinetics shown here evolve on the ten- to hundred-picosecond timescale in a manner similar to the data obtained for single-stranded DNA.[3a,4a] The long-lived states visible in Figure 1 b have amplitudes which amount to about 50 % of the initial bleached signal. The major feature of these long-lasting absorbance changes in calf thymus DNA show the following characteristic properties: First, the long-lived absorption-difference spectra differ from the bleached signals observed at short delay times. Second, the dynamics of the slow absorbance changes can be qualitatively modeled by two time constants ($\tau_1 = 40$ ps, $\tau_2 = 210$ ps). Given the complexity of the natural DNA, these time constants are within the range of previous publications.[3a,17] The present IR experiments follow transient species populated to a significant percentage (ca. 50 %), whereas long-lived transients with small relative amplitude, such as those found with emission measurements, are not addressed here.[13a] Third, and most important, are the spectra associated to the two long decay times (Figure 1 c). The two decay spectra $D_1(\nu)$ and $D_2(\nu)$ show clear differences. In the 40 ps decay spectrum, marker bands for the bases cytosine (C) and guanine (G) are dominant, while the 210 ps decay spectrum shows predominant contributions from adenine (A) and thymine (T). These spectral differences were also obtained when we subtracted spectra measured at late times from those measured at early times. This method excludes fitting artifacts (Figure S5).

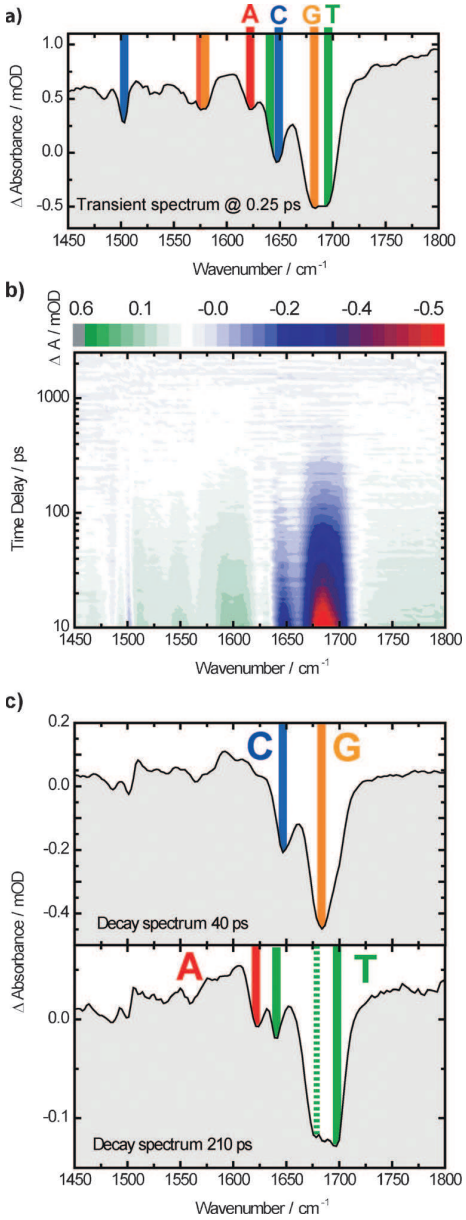

Figure 1. a) Transient difference IR spectrum at 0.25 ps after excitation at 266 nm. The marker band positions of the nucleobases Adenine (A), cytosine (C), guanine (G), thymine (T) are marked with coloured bars. b) Absorbance-change data at longer delay times in a contour plot. The cooling procedure before 10 ps is omitted. c) Decay-associated spectra $D_1(\nu)$ and $D_2(\nu)$ of slowly decaying species associated with the decay constants $\tau_1 = 40$ ps and $\tau_2 = 210$ ps.

The data show clearly that the bands for the nucleotides connected through Watson–Crick base pairing are linked in the decay process. The data show furthermore that the lifetimes of G and C are shorter than those of A and T.

If the long-lived states in the double-stranded system are assumed to be intrastrand charge-transfer states, one would expect a complex decay scheme. Different base sequences should give rise to different decay times since the recombination of charge-separated states is determined according to the Marcus theory by the redox difference between the involved bases.[3c] Such behavior has indeed been observed in single-stranded DNA. One would consequently expect a complex decay pattern in line with the extreme sequence heterogeneity of natural calf thymus DNA. For example, the lifetime of the GA exciplex is known to be around 300 ps,[4a] which is much longer than the observed times in the

DNA duplex. It is this joint decay of G and C on the one side and of A and T on the other that lead us to conclude that Watson–Crick base pairing and not base stacking controls the lifetime of the excited states.

The involvement of interstrand base pairing was further investigated in defined single- and double-stranded oligonucleotides. At first, we designed two complementary single strands with nucleotides selected in such a way that for each strand, one specific base, namely 2′-deoxyguanosine (G) or 5-methyl-2′-deoxycytidine (^{m}C), could be selectively excited by UV light at 295 nm (Figure S6).[4a] Investigation of these two DNA single strands (U^{m}CUUUUUU, AAAAAAGA; Figure 2a) showed long-lived excited states with marker bands

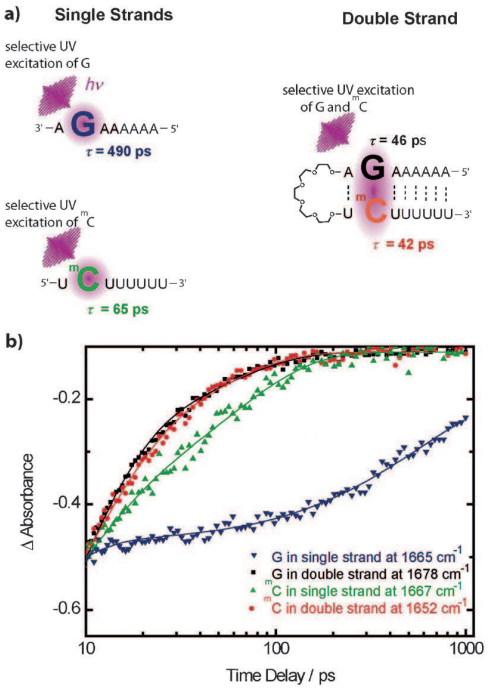

Figure 2. a) Picosecond pulses of UV light at 295 nm allow selective excitation of the 2′-deoxyguanosine (G) residue in the AAAAAAGA and the 5-methyl-2′-deoxycytidine (mC) residue in the UmCUUUUUU oligonucleotide. In the corresponding double-stranded hairpin AAAAAAGA·UmCUUUUUU, only G and mC are excited. b) Time-dependent absorption changes in the IR spectrum (normalized) recorded at the marker band positions of G and mC for the single- and double-stranded samples. The transients are fitted with a sum of exponentials (lines).

for charge-separated states (Figure S7). The charge-separated state $^{m}C^{+}U^{\bullet-}$ decays in U^{m}CUUUUUU with a lifetime of 65 ps. The charge-separated state $G^{\bullet+}A^{\bullet-}$ in AAAAAAGA vanishes with a lifetime of 490 ps. The temporal progression can be clearly seen by the positions of the respective ground-state bands of mC and G (Figure 2b, green and blue, respectively). The results fully agree with previous data obtained with other single-stranded DNA.[4a] We next prepared a duplex with the same sequence. To obtain a stable structure, we connected the strands through a hexaethylene glycol linker (Figure 2a) to give a hairpin structure (Figure S8, S9). In this duplex, the mC and G residues were selectively excited and the ground-state recovery of the mC and G bands in the duplex could be monitored separately as a result of their distinct absorbance bands in the mid-IR region. The transients at 1678 cm^{-1} (marker band for G; black) and 1652 cm^{-1} (marker band for ^{m}C; red) in the double-stranded hairpin are plotted in Figure 2b. It is evident that the decay of the long-lived excited states of ^{m}C and G is much faster in the duplex than in the corresponding single strands. More importantly, we observe very similar time constants of ca. 40 ps for the decay of both ^{m}C and the G in the duplex, whereas in the single strands, the excited states of these bases decay much more slowly with vastly different time constants. This effect cannot be caused by structural differences between the single- and the double-stranded DNA since charge-transfer states are nearly independent of base-stacking geometry.[18] The decay of the excited states of G and ^{m}C are thus coupled in the duplex and it is this coupling that blocks formation of the reactive radical-type charge-transfer states. Furthermore, the time constant for the GC pair in the artificial hairpin is the same as in natural calf thymus DNA. These results show directly that the hydrogen bonds of the base pairs control the formation and decay of the long-lived excited states. Our data suggest that interstrand proton transfer initiated by photoexcitation of the DNA is the reason for the concerted decay of paired bases. Indeed, proton transfer between paired bases caused by intrastrand charge transfer after UV excitation has been postulated in the literature based on hydrogen/deuterium isotope effects.[3a,19] The observed concerted decay of excitation in paired bases could also be explained by a model consisting of interstrand charge transfer coupled to proton transfer.[6] However, the long time constants observed in the present experiments stand in contrast to the proposed subpicosecond decay. Besides these proton transfer processes induced by charge transfer, a mechanism involving double proton transfer induced directly by the electronic excitation could explain the observations.[20] As a common feature of these models, the excited state decay is related to interstrand proton transfer and the observed changes in the IR-absorption spectrum originate from the modified arrangement of hydrogen bonds in the base pairs.

The molecular processes following the excitation of the nucleobases are illustrated in Figure 3. In monomers, the optically excited $\pi\pi^*$ state mostly decays fast by internal conversion to the ground state. In single strands, base stacking enables photochemical reactions between neighboring bases (e.g., to give a cyclobutane pyrimidine dimer (CPD)[15b,c] or a 6–4 lesion[15a]) and gives rise to a considerable number of long-lived radical-pair states. These charge-separated states are precursors of the harmful 6–4 lesion in DNA[21] and possibly induce oxidative as well as reductive damage.[22] Because base stacking enables the formation of charge-transfer states, it is the stacking which is responsible for DNA damage (Figure 3). Base pairing through Watson–Crick hydrogen bonds opens up new decay channels through proton transfer[23] and may deactivate dangerous charge-transfer states.

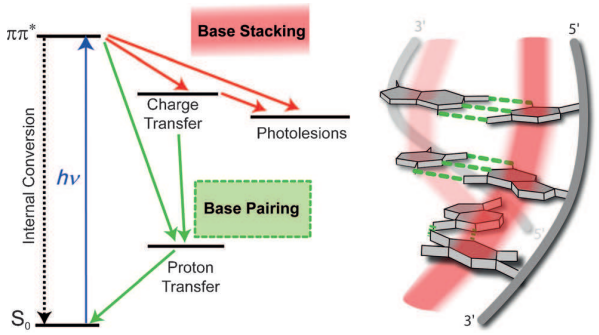

Figure 3. Base stacking in the DNA strands supports the ordered arrangement of bases, which is a prerequisite for many of the functions of DNA. However, the stacking also leads to the formation of photolesions, either directly from the originally excited ππ* state or through charge-separated intermediates. Base pairing between the bases of two complementary strands opens up a new decay channel which deactivates the ππ*[10] and charge-separated states. Base pairing thus counteracts the destructive action of charge-separated states, thereby supporting the integrity of the genetic information.

Received: June 16, 2014
Revised: July 22, 2014
Published online: September 4, 2014

Keywords: base pairing · DNA photochemistry · excited-state decay · femtosecond IR spectroscopy · proton transfer

[1] a) J. S. Taylor, *Acc. Chem. Res.* **1994**, *27*, 76 – 82; b) G. P. Pfeifer, Y.-H. You, A. Besaratinia, *Mutat. Res. Fundam. Mol. Mech. Mutagen.* **2005**, *571*, 19 – 31.
[2] a) J.-M. L. Pecourt, J. Peon, B. Kohler, *J. Am. Chem. Soc.* **2001**, *123*, 10370 – 10378; b) C. E. Crespo-Hernández, B. Cohen, P. M. Hare, B. Kohler, *Chem. Rev.* **2004**, *104*, 1977 – 2020.
[3] a) C. E. Crespo-Hernández, B. Cohen, B. Kohler, *Nature* **2005**, *436*, 1141 – 1144; b) C. T. Middleton, K. de La Harpe, C. Su, Y. K. Law, C. E. Crespo-Hernández, B. Kohler, *Annu. Rev. Phys. Chem.* **2009**, *60*, 217 – 239; c) T. Takaya, C. Su, K. d. L. Harpe, C. E. Crespo-Hernández, B. Kohler, *Proc. Natl. Acad. Sci. USA* **2008**, *105*, 10285 – 10290.
[4] a) D. B. Bucher, B. M. Pilles, T. Carell, W. Zinth, *Proc. Natl. Acad. Sci. USA* **2014**, *111*, 4369 – 4374; b) G. W. Doorley, M. Wojdyla, G. W. Watson, M. Towrie, A. W. Parker, J. M. Kelly, S. J. Quinn, *J. Phys. Chem. Lett.* **2013**, *4*, 2739 – 2744.
[5] a) G. Olaso-González, M. Merchán, L. Serrano-Andrés, *J. Am. Chem. Soc.* **2009**, *131*, 4368 – 4377; b) R. Improta, V. Barone, *Angew. Chem. Int. Ed.* **2011**, *50*, 12016 – 12019; *Angew. Chem.* **2011**, *123*, 12222 – 12225.
[6] a) A. L. Sobolewski, W. Domcke, *Phys. Chem. Chem. Phys.* **2004**, *6*, 2763 – 2771; b) S. Perun, A. L. Sobolewski, W. Domcke, *J. Phys. Chem. A* **2006**, *110*, 9031 – 9038.
[7] T. Schultz, E. Samoylova, W. Radloff, I. V. Hertel, A. L. Sobolewski, W. Domcke, *Science* **2004**, *306*, 1765 – 1768.
[8] a) N. K. Schwalb, T. Michalak, F. Temps, *J. Phys. Chem. B* **2009**, *113*, 16365 – 16376; b) N. K. Schwalb, F. Temps, *J. Am. Chem. Soc.* **2007**, *129*, 9272 – 9273.
[9] a) A. Abo-Riziq, L. Grace, E. Nir, M. Kabelac, P. Hobza, M. S. d. Vries, *Proc. Natl. Acad. Sci. USA* **2005**, *102*, 20 – 23; b) A. L. Sobolewski, W. Domcke, C. Hättig, *Proc. Natl. Acad. Sci. USA* **2005**, *102*, 17903 – 17906.
[10] a) F.-A. Miannay, Á. Bányász, T. Gustavsson, D. Markovitsi, *J. Am. Chem. Soc.* **2007**, *129*, 14574 – 14575; b) I. Vayá, F.-A. Miannay, T. Gustavsson, D. Markovitsi, *ChemPhysChem* **2010**, *11*, 987 – 989; c) J. Brazard, A. K. Thazhathveetil, I. Vayá, F. D. Lewis, T. Gustavsson, D. Markovitsi, *Photochem. Photobiol. Sci.* **2013**, *12*, 1453 – 1459.
[11] a) C. E. Crespo-Hernández, K. de La Harpe, B. Kohler, *J. Am. Chem. Soc.* **2008**, *130*, 10844 – 10845; b) L. Biemann, S. A. Kovalenko, K. Kleinermanns, R. Mahrwald, M. Markert, R. Improta, *J. Am. Chem. Soc.* **2011**, *133*, 19664 – 19667; c) K. de La Harpe, B. Kohler, *J. Phys. Chem. Lett.* **2011**, *2*, 133 – 138; d) I. Buchvarov, Q. Wang, M. Raytchev, A. Trifonov, T. Fiebig, *Proc. Natl. Acad. Sci. USA* **2007**, *104*, 4794 – 4797.
[12] B. Kohler, *J. Phys. Chem. Lett.* **2010**, *1*, 2047 – 2053.
[13] a) I. Vayá, T. Gustavsson, F.-A. Miannay, T. Douki, D. Markovitsi, *J. Am. Chem. Soc.* **2010**, *132*, 11834 – 11835; b) I. Vayá, T. Gustavsson, T. Douki, Y. Berlin, D. Markovitsi, *J. Am. Chem. Soc.* **2012**, *134*, 11366 – 11368.
[14] N. K. Schwalb, F. Temps, *Science* **2008**, *322*, 243 – 245.
[15] a) K. Haiser, B. P. Fingerhut, K. Heil, A. Glas, T. T. Herzog, B. M. Pilles, W. J. Schreier, W. Zinth, R. de Vivie-Riedle, T. Carell, *Angew. Chem. Int. Ed.* **2012**, *51*, 408 – 411; *Angew. Chem.* **2012**, *124*, 421 – 424; b) W. J. Schreier, J. Kubon, N. Regner, K. Haiser, T. E. Schrader, W. Zinth, P. Clivio, P. Gilch, *J. Am. Chem. Soc.* **2009**, *131*, 5038 – 5039; c) W. J. Schreier, T. E. Schrader, F. O. Koller, P. Gilch, C. E. Crespo-Hernández, V. N. Swaminathan, T. Carell, W. Zinth, B. Kohler, *Science* **2007**, *315*, 625 – 629.
[16] M. Banyay, M. Sarkar, A. Gräslund, *Biophys. Chem.* **2003**, *104*, 477 – 488.
[17] G. W. Doorley, D. A. McGovern, M. W. George, M. Towrie, A. W. Parker, J. M. Kelly, S. J. Quinn, *Angew. Chem. Int. Ed.* **2009**, *48*, 123 – 127; *Angew. Chem.* **2009**, *121*, 129 – 133.
[18] a) J. Chen, B. Kohler, *J. Am. Chem. Soc.* **2014**, *136*, 6362 – 6372; b) K. de La Harpe, C. E. Crespo-Hernández, B. Kohler, *ChemPhysChem* **2009**, *10*, 1421 – 1425.
[19] K. de La Harpe, C. E. Crespo-Hernández, B. Kohler, *J. Am. Chem. Soc.* **2009**, *131*, 17557 – 17559.
[20] a) S. Takeuchi, T. Tahara, *Proc. Natl. Acad. Sci. USA* **2007**, *104*, 5285 – 5290; b) A. Douhal, S. H. Kim, A. H. Zewail, *Nature* **1995**, *378*, 260 – 263.
[21] A. Banyasz, T. Douki, R. Improta, T. Gustavsson, D. Onidas, I. Vayá, M. Perron, D. Markovitsi, *J. Am. Chem. Soc.* **2012**, *134*, 14834 – 14845.
[22] S. Kanvah, J. Joseph, G. B. Schuster, R. N. Barnett, C. L. Cleveland, U. Landman, *Acc. Chem. Res.* **2010**, *43*, 280 – 287.
[23] M. Dittmann, F. F. Graupner, B. März, S. Oesterling, R. de Vivie-Riedle, W. Zinth, M. Engelhard, W. Lüttke, *Angew. Chem. Int. Ed.* **2014**, *53*, 591 – 594; *Angew. Chem.* **2014**, *126*, 602 – 605.

Angewandte Chemie
Eine Zeitschrift der Gesellschaft Deutscher Chemiker

Supporting Information

69451 Weinheim, Germany

Watson–Crick Base Pairing Controls Excited-State Decay in Natural DNA**

Dominik B. Bucher, Alexander Schlueter, Thomas Carell, and Wolfgang Zinth**

anie_201406286_sm_miscellaneous_information.pdf

1. Materials and sample preparation

The double stranded calf thymus DNA was purchased from Merck Millipore (Calbiochem, 2618 Deoxyribonucleic Acid, Sodium Salt, Calf Thymus). The calf thymus DNA was dissolved two days prior to the experiment in buffered (50mM phosphate buffer) D_2O solution with a concentration of 3.5 mg/mL. The oligonucleotides and the hairpin were provided by IBA GmbH and used with a concentration of 5 mM. The hairpin was annealed before measurement (80 °C to 20 °C in 3 h).

2. IR-band assignment

Band assignments for the nucleobases are complicated due to the shift of the absorbance bands upon the hybridisation process. For that reason, FTIR spectra of single bases and double stranded oligonucleotides were recorded and compared (Figure S1). Figure S1a shows the absorbance change for A-T base pairing, Figure S1b for G-C base pairing. The spectra of the single and double strands are plotted on the same absorbance scale thus they are directly comparable.
In the bottom part of Figure S1a, the single strands of dA_{18} (red) and dT_{18} (green) are plotted. The sum of both spectra is shown in grey. Annealing both strands with the same concentration results in a spectrum, which deviates considerably from the sum spectrum. Upon duplexation, the intensities of the absorbance bands are strongly changing: The A-band at 1623 cm^{-1} loses amplitude. The three absorbance bands of T between 1600 and 1700 cm^{-1} show also a change in intensity and shifts of their spectral position. Additionally, the band assignment in the double strand is supported by the literature values[1].
In Figure S1b the same experiment has been performed for the G-C base pair. In this experiment, no homooligomer of G could be used, since these sequences form G quadruplexes and do not allow to determine the absorbance spectra of the G single strand. Therefore, we compared the spectra of the G and C mononucleotides with the double strand formed by the alternating sequence d(GCGCCGCG)·d(CGCGGCGC) (Figure S1b). In the monomer case, the absorbance bands at 1650 cm^{-1} can hardly be distinguished between G and C. However, in the double strand, these bands are well separated allowing a clear distinction of G and C in the duplex strand[1]. Unfortunately, the characteristic isolated absorbance bands of C at 1505 cm^{-1} and of G at 1580 cm^{-1} are nearly vanishing upon base pairing and can thus not be used as marker bands. Using the marker bands at 1650 cm^{-1} and 1683 cm^{-1}, we are able to assign the different bands of the IR absorbance spectrum of calf thymus DNA (Figure S2).
In table S1 the most intense marker bands of all four nucleobases in the double strand are shown together with literature values. All marker band positions from the FTIR measurements, the marker bands seen in the time-resolved calf thymus DNA experiments and the literature values[1] are listed in Table S1.

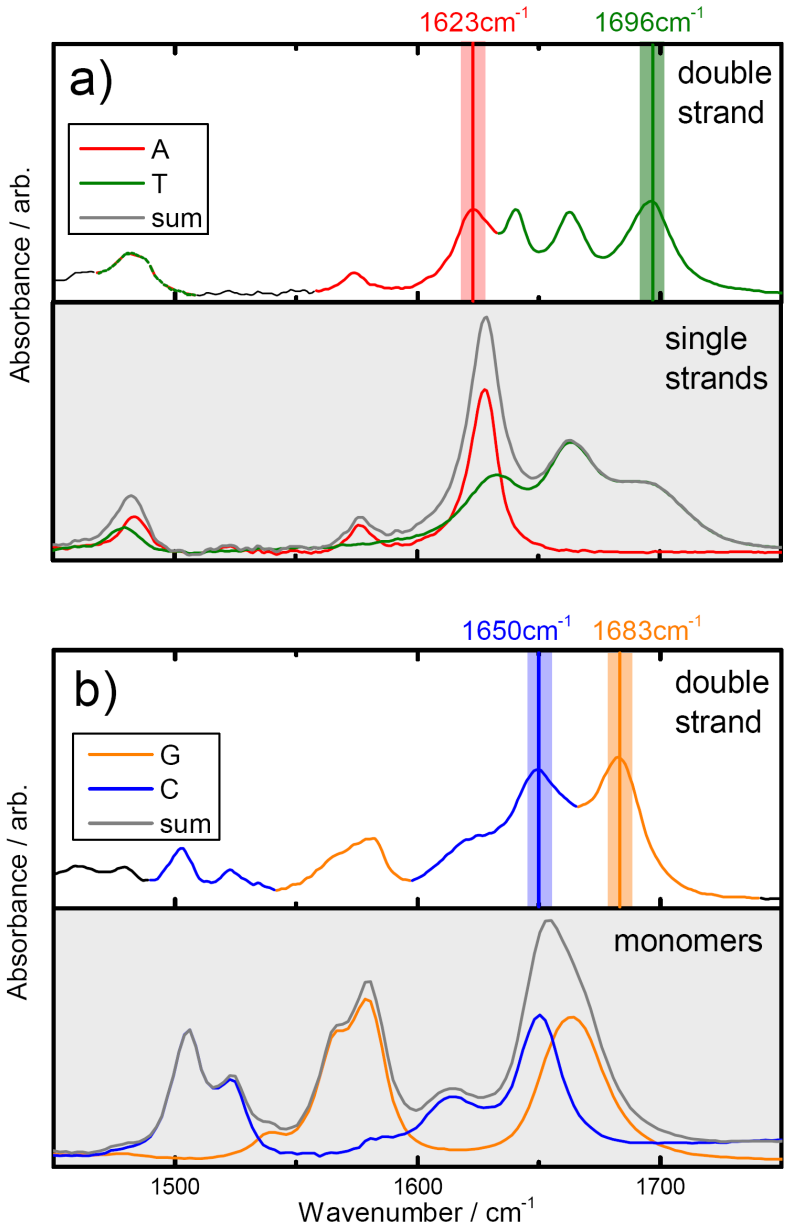

Supporting Figure S1: IR-absorbance spectra of single- and double-stranded DNA. Base pairing leads to changes of the absorbance spectra of the nucleobases upon double strand formation.

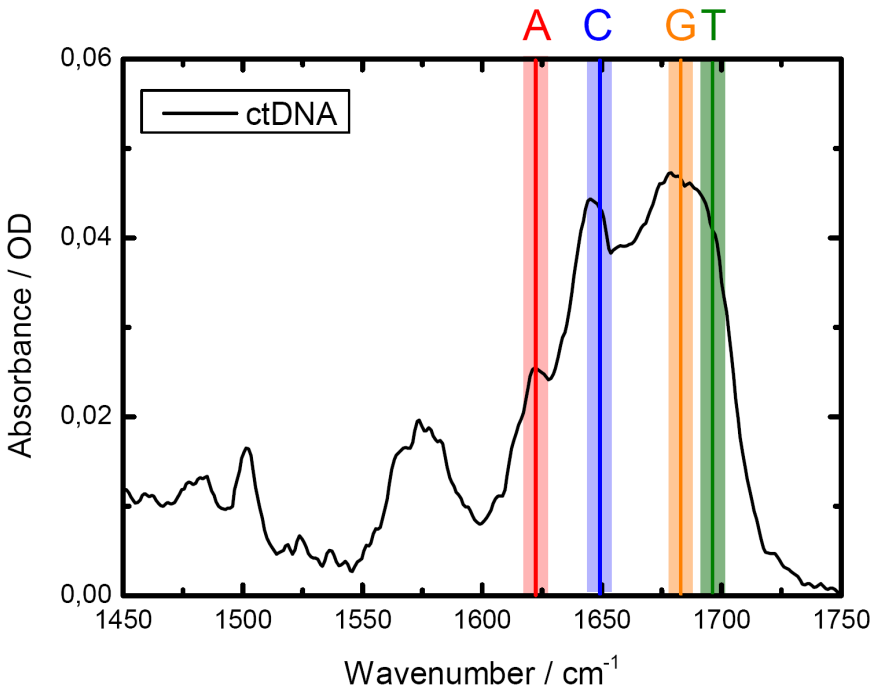

Supporting Figure S2: Absorbance spectrum of calf thymus DNA

	FTIR double strand	Time resolved experiment	Literature[1]
A	1574		1576-1579
	1623	1622	1622-1632
T	1640	1640	1641-1645
	1662	1676	1655-1671
	1696	1696	1691-1698
G	1581		1575-1590
	1683	1683	1678-1689
C	1503		1498-1506
	1650	1647	1647-1655

Supporting Table S1: Marker bands of A, T, G and C in double-stranded DNA

The mid IR marker bands of the steady state FTIR experiment match most of the marker bands of the time resolved experiment. However, in the 210 ps decay spectrum of calf thymus DNA a band at 1676 cm^{-1} cannot be assigned directly. Both bases, G and T absorb in this spectral regime. Since we can fix the position of the G band by the initial bleach signal and the 40 ps decay spectrum to 1683 cm^{-1}, we tentatively assign the band at 1676 cm^{-1} to a strongly blue shifted T band. This is further supported by the FTIR experiment presented in Figure S3. Here, the IR absorbance spectrum of the alternating double strand $d(CA)_{10}{\cdot}d(TG)_{10}$ is shown and compared to the spectrum of the double strands containing exclusively either A-T or G-C (see also Figure S1). Although the base pairing is identical, we observe strong shifts of the absorbance bands showing us that the environment of the nucleobases may play an important role. The T absorbance band at 1662 cm^{-1} is not observable in the heterogeneous sequence $d(CA)_{10}{\cdot}$ $d(TG)_{10}$. Either the band has lost its intensity or it is shifted and overlaps with other bands, which supports our assignment in the time resolved experiment.

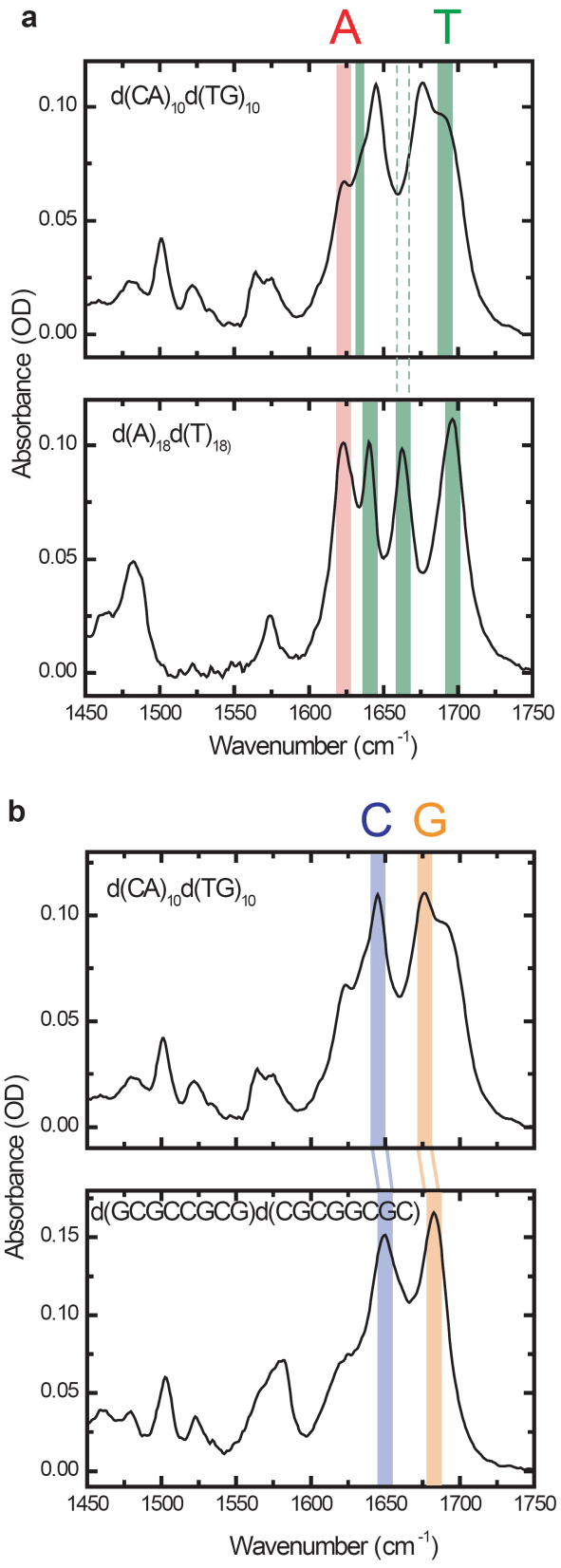

Supporting Figure S3: Effect of the sequence on the absorbance spectra of the nucleobases in double strands

3. Fitting procedure of the calf thymus DNA data

The absorbance data from the first 5 ps when the initial decay of the original excited state and vibrational cooling occur were excluded from the fitting procedure since cooling leads to a non-exponential behaviour which complicates the fit. Furthermore, this timescale is not of interest for this study. Thus, the data for calf thymus DNA was globally fitted for decay times larger than 5 ps with three exponential functions and one long lasting component.

$$\Delta A(\nu, t_D) = \sum_{i=0}^{2} D_i(\nu) \cdot \exp\left(-\frac{t_D}{\tau_i}\right) + D_3(\nu)$$

Three time constants, τ_0 = 6 ps, τ_1 = 40 ps and τ_2 = 210 ps were necessary to reproduce the data satisfactory. τ_0 represents the tail of the cooling process, whereas τ_1 and τ_2 are discussed in the main part of the publication. D_3, the long lasting component, is an offset which is caused by long-lived states and heated water. For each of the time constants, a decay associated difference spectrum is calculated which is shown in Figure S4. All three decay associated spectra exhibit distinctly different spectral characteristics.

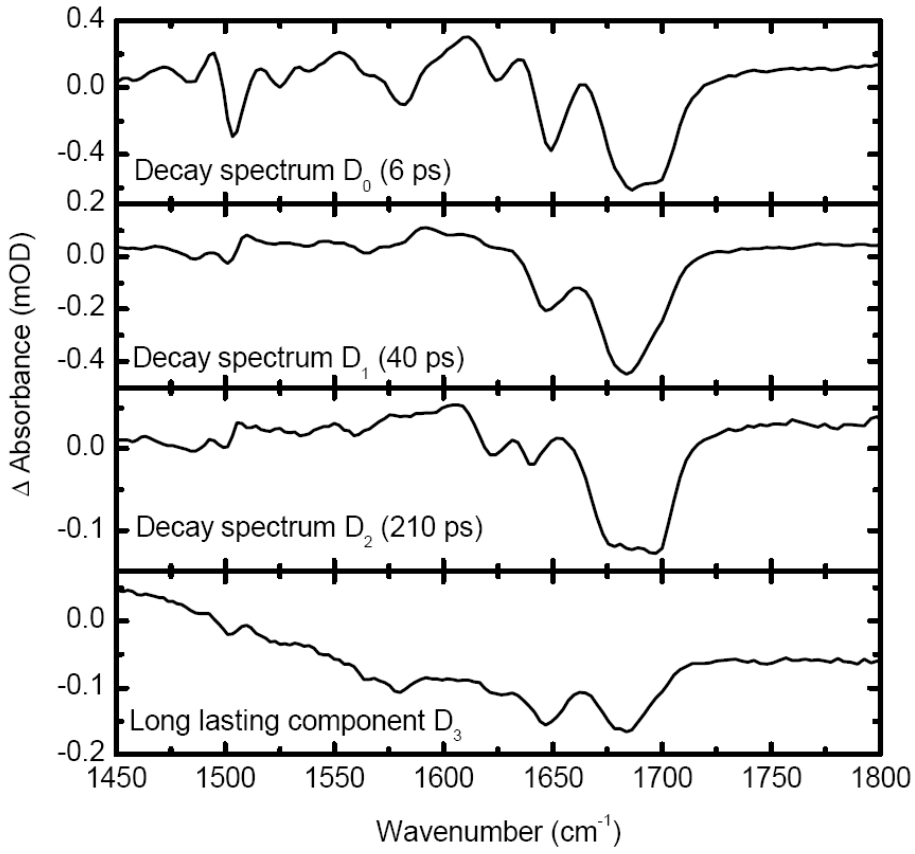

Supporting Figure S4: Decay associated difference spectra D_0 (τ_0 = 6 ps), D_1 (τ_1 = 40 ps), D_2 (τ_2 = 210 ps) and the long lasting component D_3

To show that the spectral features represented by the decay spectra D_1 and D_2 are independent of the special model assumption, we used an independent method to extract of these spectral features. We subtracted absorbance data recorded at late times from those recorded at early times and plotted these spectra together with the decay spectra D_1 and D_2 (Figure S5). We could reproduce the decay spectrum D_1 by subtracting the transient spectrum at 40 ps from

one at 20 ps and D_2 by subtracting the transient spectrum at 2500 ps from that at 100 ps. This unequivocally shows that the spectral changes are not fitting artefacts. The same trend can be observed in the contour plot (see Figure 1b).

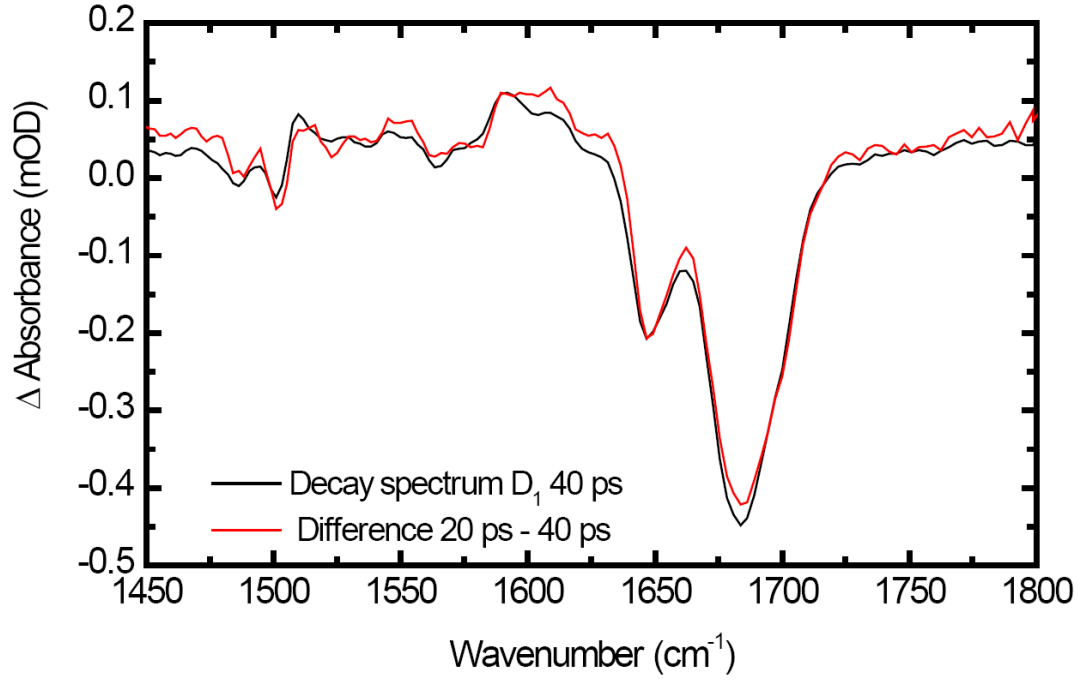

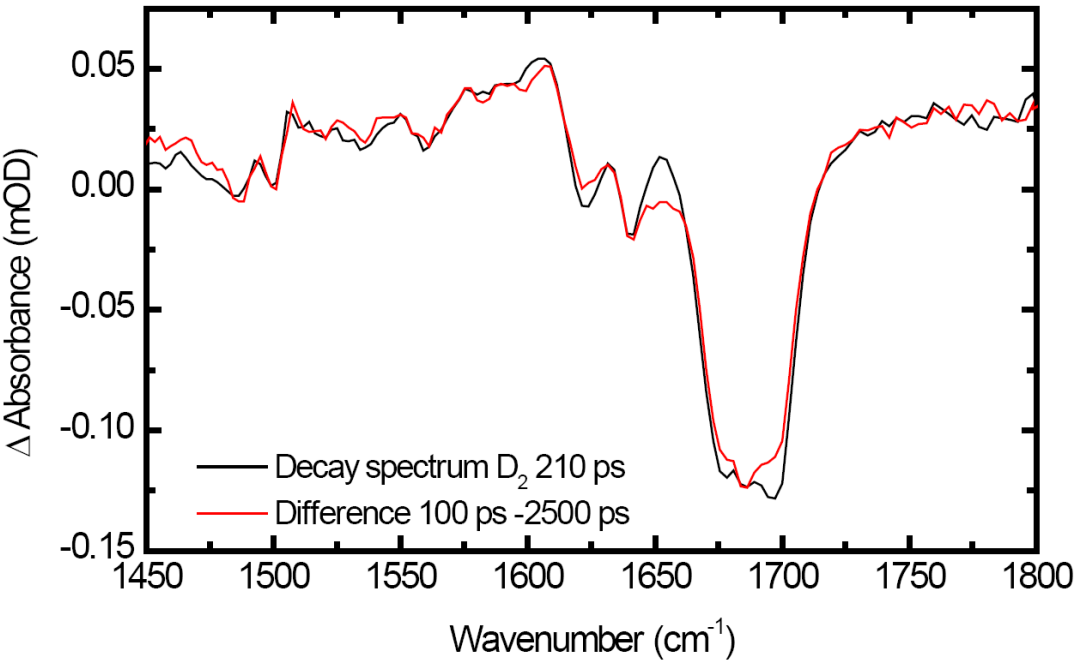

Supporting Figure S5: Comparison of the decay spectra D_1 and D_2 of the calf thymus DNA with difference transient spectra recorded at the given times.

The long-lasting component D_3 is mainly caused by the absorption change of the heated water surrounding the DNA[2]. Furthermore we observed a small bleach at the G and C position. This bleach is caused by a non-linear, intensity-dependent process, presumably by two-photon

ionization. In contrast, features related to τ_0, τ_1 and τ_2 do not depend on the excitation intensity and thus are not influenced by the two-photon process. The spectral signature of this long-lived component is constant over the investigated time window. For this reason, we subtracted the spectrum of the long lasting-component for the contour plot in Figure 1. We also calculated the number of absorbed photons/number of bases which gives a value of 9%. This low value cannot be reduced due to the low absorbance coefficients in the IR. Experiments with reduced precision show that down to an excitation of 4% no deviation of the general behavior was observed.

4. Characterization of the hairpin sample

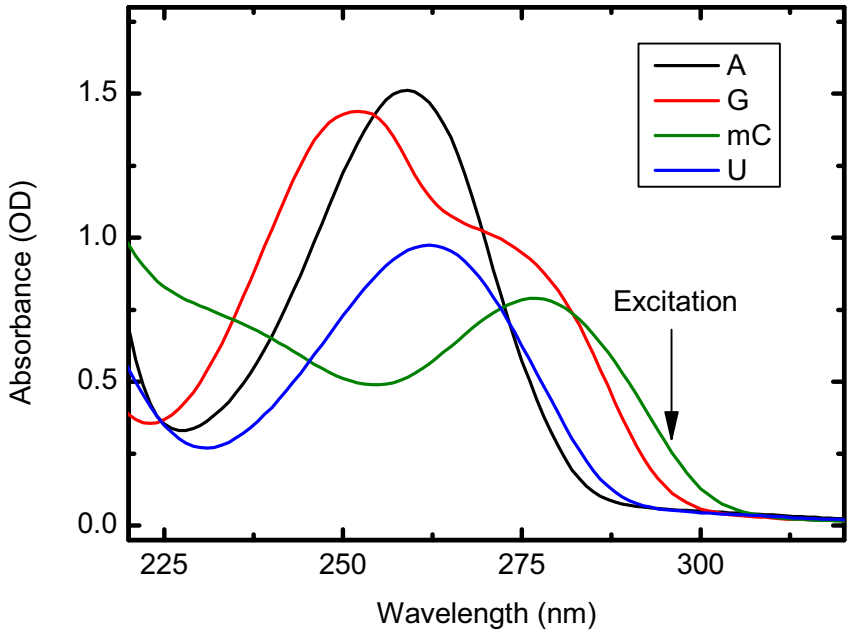

Supporting Figure S6: Absorbance spectra of the 10 mM solutions of A, G, mC and U in phosphate buffer

The absorbance spectra of 2'-deoxyguanosine monophosphate (G), 2'-deoxy-5-methylcytidine (mC) are red shifted or have red-shifted wings in comparison to 2'-deoxyadenosine monophosphate (A) and uridine monophosphate (U). This allows to construct oligonucleotides in which we can achieve a selective excitation of dmC and dG by light pulses at 295 nm (arrow). The spectra were recorded with a UV/Vis spectrophotometer (Perkin-Elmer, Lambda 750) in cuvettes with a thickness of 100 µm.

The transient absorption data of the single strand samples AAAAAAGA and UmCUUUUUU were globally fitted with the same procedure as published in Ref [3]. The decay associated spectrum for the long-lived state is shown in the bottom part for AAAAAAGA in Figure S7a and in Figure S7b for UmCUUUUUU. In the upper part of the figures the difference spectra of the radical cations of G and mC are shown[3-4]. The cation marker bands (colored) are directly visible in these spectra. They also appear in the spectra (lower part) of AAAAAAGA and UmCUUUUUU. In UmCUUUUUU, the violet colored marker bands are caused by the

$U^{\bullet-}$, which has been assigned previously[3]. These results are in accordance with previous data and show directly the occurrence of charge-separated states in the single-stranded oligonucleotides.

The stability of the AAAAAAGA·UmCUUUUUU hairpin (3 μM) was investigated by determining the melting curve. Temperature dependent absorption at 266 nm was recorded on a Jasco-V650 UV/VIS spectrophotometer with a temperature-controlled sample holder, which gives a melting point of 47 °C (Figure S8). Thus, the hexaethylene glycole linked sequence forms stable duplexes at room temperature.

The structure of the hairpin DNA in solutions was determined with CD spectroscopy in 50 mM phosphate buffer solution (3 μM). The positive band at 274 nm with a zero crossing at 254 nm and a negative band at 245 nm shows clearly, that the hexaethylene glycole linked hairpin forms a B-DNA[5] (Figure S9). The CD experiments have been recorded using a Jasco J-810 CD spectrophotometer at room temperature.

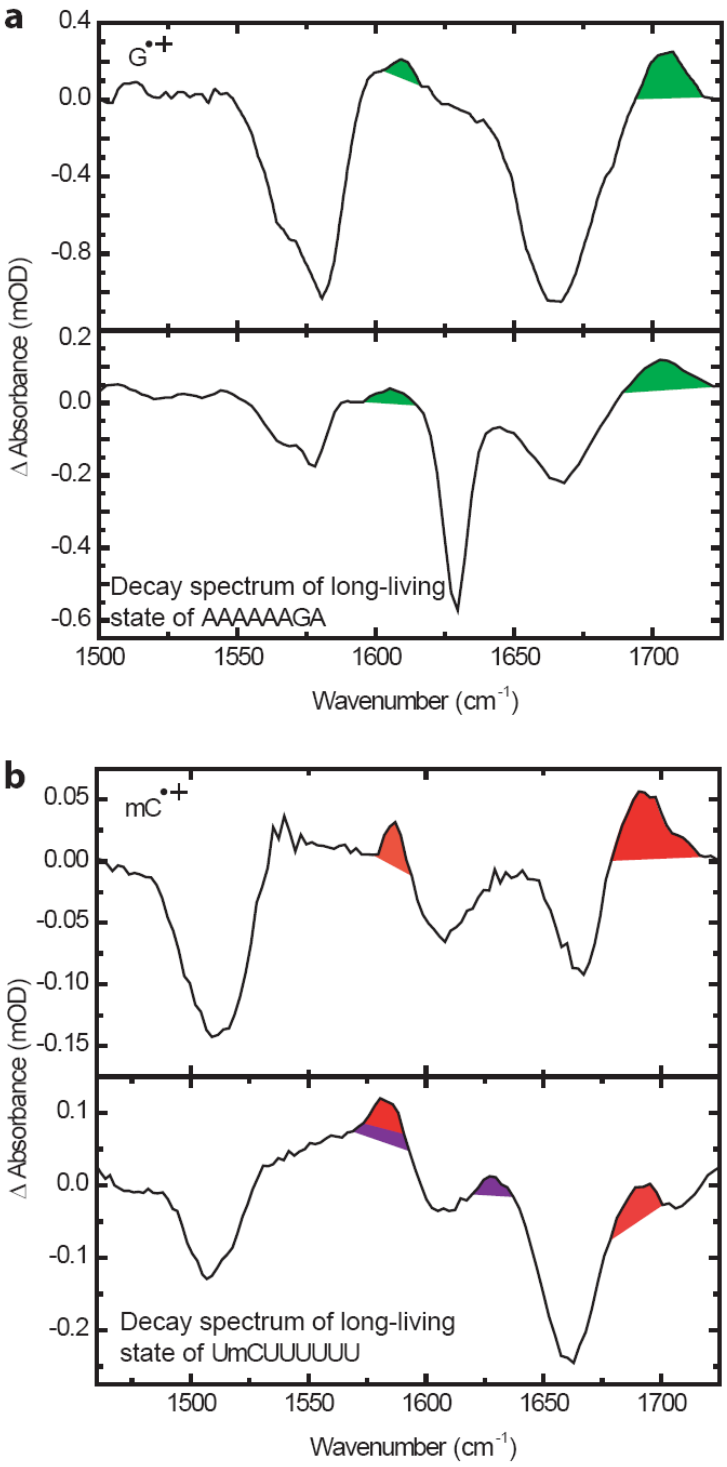

Supporting Figure S7: Identification of marker bands in the decay spectrum of the long-lived state in AAAAAAGA (a) and UmCUUUUUU (b). Marker bands of $G^{\bullet+}$ (green), $mC^{\bullet+}$ (red) and $U^{\bullet-}$ (violet) are color-coded

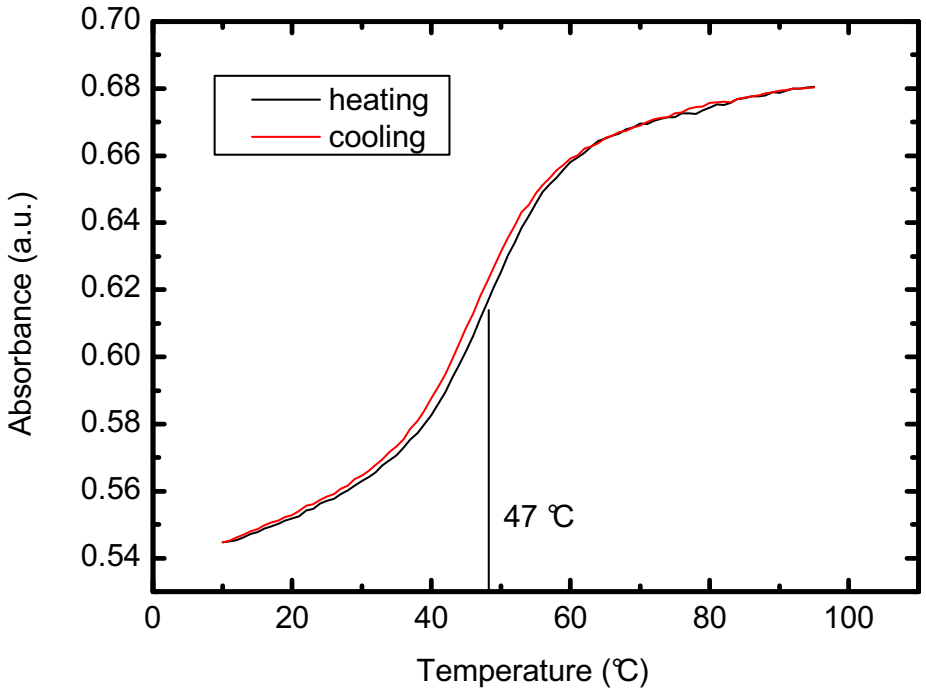

Supporting Figure S8: Melting curve of the AAAAAAGA·UmCUUUUUU hairpin

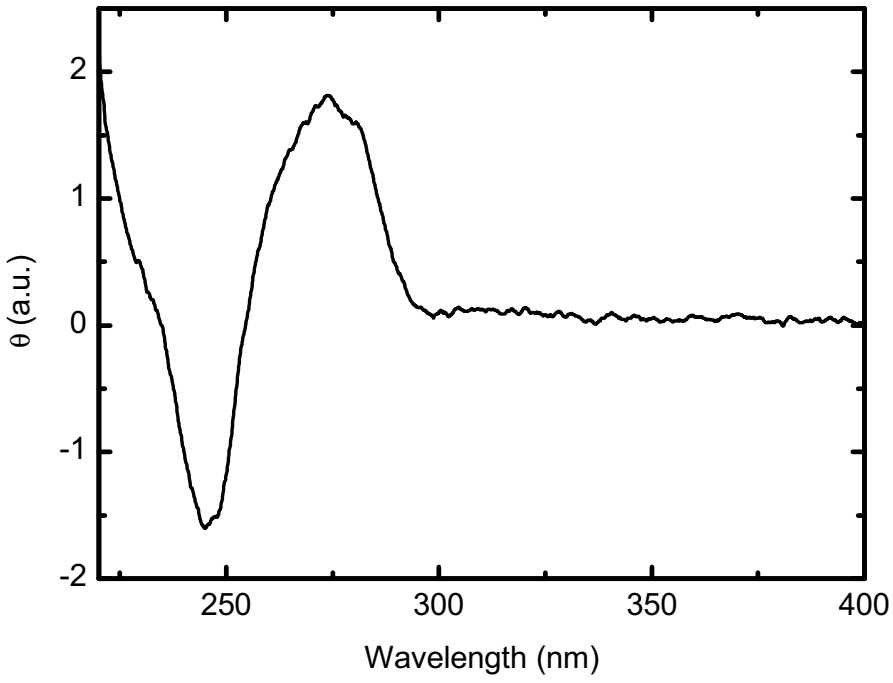

Supporting Figure S9: CD spectrum of the AAAAAAGA·UmCUUUUUU hairpin

5. Fitting procedure for the oligonucleotides

The time dependencies of the absorption changes of the duplex hairpin shown in Figure 2 in the main text were recorded at the peak positions of the absorption bands of mC and G. Note that the corresponding absorbance bands are shifted in the duplex relative to those of the single strand, as described in the "band assignment" chapter. The transients were fitted with a sum of two exponentials, which is sufficient to reproduce the data and can be judged from the solid line in Figure 2 in the main text. The short time constant is used to describe remaining absorption changes from the cooling, whereas the second time constant reproduces the decay of the long-lived state.

6. Experimental setup

The UV-pump IR-probe measurements are based on a Ti-sapphire laser-amplifier system (Tsunami/Spitfire Pro, Spectra Physics) with 100 fs pulses at 800 nm and a repetition rate of 1 kHz. Excitation pulses were obtained by harmonic generation (266 nm) or by a frequency doubled two stages noncolinear optical parametric amplifier (295 nm). The 266 nm pulses were stretched via propagation in fused silica to a duration of ca. 1ps to minimize two-photon reactions. Excitation energies were 0.5- 1μJ with a beam diameter at the sample position of 150 μm. The probe pulse in the mid-IR was generated by a combination of a non-collinear and a collinear optical parametric amplifier, followed by a difference frequency mixing in a $AgGaS_2$-crystal. The IR pulse passing the sample was spectrally dispersed (Brucker, Chromex 250 IS) and detected by a 64 channel MCT array (Infrared Systems Development, IR-0144). All experiments were performed under magic angle conditions and at room temperature. The sample volume was exchanged between two consecutive excitation pulses in a 100 μm flow cuvette with BaF_2 windows.

References:

[1] M. Banyay, M. Sarkar, A. Gräslund, *Biophysical Chemistry* **2003**, *104*, 477-488.

[2] W. J. Schreier, T. E. Schrader, F. O. Koller, P. Gilch, C. E. Crespo-Hernández, V. N. Swaminathan, T. Carell, W. Zinth, B. Kohler, *Science* **2007**, *315*, 625-629.

[3] D. B. Bucher, B. M. Pilles, T. Carell, W. Zinth, *Proceedings of the National Academy of Sciences* **2014**, *111*, 4369-4374.

[4] D. B. Bucher, B. M. Pilles, T. Pfaffeneder, T. Carell, W. Zinth, *ChemPhysChem* **2014**, *15*, 420-423.

[5] M. Vorlickova, I. Kejnovska, K. Bednrova, D. Renciuk, J. Kypr, *Chirality* **2012**, *24*, 691-698.

5 Summary and Outlook

Absorption of UV-light by the nucleobases in DNA can induce photochemical reactions leading to lesions which may result in cell death or cancer [8, 9, 10, 11, 12, 13]. To minimize these lesions in the genome nature has evolved sophisticated protection and repair mechanisms [5, 6, 7]. In addition to these biological based protection systems, DNA protects itself from damaging photoreactions by having extraordinary photophysical and photochemical properties [24]. The photostability of DNA monomers is well understood [26, 47]. All natural nucleobases have extremely short excited state lifetimes, reducing the probability to undergo damaging photochemical reactions. This ultrafast deactivation is a special property of natural bases, since structural modifications lead to longer-living excited states and thus to higher photoreactivity. However, the biological important molecules are DNA single and double strands, which are stabilized by base stacking and base pairing. It is known that base stacking causes long-living excited states in single strands. However, the underlying molecular processes are under discussion (section 2.2.1.2). In addition the influence of base pairing in DNA double strands on the excited state dynamics is largely unknown (section 2.2.1.3).

Thus, the aim of this thesis was to characterize the photophysical processes occurring after light absorption in the biological important DNA single and double strands. Especially the structural influence of base stacking and base pairing on the excited state dynamics of nucleobases should be investigated. All investigations of this thesis were based on ultrafast IR-spectroscopy. The fingerprint absorbance bands in the mid-IR enabled the distinction of the four DNA bases, which provided a detailed insight into the photophysical processes of each base in its natural environment.

The photophysics of single-stranded DNA – Influence of base stacking

In the first part of this thesis, the influence of base stacking has been investigated. For this reason, single-stranded DNA has been used, where base pairing is absent and where base stacking is the dominant interaction between adjacent bases. In these experiments, specially designed oligonucleotides were used which allowed to selectively excite one base in the strand (the minor natural base 5-methyl-2′-deoxycytidine (mC) or guanine (G)) at 295 nm. Due to the characteristic absorbance bands in the IR, vibrational spectroscopy was used to selectively probe the excited state dynamics of each nucleobase in these strands. Thus, not only the excited state decay of the excited base could be monitored individually, but also processes occurring on neighboring bases, which were not directly involved in the excitation process, could be probed. With this new approach – selective excitation and selective probing in the IR – the photophysical processes in single-stranded DNA could be elucidated (Fig. 5.1).

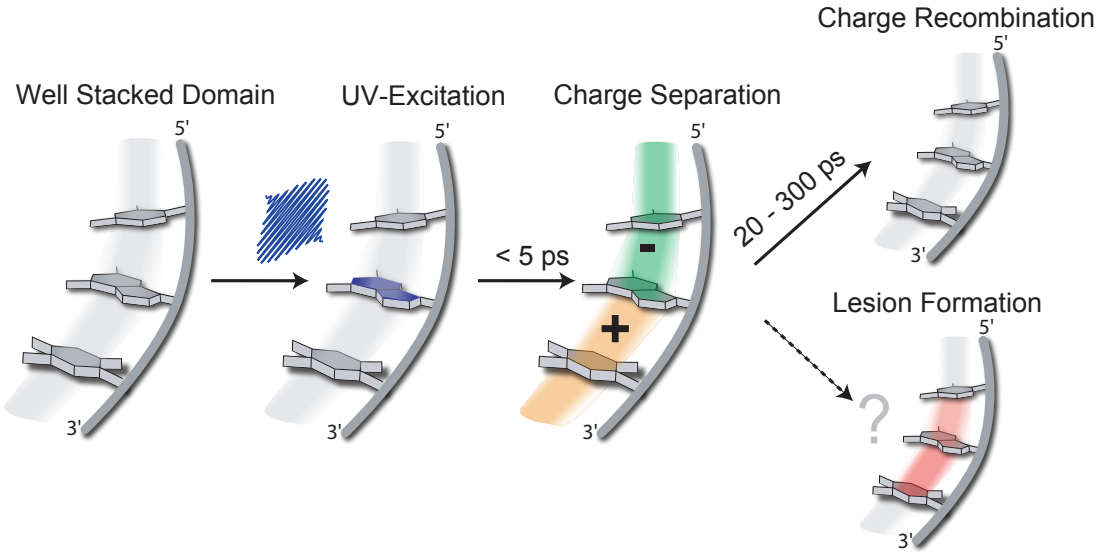

Figure 5.1 – Model for the excited state decay of single-stranded stacked DNA.

It could be shown that base stacking leads to long-living states on the 100 ps time scale with amplitudes of up to 40%, in accordance with literature. Interestingly, the mid-IR probing revealed that not only the directly excited base (mC or G) is involved in the long-living excited state, but also adjacent bases. The molecular nature of the long-living state could be identified by its transient IR-spectrum which showed characteristic absorbance bands. For the identification of a possible charge transfer state, a reference spectrum of the mC radical cation was recorded by a two-photon ionization process. Marker bands of the mC radical cation as well as of other base radical cations and anions could be identified in the IR-spectrum of the long-living state. Thus, light excitation leads to charge transfer states between adjacent bases in DNA single strands. The charge transfer is directed by the redox potential of the involved nucleobases and is thus governed by the base sequence.

Additional investigations could show that the charge separated states are delocalized in stacked domains of about 3-4 bases along the DNA strand. Charge delocalization has been postulated in the DNA charge transport community, but a spectroscopic evidence has not been published so far. Thus, DNA photophysics and DNA charge transport are strongly related research topics and are based on similar mechanisms.

In future, the question of biological consequences of reactive radicals induced by UV-light in DNA should be addressed. It is not known, if these long-living charge transfer states can overcome the Coulomb attraction and migrate along DNA, which would implicate reductive or oxidative lesion formation. These kind of lesions have not been considered in UV-induced damage formation in DNA before. Thus, future biochemical experiments have to characterize potential lesions induced by the charge transfer states in DNA. In addition, a possible reductive repair of CPD lesions by the charge transfer states should also be considered.

The photophysics of double-stranded DNA – Influence of base pairing

In the second part of this thesis, the influence of base pairing has been investigated in a natural sample – the calf thymus DNA and in oligonucleotide model systems. IR-marker bands for each of the four nucleobases have been identified and assigned to the IR-spectrum of complex natural calf thymus DNA. This allowed the observation of the excited state decay of each nucleobase individually after non-selective excitation of all bases of the calf thymus DNA at 266 nm. Thus, the excited state dynamics of each of the four nucleobases in their natural environment have been observed for the first time. According to the literature, the excited state decay in double-stranded DNA is controlled by base stacking and results in the formation of charge transfer states. As a consequence a complex decay mechanism caused by the charge transfer states depending on the involved sequence has been expected (as described in the previous paragraph). However, in contrast to this scientific consensus, an unexpectedly simple decay scheme has been discovered. The excited states of bases connected by the Watson-Crick hydrogen bonds decay in a concerted way with a joint time constant of 40 ps for the G-C and 210 ps for the A-T base pair.

This surprising result was further verified by comparing the excited state decay in single- and double-stranded model systems. In single strands, charge transfer states were detected, supporting the observations made in the first part of the thesis. Upon formation of double strands by merging the single strands, the charge transfer states were quenched. These results directly showed that base stacking is not the dominant interaction for the photophysical processes as suggested in literature. On the contrary, it is the base pairing, which controls the excited state dynamics in the natural DNA duplex (Fig. 5.2). The strong influence of the base pairing hydrogen bonds on the excited state decay points to the involvement of a proton transfer in the excited state deactivation. This proton transfer presumably bypasses the population of the reactive charge transfer states. Thus, the double helical structure with its Watson-Crick base pairing scheme is presumably responsible for the low photoreactivity of DNA.

Three basic mechanisms – the excited state tautomerization, the interstrand electron driven proton transfer or the intrastrand electron induced proton transfer – are conceivable. However, the results could not distinguish between these models, mainly due to the complexity of the investigated systems. Further time-resolved experiments in combination

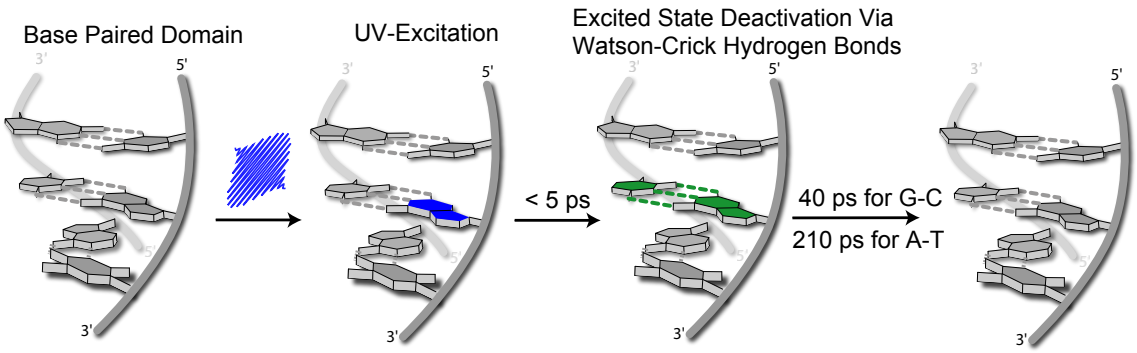

Figure 5.2 – Model for the excited state decay of double-stranded, Watson-Crick base paired DNA.

with quantum chemical simulations have to address the question of the proton transfer mechanism in future.

In summary, it could be shown that base stacking causes reactive charge transfer states, which are delocalized along the DNA strand (Fig. 5.1). This is in strong contrast to the effective excited state deactivation mechanisms in single nucleobases. As a consequence base stacking is potentially responsible for DNA damage. However, upon Watson-Crick base pairing, these charged radical states are quenched (Fig. 5.2). Thus, the double helical structure opens up an additional decay channel, improving the photostability and protects DNA from photolesions. The results demonstrate, that the molecular mechanism of the excited state decay is changing with each step of further complexity – from the single base to natural DNA.

List of Figures

Nomenclature

A	adenine
BBO	beta barium borate
BER	base excision repair
C	cytosine
CPD	cyclobutane pyrimidine dimer
dAMP	adenosine monophosphate monomer
DFM	difference frequency mixing
DNA	deoxyribonucleic acid
FTIR	Fourier Transform Infrared Spectroscopy
G	guanine
HOMO	highest occupied molecular orbital
LUMO	lowest unoccupied molecular orbital
mC	5-methyl-2'-deoxycytidine
NER	nucleotide excision repair
NIR	near infrared
NOPA	non-collinear optical parametric amplifier
OPA	optical parametric amplifier
RNA	ribonucleic acid
SFG	sum frequency mixing
T	thymine
U	uracil
WL	white light

Bibliography

[1] Albert L. Lehninger, David L. Nelson, and M. Michael Cox. *Prinzipien der Biochemie*. Spektrum Akademischer Verlag GmbH, Heidelberg, Berlin, Oxford, 2nd edition, 1994.

[2] Bruce Alberts, Alexander Johnson, Julian Lewis, Martin Raff, Keith Roberts, and Peter Walter. *The Molecular Biology of the Cell*. Garland Science, Taylor & Francis Group, New York, 5th edition, 2008.

[3] Lubert Stryer. Biochemistry. W. H. Freeman and Company, New York, 7th edition, 2012.

[4] Nicholas E. Geacintov and Suse Broyde. *The Chemical Biology Of DNA Damage*. WILEY-VCH Verlag GmbH & Co. KGaA, Weinheim, 2010.

[5] Jan H. J. Hoeijmakers. Genome maintenance mechanisms for preventing cancer. *Nature*, 411(6835):366, May 2001.

[6] Alberto Ciccia and Stephen J. Elledge. The DNA damage response: Making it safe to play with knives. *Molecular Cell*, 40(2):179–204, October 2010.

[7] Wei Yang. Surviving the sun: Repair and bypass of DNA UV lesions. *Protein Science : A Publication of the Protein Society*, 20(11):1781–1789, November 2011.

[8] John Stephen Taylor. DNA, sunlight, and skin cancer. *J. Chem. Educ.*, 67(10):835, 1990.

[9] John Stephen Taylor. Unraveling the molecular pathway from sunlight to skin cancer. *Accounts of Chemical Research*, 27(3):76–82, March 1994.

[10] H. S. Black, F. R. deGruijl, P. D. Forbes, J. E. Cleaver, H. N. Ananthaswamy, E. C. deFabo, S. E. Ullrich, and R. M. Tyrrell. Photocarcinogenesis: an overview. *Journal of Photochemistry and Photobiology B: Biology*, 40(1):29–47, August 1997.

[11] Deevya L. Narayanan, Rao N. Saladi, and Joshua L. Fox. Review: Ultraviolet radiation and skin cancer. *International Journal of Dermatology*, 49(9):978–986, September 2010.

[12] D. E. Brash, J. A. Rudolph, J. A. Simon, A. Lin, G. J. McKenna, H. P. Baden, A. J. Halperin, and J. Ponten. A role for sunlight in skin cancer: UV-induced p53 mutations in squamous cell carcinoma. *Proceedings of the National Academy of Sciences*, 88(22):10124–10128, November 1991.

[13] Gerd P. Pfeifer, Young-Hyun You, and Ahmad Besaratinia. Mutations induced by ultraviolet light. *Mutation Research/Fundamental and Molecular Mechanisms of Mutagenesis*, 571(1-2):19–31, April 2005.

[14] Howard W. Rogers, Martin A. Weinstock, Ashlynne R. Harris, Michael R. Hinckley, Steven R. Feldman, Alan B. Fleischer, and Brett M. Coldiron. Incidence estimate of nonmelanoma skin cancer in the United States, 2006. *Archives of Dermatology*, 146(3):283–287, March 2010.

[15] Infographics American Cancer Society. Available from URL: http://www.cancer.org/research/infographicgallery/skin-cancer-prevention [accessed 2014, september 22].

[16] Amaya Viros, Berta Sanchez-Laorden, Malin Pedersen, Simon J. Furney, Joel Rae, Kate Hogan, Sarah Ejiama, Maria Romina Girotti, Martin Cook, Nathalie Dhomen, and Richard Marais. Ultraviolet radiation accelerates BRAF-driven melanomagenesis by targeting TP53. *Nature*, 511(7510):478–482, July 2014.

[17] Eran Hodis, Ian R. Watson, Gregory V. Kryukov, Stefan T. Arold, Marcin Imielinski, Jean-Philippe Theurillat, Elizabeth Nickerson, Daniel Auclair, Liren Li, Chelsea Place, Daniel DiCara, Alex H. Ramos, Michael S. Lawrence, Kristian Cibulskis, Andrey Sivachenko, Douglas Voet, Gordon Saksena, Nicolas Stransky, Robert C. Onofrio, Wendy Winckler, Kristin Ardlie, Nikhil Wagle, Jennifer Wargo, Kelly Chong, Donald L. Morton, Katherine Stemke-Hale, Guo Chen, Michael Noble, Matthew Meyerson, John E. Ladbury, Michael A. Davies, Jeffrey E. Gershenwald, Stephan N. Wagner, Dave S. B. Hoon, Dirk Schadendorf, Eric S. Lander, Stacey B. Gabriel, Gad Getz, Levi A. Garraway, and Lynda Chin. A landscape of driver mutations in melanoma. *Cell*, 150(2):251–263, July 2012.

[18] Michael Krauthammer, Yong Kong, Byung Hak Ha, Perry Evans, Antonella Bacchiocchi, James P. McCusker, Elaine Cheng, Matthew J. Davis, Gerald Goh, Murim Choi, Stephan Ariyan, Deepak Narayan, Ken Dutton-Regester, Ana Capatana, Edna C. Holman, Marcus Bosenberg, Mario Sznol, Harriet M. Kluger, Douglas E. Brash, David F. Stern, Miguel A. Materin, Roger S. Lo, Shrikant Mane, Shuangge Ma, Kenneth K. Kidd, Nicholas K. Hayward, Richard P. Lifton, Joseph Schlessinger, Titus J. Boggon, and Ruth Halaban. Exome sequencing identifies recurrent somatic RAC1 mutations in melanoma. *Nature Genetics*, 44(9):1006–1014, September 2012.

[19] Michael F. Berger, Eran Hodis, Timothy P. Heffernan, Yonathan Lissanu Deribe, Michael S. Lawrence, Alexei Protopopov, Elena Ivanova, Ian R. Watson, Elizabeth Nickerson, Papia Ghosh, Hailei Zhang, Rhamy Zeid, Xiaojia Ren, Kristian Cibulskis, Andrey Y. Sivachenko, Nikhil Wagle, Antje Sucker, Carrie Sougnez, Robert Onofrio, Lauren Ambrogio, Daniel Auclair, Timothy Fennell, Scott L. Carter, Yotam Drier, Petar Stojanov, Meredith A. Singer, Douglas Voet, Rui Jing, Gordon Saksena, Jordi Barretina, Alex H. Ramos, Trevor J. Pugh, Nicolas Stransky, Melissa Parkin, Wendy Winckler, Scott Mahan, Kristin Ardlie, Jennifer Baldwin, Jennifer Wargo, Dirk

Schadendorf, Matthew Meyerson, Stacey B. Gabriel, Todd R. Golub, Stephan N. Wagner, Eric S. Lander, Gad Getz, Lynda Chin, and Levi A. Garraway. Melanoma genome sequencing reveals frequent PREX2 mutations. *Nature*, 485(7399):502–506, May 2012.

[20] American Cancer Society. Cancer Facts & Figures 2014. Atlanta: American Cancer Society; 2014.

[21] The Surgeon General's Call to Action to Prevent Skin Cancer. U.S. Department of Health and Human Services. Washington, DC: U.S. Departement of Health and Human Services, Office of the Surgeon General; 2014.

[22] Jan H.J. Hoeijmakers. DNA damage, aging, and cancer. *New England Journal of Medicine*, 361(15):1475–1485, October 2009.

[23] Vivek T. Natarajan, Parul Ganju, Amrita Ramkumar, Ritika Grover, and Rajesh S. Gokhale. Multifaceted pathways protect human skin from UV radiation. *Nature Chemical Biology*, 10(7):542–551, July 2014.

[24] Jean Cadet and Paul Vigny. The photochemistry of nucleic acid in bioorganic photochemistry. In *Bioorganic Photochemistry, Photochemistry and the Nucleic Acids*, pages 1–272. John Wiley & Sons, Inc., New York, 1990.

[25] Marco Montalti, Alberto Credi, Luca Prodi, and M. Theresa Gandolfi. *Handbook of Photochemistry*. Taylor & Francis Group, Boca Raton, 3rd edition, 2006.

[26] Carlos E. Crespo-Hernandez, Boiko Cohen, Patrick M. Hare, and Bern Kohler. Ultrafast excited-state dynamics in nucleic acids. *Chemical Reviews*, 104(4):1977–2020, April 2004.

[27] Armen Y. Mulkidjanian, Dmitry A. Cherepanov, and Michael Y. Galperin. Survival of the fittest before the beginning of life: selection of the first oligonucleotide-like polymers by UV light. *BMC Evolutionary Biology*, 3(1):12, May 2003.

[28] Luis Serrano-Andres and Manuela Merchan. Are the five natural DNA/RNA base monomers a good choice from natural selection?: A photochemical perspective. *Journal of Photochemistry and Photobiology C: Photochemistry Reviews*, 10(1):21–32, March 2009.

[29] Charles S. Cockell and Gerda Horneck. The history of the UV radiation climate of the earth-theoretical and space-based observations. *Photochemistry and Photobiology*, 73(4):447–451, April 2001.

[30] Charles R. Cantor and Paul. R. Schimmel. The behaviour of biological macromolecules. In *Biophysical Chemistry*, volume III. W. H. Freeman and Company, San Francisco, 1980.

[31] Eric T. Kool. Hydrogen bonding, base stacking, and steric effects in DNA replication. *Annual Review of Biophysics & Biomolecular Structure*, 30(1):1–22, June 2001.

[32] Victor A. Bloomfield, Donald M. Crothers, and Ignoco Tinoco (jun). *Nucleic Acids: Structures, Properties, and Functions*. University Science Books, Sausalito, 2000.

[33] Kevin M. Guckian, Barbara A. Schweitzer, Rex X.-F. Ren, Charles J. Sheils, Deborah C. Tahmassebi, and Eric T. Kool. Factors contributing to aromatic stacking in water: Evaluation in the context of DNA. *Journal of the American Chemical Society*, 122(10):2213–2222, February 2000.

[34] Benedict W. Bangerter and Sunney I. Chan. Proton magnetic resonance studies of ribose dinucleoside monophosphates in aqueous solution. II. nature of the base-stacking interaction in adenylyl-(3' - 5')-cytidine and cytidylyl-(3' - 5')adenosine. *Journal of the American Chemical Society*, 91(14):3910–3921, July 1969.

[35] J. D. Watson and F. H. C. Crick. Molecular structure of nucleic acids: A structure for deoxyribose nucleic acid. *Nature*, 171(4356):737–738, April 1953.

[36] Hans Ulrich Koecke, Peter Emschermann, and Eckhart Haerle. *Biologie*. F. K. Schattauer Verlagsgesellschaft mbH, Stuttgart, 4th edition, 2000.

[37] Peter Yakovchuk, Ekaterina Protozanova, and Maxim D. Frank-Kamenetskii. Base-stacking and base-pairing contributions into thermal stability of the DNA double helix. *Nucleic Acids Research*, 34(2):564–574, January 2006.

[38] Narendra Narayana and Michael A. Weiss. Crystallographic analysis of a sex-specific enhancer element: sequence-dependent DNA structure, hydration, and dynamics. *Journal of Molecular Biology*, 385(2):469–490, January 2009.

[39] *DeLano Scientific LLC, 400 Oyster Point Blvd., Suite 213, South San Francisco, CA 94080-1918, USA. http://www.pymol.org.*

[40] Mattanjah S. de Vries and Pavel Hobza. Gas-phase spectroscopy of biomolecular building blocks. *Annual Review of Physical Chemistry*, 58(1):585–612, 2007.

[41] Hiroyuki Saigusa. Excited-state dynamics of isolated nucleic acid bases and their clusters. *Journal of Photochemistry and Photobiology C: Photochemistry Reviews*, 7(4):197–210, December 2006.

[42] Thomas Gustavsson, Alexei Sharonov, and Dimitra Markovitsi. Thymine, thymidine and thymidine 5'-monophosphate studied by femtosecond fluorescence upconversion spectroscopy. *Chemical Physics Letters*, 351(3-4):195–200, January 2002.

[43] Paraic M. Keane, Michal Wojdyla, Gerard W. Doorley, Graeme W. Watson, Ian P. Clark, Gregory M. Greetham, Anthony W. Parker, Michael Towrie, John M. Kelly, and Susan J. Quinn. A comparative picosecond transient infrared study of 1-methylcytosine and 5'-dCMP that sheds further light on the excited states of cytosine derivatives. *Journal of the American Chemical Society*, 133(12):4212–4215, March 2011.

[44] Patrick M. Hare, Carlos E. Crespo-Hernandez, and Bern Kohler. Internal conversion to the electronic ground state occurs via two distinct pathways for pyrimidine bases in aqueous solution. *Proceedings of the National Academy of Sciences of the United States of America*, 104(2):435–440, January 2007.

[45] D. Onidas, D. Markovitsi, S. Marguet, A. Sharonov, and T. Gustavsson. Fluorescence properties of DNA nucleosides and nucleotides: A refined steady-state and femtosecond investigation. *The Journal of Physical Chemistry B*, 106(43):11367–11374, October 2002.

[46] Karl Kleinermanns, Dana Nachtigallova, and Mattanjah S. de Vries. Excited state dynamics of DNA bases. *International Reviews in Physical Chemistry*, 32(2):308–342, 2013.

[47] Chris T. Middleton, Kimberly de La Harpe, Charlene Su, Yu Kay Law, Carlos E. Crespo-Hernandez, and Bern Kohler. DNA excited-state dynamics: From single bases to the double helix. *Annual Review of Physical Chemistry*, 60(1):217–239, May 2009.

[48] *ISO 21348 Definitions of Solar Irradiance Spectral Categories.*

[49] Vincenzo Balzani, Paola Ceroni, and Alberto Juris. *Photochemistry and Photophysics.* WILEY-VCH Verlag GmbH & Co. KGaA, Weinheim, 2014.

[50] W. Zinth, B. P. Fingerhut, T. T. Herzog, G. R. Ryseck, K. Haiser, F. F. Graupner, K. Heil, P. Gilch, W. J. Schreier, T. Carell, and R. de Vivie-Riedle. Ultrafast spectroscopy of UV-induced DNA-lesions - on the search for strategies which keep DNA alive. *EPJ Web of Conferences*, (41):07005–p.1, February 2013.

[51] Malcolm Daniels and William Hauswirth. Fluorescence of the purine and pyrimidine bases of the nucleic acids in neutral aqueous solution at 300 k. *Science*, 171(3972):675–677, February 1971.

[52] S. J. Strickler and Robert A. Berg. Relationship between absorption intensity and fluorescence lifetime of molecules. *The Journal of Chemical Physics*, 37(4):814–822, 1962.

[53] Boiko Cohen, Carlos E. Crespo-Hernandez, and Bern Kohler. Strickler-berg analysis of excited singlet state dynamics in DNA and RNA nucleosides. *Faraday Discussions*, 127:137, 2004.

[54] Joseph R. Lakowicz. *Principles of Fluorescence Spectroscopy.* Springer Science+Business Media, New York, 3rd edition, 2010.

[55] Patrik R. Callis. Polarized fluorescence and estimated lifetimes of the DNA bases at room temperature. *Chemical Physics Letters*, 61(3):568–570, March 1979.

[56] A. A. Oraevsky, A. V. Sharkov, and D. N. Nikogosyan. Picosecond study of electronically excited singlet states of nucleic acid components. *Chemical Physics Letters*, 83(2):276–280, October 1981.

[57] Jean-Pierre Ballini, Malcolm Daniels, and Paul Vigny. Wavelength-resolved lifetime measurements of emissions from DNA components and poly rA at room temperature excited with synchrotron radiation. *Journal of Luminescence*, 27(4):389–400, December 1982.

[58] Jean-Marc L. Pecourt, Jorge Peon, and Bern Kohler. Ultrafast internal conversion of electronically excited RNA and DNA nucleosides in water. *Journal of the American Chemical Society*, 122(38):9348–9349, September 2000.

[59] Jorge Peon and Ahmed H. Zewail. DNA/RNA nucleotides and nucleosides: direct measurement of excited-state lifetimes by femtosecond fluorescence up-conversion. *Chemical Physics Letters*, 348(3-4):255–262, November 2001.

[60] Boiko Cohen, Patrick M. Hare, and Bern Kohler. Ultrafast excited-state dynamics of adenine and monomethylated adenines in solution: Implications for the nonradiative decay mechanism. *Journal of the American Chemical Society*, 125(44):13594–13601, November 2003.

[61] Jean-Marc L. Pecourt, Jorge Peon, and Bern Kohler. DNA excited-state dynamics: Ultrafast internal conversion and vibrational cooling in a series of nucleosides. *Journal of the American Chemical Society*, 123(42):10370–10378, October 2001.

[62] Yuyuan Zhang, Roberto Improta, and Bern Kohler. Mode-specific vibrational relaxation of photoexcited guanosine 5-monophosphate and its acid form: a femtosecond broadband mid-IR transient absorption and theoretical study. *Physical Chemistry Chemical Physics*, 16(4):1487–1499, December 2013.

[63] S. Brondsted Nielsen, J. U. Andersen, J. S. Forster, P. Hvelplund, B. Liu, U. V. Pedersen, and S. Tomita. Photodestruction of adenosine 5'-monophosphate (AMP) nucleotide ions in vacuo: Statistical versus nonstatistical processes. *Physical Review Letters*, 91(4):048302, July 2003.

[64] Chris T. Middleton, Boiko Cohen, and Bern Kohler. Solvent and solvent isotope effects on the vibrational cooling dynamics of a DNA base derivative. *The Journal of Physical Chemistry A*, 111(42):10460–10467, October 2007.

[65] Samir Kumar Pal and Ahmed H. Zewail. Dynamics of water in biological recognition. *Chemical Reviews*, 104(4):2099–2124, April 2004.

[66] Mario Barbatti, Adelia J. A. Aquino, Jaroslaw J. Szymczak, Dana Nachtigallova, Pavel Hobza, and Hans Lischka. Relaxation mechanisms of UV-photoexcited DNA and RNA nucleobases. *Proceedings of the National Academy of Sciences*, 107(50):21453–21458, December 2010.

[67] Wolfgang Domcke and David R. Yarkony. Role of conical intersections in molecular spectroscopy and photoinduced chemical dynamics. *Annual Review of Physical Chemistry*, 63(1):325–352, 2012.

[68] Spiridoula Matsika and Pascal Krause. Nonadiabatic events and conical intersections. *Annual Review of Physical Chemistry*, 62(1):621–643, 2011.

[69] Nina Ismail, Lluis Blancafort, Massimo Olivucci, Bern Kohler, and Michael A. Robb. Ultrafast decay of electronically excited singlet cytosine via a pi,pi* to nO,pi* state switch. *Journal of the American Chemical Society*, 124(24):6818–6819, June 2002.

[70] M. K. Shukla and Jerzy Leszczynski. Electronic spectra, excited state structures and interactions of nucleic acid bases and base assemblies: A review. *Journal of Biomolecular Structure and Dynamics*, 25(1):93–118, 2007.

[71] Thomas Gustavsson, Roberto Improta, and Dimitra Markovitsi. DNA/RNA: Building blocks of life under UV irradiation. *The Journal of Physical Chemistry Letters*, 1(13):2025–2030, July 2010.

[72] Brant E. Billinghurst, Ralph Yeung, and Glen R. Loppnow. Excited-state structural dynamics of 5-fluorouracil. *The Journal of Physical Chemistry A*, 110(19):6185–6191, May 2006.

[73] Brant E. Billinghurst and Glen R. Loppnow. Excited-state structural dynamics of cytosine from resonance raman spectroscopy. *The Journal of Physical Chemistry A*, 110(7):2353–2359, February 2006.

[74] B. K. McFarland, J. P. Farrell, S. Miyabe, F. Tarantelli, A. Aguilar, N. Berrah, C. Bostedt, J. D. Bozek, P. H. Bucksbaum, J. C. Castagna, R. N. Coffee, J. P. Cryan, L. Fang, R. Feifel, K. J. Gaffney, J. M. Glownia, T. J. Martinez, M. Mucke, B. Murphy, A. Natan, T. Osipov, V. S. Petrovic, S. Schorb, Th Schultz, L. S. Spector, M. Swiggers, I. Tenney, S. Wang, J. L. White, W. White, and M. Guehr. Ultrafast X-ray Auger probing of photoexcited molecular dynamics. *Nature Communications*, 5(4235), June 2014.

[75] Mario Barbatti. Photorelaxation induced by water-chromophore electron transfer. *Journal of the American Chemical Society*, 136(29):10246–10249, July 2014.

[76] Deniz Tuna, Andrzej L. Sobolewski, and Wolfgang Domcke. Mechanisms of ultrafast excited-state deactivation in adenosine. *The Journal of Physical Chemistry A*, 118(1):122–127, December 2013.

[77] Rosalie J. Malone, Angela M. Miller, and Bern Kohler. Singlet excited-state lifetimes of cytosine derivatives measured by femtosecond transient absorption. *Photochemistry and Photobiology*, 77(2):158–164, 2003.

[78] Zachary D. Smith and Alexander Meissner. DNA methylation: roles in mammalian development. *Nature Reviews Genetics*, 14(3):204–220, March 2013.

[79] Don-Marc Franchini, Kerstin-Maike Schmitz, and Svend K. Petersen-Mahrt. 5-methylcytosine DNA demethylation: More than losing a methyl group. *Annual Review of Genetics*, 46(1):419–441, 2012.

[80] Stella Tommasi, Mikhail F. Denissenko, and Gerd P. Pfeifer. Sunlight induces pyrimidine dimers preferentially at 5-methylcytosine bases. *Cancer Research*, 57(21):4727 –4730, November 1997.

[81] Young-Hyun You, Chun Li, and Gerd P Pfeifer. Involvement of 5-methylcytosine in sunlight-induced mutagenesis. *Journal of Molecular Biology*, 293(3):493–503, October 1999.

[82] Luis Serrano-Andres, Manuela Merchan, and Antonio C. Borin. Adenine and 2-aminopurine: Paradigms of modern theoretical photochemistry. *Proceedings of the National Academy of Sciences*, 103(23):8691–8696, June 2006.

[83] Patrick M. Hare, Carlos E. Crespo-Hernandez, and Bern Kohler. Solvent-dependent photophysics of 1-cyclohexyluracil: Ultrafast branching in the initial bright state leads nonradiatively to the electronic ground state and a long-lived 1npi* state. *The Journal of Physical Chemistry B*, 110(37):18641–18650, September 2006.

[84] Patrick M. Hare, Chris T. Middleton, Kristin I. Mertel, John M. Herbert, and Bern Kohler. Time-resolved infrared spectroscopy of the lowest triplet state of thymine and thymidine. *Chemical Physics*, 347(1-3):383–392, May 2008.

[85] Christel M. Marian. A new pathway for the rapid decay of electronically excited adenine. *The Journal of Chemical Physics*, 122(10):104314, March 2005.

[86] Mario Barbatti, Adelia J. A. Aquino, Jaroslaw J. Szymczak, Dana Nachtigallova, and Hans Lischka. Photodynamical simulations of cytosine: characterization of the ultrafast bi-exponential UV deactivation. *Physical Chemistry Chemical Physics*, 13(13):6145–6155, March 2011.

[87] Lluis Blancafort. Energetics of cytosine singlet excited-state decay paths - A difficult case for CASSCF and CASPT2. *Photochemistry and Photobiology*, 83(3):603–610, May 2007.

[88] Susan Quinn, Gerard W. Doorley, Graeme W. Watson, Alexander J. Cowan, Michael W. George, Anthony W. Parker, Kate L. Ronayne, Michael Towrie, and John M. Kelly. Ultrafast IR spectroscopy of the short-lived transients formed by UV excitation of cytosine derivatives. *Chemical Communications*, page 2130, 2007.

[89] Raj K. Bansal. *Synthetic Approaches in Organic Chemistry*. Jones and Bartlett Publishers International, Inc., London, 1998.

[90] M. A. El-Sayed. Spin-orbit coupling and the radiationless processes in nitrogen heterocyclics. *The Journal of Chemical Physics*, 38(12):2834–2838, June 1963.

[91] Francisco Bosca, Virginie Lhiaubet-Vallet, M. Consuelo Cuquerella, Jose V. Castell, and Miguel A. Miranda. The triplet energy of thymine in DNA. *Journal of the American Chemical Society*, 128(19):6318–6319, April 2006.

[92] J. Isaksson, S. Acharya, J. Barman, P. Cheruku, and J. Chattopadhyaya. Single-stranded adenine-rich DNA and RNA retain structural characteristics of their respective double-stranded conformations and show directional differences in stacking pattern. *Biochemistry*, 43(51):15996–16010, November 2004.

[93] Carlos E. Crespo-Hernandez and Bern Kohler. Influence of secondary structure on electronic energy relaxation in adenine homopolymers. *The Journal of Physical Chemistry B*, 108(30):11182–11188, July 2004.

[94] Bern Kohler. Nonradiative decay mechanisms in DNA model systems. *The Journal of Physical Chemistry Letters*, 1(13):2047–2053, July 2010.

[95] Dimitra Markovitsi, Alexei Sharonov, Delphine Onidas, and Thomas Gustavsson. The effect of molecular organisation in DNA oligomers studied by femtosecond fluorescence spectroscopy. *ChemPhysChem*, 4(3):303–305, March 2003.

[96] Dimitra Markovitsi, Thomas Gustavsson, and Alexei Sharonov. Cooperative effects in the photophysical properties of self-associated triguanosine diphosphates. *Photochemistry and Photobiology*, 79(6):526–530, June 2004.

[97] Irene Conti, Piero Altoe, Marco Stenta, Marco Garavelli, and Giorgio Orlandi. Adenine deactivation in DNA resolved at the CASPT2//CASSCF/AMBER level. *Physical Chemistry Chemical Physics*, 12(19):5016–5023, May 2010.

[98] Dana Nachtigallova, Tomas Zeleny, Matthias Ruckenbauer, Thomas Mueller, Mario Barbatti, Pavel Hobza, and Hans Lischka. Does stacking restrain the photodynamics of individual nucleobases? *Journal of the American Chemical Society*, 132(24):8261–8263, June 2010.

[99] M. Kasha, H. R. Rawls, and M. Ashraf El-Bayoumi. The exciton model in molecular spectroscopy. *Pure and Applied Chemistry*, 11(3-4), January 1965.

[100] J. Eisinger and R. G. Shulman. Excited electronic states of DNA. *Science*, 161(3848):1311–1319, September 1968.

[101] B. Bouvier, T. Gustavsson, D. Markovitsi, and P. Millie. Dipolar coupling between electronic transitions of the DNA bases and its relevance to exciton states in double helices. *Chemical Physics*, 275(1-3):75–92, January 2002.

[102] Benjamin Bouvier, Jean-Pierre Dognon, Richard Lavery, Dimitra Markovitsi, Philippe Millie, Delphine Onidas, and Krystyna Zakrzewska. Influence of conformational dynamics on the exciton states of DNA oligomers. *The Journal of Physical Chemistry B*, 107(48):13512–13522, December 2003.

[103] Emanuela Emanuele, Krystyna Zakrzewska, Dimitra Markovitsi, Richard Lavery, and Philippe Millie. Exciton states of dynamic DNA double helices: Alternating dCdG sequences. *The Journal of Physical Chemistry B*, 109(33):16109–16118, August 2005.

[104] Dimitra Markovitsi, Francis Talbot, Thomas Gustavsson, Delphine Onidas, Elodie Lazzarotto, and Sylvie Marguet. Molecular spectroscopy: Complexity of excited-state dynamics in DNA. *Nature*, 441(7094):E7, June 2006.

[105] Dimitra Markovitsi, Delphine Onidas, Thomas Gustavsson, Francis Talbot, and Elodie Lazzarotto. Collective behavior of franck-condon excited states and energy transfer in DNA double helices. *Journal of the American Chemical Society*, 127(49):17130–17131, December 2005.

[106] Dimitra Markovitsi, Thomas Gustavsson, and Akos Banyasz. Absorption of UV radiation by DNA: Spatial and temporal features. *Mutation Research/Reviews in Mutation Research*, 704(1-3):21–28, April 2010.

[107] Dimitra Markovitsi, Thomas Gustavsson, and Francis Talbot. Excited states and energy transfer among DNA bases in double helices. *Photochemical & Photobiological Sciences*, 6(7):717–724, July 2007.

[108] Dimitra Markovitsi, Thomas Gustavsson, and Ignacio Vaya. Fluorescence of DNA duplexes: From model helices to natural DNA. *The Journal of Physical Chemistry Letters*, 1(22):3271–3276, November 2010.

[109] Alexander A. Voityuk. Effects of dynamic disorder on exciton delocalization and photoinduced charge separation in DNA. *Photochemical & Photobiological Sciences*, 12(8):1303–1309, August 2013.

[110] Ivan Buchvarov, Qiang Wang, Milen Raytchev, Anton Trifonov, and Torsten Fiebig. Electronic energy delocalization and dissipation in single- and double-stranded DNA. *Proceedings of the National Academy of Sciences*, 104(12):4794–4797, March 2007.

[111] Charlene Su, Chris T. Middleton, and Bern Kohler. Base-stacking disorder and excited-state dynamics in single-stranded adenine homo-oligonucleotides. *The Journal of Physical Chemistry B*, 116(34):10266–10274, August 2012.

[112] Carlos E. Crespo-Hernandez, Boiko Cohen, and Bern Kohler. Base stacking controls excited-state dynamics in AT DNA. *Nature*, 436(7054):1141–1144, August 2005.

[113] Carlos E. Crespo-Hernandez, Boiko Cohen, and Bern Kohler. Molecular spectroscopy: Complexity of excited-state dynamics in DNA (reply). *Nature*, 441(7094):E8–E8, June 2006.

[114] Susan L. Mattes and Samir Farid. Exciplexes and electron transfer reactions. *Science*, 226(4677):917–921, November 1984.

[115] J Eisinger, M Gueron, R G Shulman, and T Yamane. Excimer fluorescence of dinucleotides, polynucleotides, and DNA. *Proceedings of the National Academy of Sciences of the United States of America*, 55(5):1015–1020, May 1966.

[116] Tomohisa Takaya, Charlene Su, Kimberly de La Harpe, Carlos E. Crespo-Hernandez, and Bern Kohler. UV excitation of single DNA and RNA strands produces high yields of exciplex states between two stacked bases. *Proceedings of the National Academy of Sciences*, 105(30):10285–10290, July 2008.

[117] Ian R. Gould, Deniz Ege, Jacques E. Moser, and Samir Farid. Efficiencies of photoinduced electron-transfer reactions: role of the marcus inverted region in return electron transfer within geminate radical-ion pairs. *Journal of the American Chemical Society*, 112(11):4290–4301, May 1990.

[118] Wai-Ming Kwok, Chensheng Ma, and David Lee Phillips. Femtosecond time- and wavelength-resolved fluorescence and absorption spectroscopic study of the excited states of adenosine and an adenine oligomer. *Journal of the American Chemical Society*, 128(36):11894–11905, September 2006.

[119] Gloria Olaso-Gonzalez, Manuela Merchaan, and Luis Serrano-Andres. The role of adenine excimers in the photophysics of oligonucleotides. *Journal of the American Chemical Society*, 131(12):4368–4377, April 2009.

[120] Nina K Schwalb and Friedrich Temps. Base sequence and higher-order structure induce the complex excited-state dynamics in DNA. *Science*, 322(5899):243–245, October 2008.

[121] Ignacio Vaya, Thomas Gustavsson, Thierry Douki, Yuri Berlin, and Dimitra Markovitsi. Electronic excitation energy transfer between nucleobases of natural DNA. *J. Am. Chem. Soc.*, 134(28):11366–11368, 2012.

[122] Ignacio Vaya, Thomas Gustavsson, Francois-Alexandre Miannay, Thierry Douki, and Dimitra Markovitsi. Fluorescence of natural DNA: From the femtosecond to the nanosecond time scales. *Journal of the American Chemical Society*, 132(34):11834–11835, September 2010.

[123] F. Santoro, V. Barone, and R. Improta. Influence of base stacking on excited-state behavior of polyadenine in water, based on time-dependent density functional calculations. *Proceedings of the National Academy of Sciences*, 104(24):9931–9936, December 2007.

[124] F. Santoro, V. Barone, and R. Improta. Excited states decay of the a-t DNA: A PCM/TD-DFT study in aqueous solution of the (9-methyl-adenine)2 (1-methyl-thymine)2 stacked tetramer. *Journal of the American Chemical Society*, 131(42):15232–15245, October 2009.

[125] Roberto Improta and Vincenzo Barone. Interplay between "neutral" and "charge-transfer" excimers rules the excited state decay in adenine-rich polynucleotides. *Angewandte Chemie International Edition*, (50):12016–12019, October 2011.

[126] Eric R. Bittner. Lattice theory of ultrafast excitonic and charge-transfer dynamics in DNA. *The Journal of Chemical Physics*, 125(9):094909, September 2006.

[127] Lisbeth Munksgaard Nielsen, Soren Vronning Hoffmann, and Steen Brondsted Nielsen. Electronic coupling between photo-excited stacked bases in DNA and RNA strands with emphasis on the bright states initially populated. *Photochemical & Photobiological Sciences*, 12(8):1273–1285, August 2013.

[128] Akos Banyasz, Thomas Gustavsson, Delphine Onidas, Pascale Changenet-Barret, Dimitra Markovitsi, and Roberto Improta. Multi-pathway excited state relaxation of adenine oligomers in aqueous solution: A joint theoretical and experimental study. *Chemistry - A European Journal*, 19(11):3762–3774, 2013.

[129] Kimberly de La Harpe and Bern Kohler. Observation of long-lived excited states in DNA oligonucleotides with significant base sequence disorder. *The Journal of Physical Chemistry Letters*, 2(3):133–138, February 2011.

[130] Thomas Schultz, Elena Samoylova, Wolfgang Radloff, Ingolf V. Hertel, Andrzej L. Sobolewski, and Wolfgang Domcke. Efficient deactivation of a model base pair via excited-state hydrogen transfer. *Science*, 306(5702):1765–1768, March 2004.

[131] A. Douhal, S. K. Kim, and A. H. Zewail. Femtosecond molecular dynamics of tautomerization in model base pairs. *Nature*, 378(6554):260–263, November 1995.

[132] J. D. Watson and F. H. C. Crick. Genetical implications of the structure of deoxyribonucleic acid. *Nature*, 171(4361):964–967, May 1953.

[133] Per-Olov Loewdin. Proton tunneling in DNA and its biological implications. *Reviews of Modern Physics*, 35(3):724–732, July 1963.

[134] Weina Wang, Homme W. Hellinga, and Lorena S. Beese. Structural evidence for the rare tautomer hypothesis of spontaneous mutagenesis. *Proceedings of the National Academy of Sciences*, 108(43):17644–17648, October 2011.

[135] Jan Florian and Jerzy Leszczynski. Spontaneous DNA Mutations Induced by Proton Transfer in the Guanine-Cytosine Base Pairs: An Energetic Perspective. *Journal of the American Chemical Society*, 118(12):3010–3017, January 1996.

[136] Leonid Gorb, Yevgeniy Podolyan, Pawel Dziekonski, W. Andrzej Sokalski, and Jerzy Leszczynski. Double-proton transfer in adenine-thymine and guanine-cytosine base pairs. A post-hartree-fock ab initio study. *Journal of the American Chemical Society*, 126(32):10119–10129, August 2004.

[137] Satoshi Takeuchi and Tahei Tahara. The answer to concerted versus step-wise controversy for the double proton transfer mechanism of 7-azaindole dimer in solution. *Proceedings of the National Academy of Sciences*, 104(13):5285–5290, March 2007.

[138] Oh-Hoon Kwon and Ahmed H. Zewail. Double proton transfer dynamics of model DNA base pairs in the condensed phase. *Proceedings of the National Academy of Sciences*, 104(21):8703–8708, May 2007.

[139] Victor Guallar, Abderrazzak Douhal, Miquel Moreno, and Jose M. Lluch. DNA mutations induced by proton and charge transfer in the low-lying excited singlet electronic states of the DNA base pairs: A theoretical insight. *The Journal of Physical Chemistry A*, 103(31):6251–6256, August 1999.

[140] Vicenta Sauri, Joao P. Gobbo, Juan J. Serrano-Perez, Marcus Lundberg, Pedro B. Coto, Luis Serrano-Andres, Antonio C. Borin, Roland Lindh, Manuela Merchan, and Daniel Roca-Sanjuan. Proton/hydrogen transfer mechanisms in the guanine-cytosine base pair: Photostability and tautomerism. *Journal of Chemical Theory and Computation*, 9(1):481–496, January 2013.

[141] Joao Paulo Gobbo, Vicenta Sauri, Daniel Roca-Sanjuan, Luis Serrano-Andres, Manuela Merchan, and Antonio Carlos Borin. On the deactivation mechanisms of adenine-thymine base pair. *The Journal of Physical Chemistry B*, 116(13):4089–4097, April 2012.

[142] Andrzej L. Sobolewski and Wolfgang Domcke. Ab initio study of the excited-state coupled electron-proton-transfer process in the 2-aminopyridine dimer. *Chemical Physics*, 294(1):73–83, October 2003.

[143] Elena Samoylova, Wolfgang Radloff, Hans-Hermann Ritze, and Thomas Schultz. Observation of proton transfer in 2-aminopyridine dimer by electron and mass spectroscopy. *The Journal of Physical Chemistry A*, 113(29):8195–8201, July 2009.

[144] Andrzej L. Sobolewski and Wolfgang Domcke. Ab initio studies on the photophysics of the guanine-cytosine base pair. *Physical Chemistry Chemical Physics*, 6(10):2763–2771, May 2004.

[145] Serhiy Perun, Andrzej L. Sobolewski, and Wolfgang Domcke. Role of electron-driven proton-transfer processes in the excited-state deactivation of the adenine-thymine base pair. *The Journal of Physical Chemistry A*, 110(29):9031–9038, July 2006.

[146] Ali Abo-Riziq, Louis Grace, Eyal Nir, Martin Kabelac, Pavel Hobza, and Mattanjah S. de Vries. Photochemical selectivity in guanine-cytosine base-pair structures. *Proceedings of the National Academy of Sciences of the United States of America*, 102(1):20–23, April 2005.

[147] Andrzej L. Sobolewski, Wolfgang Domcke, and C. Hattig. Tautomeric selectivity of the excited-state lifetime of guanine/cytosine base pairs: The role of electron-driven

proton-transfer processes. *Proceedings of the National Academy of Sciences of the United States of America*, 102(50):17903–17906, December 2005.

[148] Nina K. Schwalb, Thomas Michalak, and Friedrich Temps. Ultrashort fluorescence lifetimes of hydrogen-bonded base pairs of guanosine and cytidine in solution. *The Journal of Physical Chemistry B*, 113(51):16365–16376, December 2009.

[149] Nina K. Schwalb and Friedrich Temps. Ultrafast electronic relaxation in guanosine is promoted by hydrogen bonding with cytidine. *Journal of the American Chemical Society*, 129(30):9272–9273, August 2007.

[150] Carlos E. Crespo-Hernandez, Kimberly de La Harpe, and Bern Kohler. Ground-state recovery following UV excitation is much slower in GC-DNA duplexes and hairpins than in mononucleotides. *Journal of the American Chemical Society*, 130(33):10844–10845, August 2008.

[151] Lars Biemann, Sergey A. Kovalenko, Karl Kleinermanns, Rainer Mahrwald, Morris Markert, and Roberto Improta. Excited state proton transfer is not involved in the ultrafast deactivation of guanine-cytosine pair in solution. *J. Am. Chem. Soc.*, 133(49):19664–19667, 2011.

[152] Monika Dargiewicz, Malgorzata Biczysko, Roberto Improta, and Vincenzo Barone. Solvent effects on electron-driven proton-transfer processes: adenine-thymine base pairs. *Physical Chemistry Chemical Physics*, 14(25):8981–8989, June 2012.

[153] Gerrit Groenhof, Lars V. Schaefer, Martial Boggio-Pasqua, Maik Goette, Helmut Grubmueller, and Michael A. Robb. Ultrafast deactivation of an excited cytosine-guanine base pair in DNA. *Journal of the American Chemical Society*, 129(21):6812–6819, May 2007.

[154] Kimberly de La Harpe, Carlos E. Crespo-Hernandez, and Bern Kohler. The excited-state lifetimes in a GC DNA duplex are nearly independent of helix conformation and base-pairing motif. *ChemPhysChem*, 10(9-10):1421–1425, 2009.

[155] Kimberly de La Harpe, Carlos E. Crespo-Hernandez, and Bern Kohler. Deuterium isotope effect on excited-state dynamics in an alternating GC oligonucleotide. *Journal of the American Chemical Society*, 131(48):17557–17559, December 2009.

[156] Jinquan Chen, Arun K. Thazhathveetil, Frederick D. Lewis, and Bern Kohler. Ultrafast excited-state dynamics in hexaethyleneglycol-linked DNA homoduplexes made of AT base pairs. *Journal of the American Chemical Society*, 135(28):10290–10293, July 2013.

[157] Steen Steenken. Electron-transfer-induced acidity/basicity and reactivity changes of purine and pyrimidine bases. Consequences of redox processes for DNA base pairs. *Free Rad. Res. Comms.*, 16(6):349–379, July 2009.

[158] Anil Kumar and Michael D. Sevilla. Proton-coupled electron transfer in DNA on formation of radiation-produced ion radicals. *Chemical Reviews*, 110(12):7002–7023, December 2010.

[159] Benjamin Elias, Caitriona Creely, Gerard W. Doorley, Martin M. Feeney, Cecile Moucheron, Andree Kirsch-DeMesmaeker, Joanne Dyer, David C. Grills, Michael W. George, Pavel Matousek, Anthony W. Parker, Michael Towrie, and John M. Kelly. Photooxidation of guanine by a ruthenium dipyridophenazine complex intercalated in a double-stranded polynucleotide monitored directly by picosecond visible and infrared transient absorption spectroscopy. *Chemistry - A European Journal*, 14(1):369–375, 2008.

[160] Chaehyuk Ko and Sharon Hammes-Schiffer. Charge-transfer excited states and proton transfer in model guanine-cytosine DNA duplexes in water. *The Journal of Physical Chemistry Letters*, 4:2540–2545, July 2013.

[161] Jean-Luc Ravanat, Thierry Douki, and Jean Cadet. Direct and indirect effects of UV radiation on DNA and its components. *Journal of Photochemistry and Photobiology B: Biology*, 63(1-3):88–102, October 2001.

[162] Thierry Douki. The variety of UV-induced pyrimidine dimeric photoproducts in DNA as shown by chromatographic quantification methods. *Photochemical & Photobiological Sciences*, 12(8):1286–1302, August 2013.

[163] Celine Desnous, Dominique Guillaume, and Pascale Clivio. Spore photoproduct: A key to bacterial eternal life. *Chemical Reviews*, 110(3):1213–1232, November 2009.

[164] Rajeshwar P. Sinha and Donat-P. Haeder. UV-induced DNA damage and repair: a review. *Photochemical & Photobiological Sciences*, 1(4):225–236, April 2002.

[165] Gengjie Lin and Lei Li. Elucidation of spore-photoproduct formation by isotope labeling. *Angewandte Chemie International Edition*, 49(51):9926–9929, December 2010.

[166] J. E. Donnellan and R. B. Setlow. Thymine photoproducts but not thymine dimers found in ultraviolet-irradiated bacterial spores. *Science*, 149(3681):308–310, July 1965.

[167] R. J. H. Davies, J. F. Malone, Y. Gan, C. J. Cardin, M. P.H. Lee, and S. Neidle. High-resolution crystal structure of the intramolecular d(TpA) thymine-adenine photoadduct and its mechanistic implications. *Nucleic Acids Research*, 35(4):1048–1053, January 2007.

[168] X Zhao, S Nadji, J L Kao, and J S Taylor. The structure of d(TpA), the major photoproduct of thymidylyl-(3'5')-deoxyadenosine. *Nucleic Acids Research*, 24(8):1554–1560, April 1996.

[169] Martin Muenzel, Claudia Szeibert, Andreas F. Glas, Daniel Globisch, and Thomas Carell. Discovery and synthesis of new UV-induced intrastrand c(4-8)g and g(8-4)c photolesions. *Journal of the American Chemical Society*, 133(14):5186–5189, March 2011.

[170] Shiv Kumar, Prakash C. Joshi, Narain D. Sharma, Samarendra N. Bose, R.Jeremy H. Davies, Naohito Takeda, and James A. McCloskey. Adenine photodimerization in deoxyadenylate sequences: elucidation of the mechanism through structural studies of a major d(ApA) photoproduct. *Nucleic Acids Research*, 19(11):2841–2847, 1991.

[171] Yinsheng Wang, John-Stephen Taylor, and Michael L. Gross. Isolation and mass spectrometric characterization of dimeric adenine photoproducts in oligodeoxynucleotides. *Chemical Research in Toxicology*, 14(6):738–745, May 2001.

[172] Narain D. Sharma and R. Jeremy H. Davies. Extent of formation of a dimeric adenine photoproduct in polynucleotides and DNA. *Journal of Photochemistry and Photobiology B: Biology*, 3(2):247–258, April 1989.

[173] Saadia Asgatay, Agathe Martinez, Stephanie Coantic-Castex, Dominique Harakat, Coralie Philippe, Thierry Douki, and Pascale Clivio. UV-induced TA photoproducts: Formation and hydrolysis in double-stranded DNA. *Journal of the American Chemical Society*, 132(30):10260–10261, July 2010.

[174] G. Fisher and H. Johns. *Photochemistry and Photobiology of Nucleic Acids*. Academic Press, New York, 1953.

[175] Helmut Goerner. Chromophore loss of uracil derivatives and polyuridylic acid in aqueous solution caused by 248 nm laser pulses and continuous UV irradiation: Mechanism of the photohydration of pyrimidines. *Journal of Photochemistry and Photobiology B: Biology*, 10(1-2):91–110, July 1991.

[176] Jean Cadet, Evelyne Sage, and Thierry Douki. Ultraviolet radiation-mediated damage to cellular DNA. *Mutation Research/Fundamental and Molecular Mechanisms of Mutagenesis*, 571(1-2):3–17, April 2005.

[177] Jung-Hoon Yoon, Chong-Soon Lee, Timothy R O' Connor, Akira Yasui, and Gerd P Pfeifer. The DNA damage spectrum produced by simulated sunlight. *Journal of Molecular Biology*, 299(3):681–693, June 2000.

[178] Jean Cadet, Lucienne Voituriez, Frank E. Hruska, Lou-Sing Kan, Frank A. A. M. de Leeuw, and Cornelis Altona. Characterization of thymidine ultraviolet photoproducts. cyclobutane dimers and 5,6-dihydrothymidines. *Canadian Journal of Chemistry*, 63(11):2861–2868, November 1985.

[179] A. A. Lamola and T. Yamane. Sensitized photodimerization of thymine in DNA. *Proceedings of the National Academy of Sciences*, 58(2):443–446, January 1967.

[180] Angelo A. Lamola and Jai P. Mittal. Solution photochemistry of thymine and uracil. *Science*, 154(3756):1560–1561, December 1966.

[181] Wai-Ming Kwok, Chensheng Ma, and David Lee Phillips. A doorway state leads to photostability or triplet photodamage in thymine DNA. *Journal of the American Chemical Society*, 130(15):5131–5139, April 2008.

[182] Wolfgang J. Schreier, Tobias E. Schrader, Florian O. Koller, Peter Gilch, Carlos E. Crespo-Hernandez, Vijay N. Swaminathan, Thomas Carell, Wolfgang Zinth, and Bern Kohler. Thymine dimerization in DNA is an ultrafast photoreaction. *Science*, 315(5812):625 –629, February 2007.

[183] Wolfgang J. Schreier, Julia Kubon, Nadja Regner, Karin Haiser, Tobias E. Schrader, Wolfgang Zinth, Pascale Clivio, and Peter Gilch. Thymine dimerization in DNA model systems: Cyclobutane photolesion is predominantly formed via the singlet channel. *Journal of the American Chemical Society*, 131(14):5038–5039, April 2009.

[184] Mahesh Hariharan, Martin McCullagh, George C. Schatz, and Frederick D. Lewis. Conformational control of thymine photodimerization in single-strand and duplex DNA containing locked nucleic acid TT steps. *Journal of the American Chemical Society*, 132(37):12856–12858, September 2010.

[185] Zhengzheng Pan, Martin McCullagh, George C. Schatz, and Frederick D. Lewis. Conformational control of thymine photodimerization in purine-containing trinucleotides. *The Journal of Physical Chemistry Letters*, 2(12):1432–1438, June 2011.

[186] Thierry Douki and Jean Cadet. Individual determination of the yield of the main UV-induced dimeric pyrimidine photoproducts in DNA suggests a high mutagenicity of CC photolesions. *Biochemistry*, 40(8):2495–2501, February 2001.

[187] Juan Jose Serrano-Perez, Israel Gonzalez-Ramirez, Pedro B. Coto, Manuela Merchan, and Luis Serrano-Andres. Theoretical insight into the intrinsic ultrafast formation of cyclobutane pyrimidine dimers in UV-irradiated DNA: Thymine versus cytosine. *The Journal of Physical Chemistry B*, 112(45):14096–14098, October 2008.

[188] Luciana Esposito, Akos Banyasz, Thierry Douki, Marion Perron, Dimitra Markovitsi, and Roberto Improta. Effect of C5-methylation of cytosine on the photoreactivity of DNA: A joint experimental and computational study of TCG trinucleotides. *Journal of the American Chemical Society*, 136(31):10838, July 2014.

[189] Wu Peng and Barbara Ramsay Shaw. Accelerated deamination of cytosine residues in UV-induced cyclobutane pyrimidine dimers leads to CC TT transitions. *Biochemistry*, 35(31):10172–10181, January 1996.

[190] M. Consuelo Cuquerella, Virginie Lhiaubet-Vallet, Francisco Bosca, and Miguel A. Miranda. Photosensitised pyrimidine dimerisation in DNA. *Chemical Science*, 2(7):1219–1232, June 2011.

[191] G. Buechi, Charles G. Inman, and E. S. Lipinsky. Light-catalyzed organic reactions. I. The reaction of carbonyl compounds with 2-methyl-2-butene in the presence of ultraviolet light. *Journal of the American Chemical Society*, 76(17):4327–4331, September 1954.

[192] Pascale Clivio, Jean Louis Fourrey, Jeannette Gasche, and Alain Favre. DNA photodamage mechanistic studies: characterization of a thietane intermediate in a model reaction relevant to "6-4 lesions". *Journal of the American Chemical Society*, 113(14):5481–5483, July 1991.

[193] Sylvie Marguet and Dimitra Markovitsi. Time-resolved study of thymine dimer formation. *J. Am. Chem. Soc.*, 127(16):5780–5781, 2005.

[194] Akos Banyasz, Thierry Douki, Roberto Improta, Thomas Gustavsson, Delphine Onidas, Ignacio Vaya, Marion Perron, and Dimitra Markovitsi. Electronic excited states responsible for dimer formation upon UV absorption directly by thymine strands: Joint experimental and theoretical study. *Journal of the American Chemical Society*, 134(36):14834–14845, September 2012.

[195] Gerald Ryseck, Thomas Schmierer, Karin Haiser, Wolfgang Schreier, Wolfgang Zinth, and Peter Gilch. The excited state decay of 1-methyl-2(1H)-pyrimidinone is an activated process. *ChemPhysChem*, 12(10):1880–1888, June 2011.

[196] Victoria Vendrell-Criado, Gemma M. Rodriguez-Muniz, M. Consuelo Cuquerella, Virginie Lhiaubet-Vallet, and Miguel A. Miranda. Photosensitization of DNA by 5-methyl-2-pyrimidone deoxyribonucleoside: (6-4) photoproduct as a possible trojan horse. *Angewandte Chemie International Edition*, 52(25):6476–6479, 2013.

[197] Hans-Achim Wagenknecht. Unraveling the pathways to UVA-induced DNA photodamage: (6-4) photoproduct as a potential "trojan horse". *ChemPhysChem*, 14(14):3197–3198, 2013.

[198] J. Dewar. On the oxidation af phenyl alcohol, and a mechanical arrangement adapted to illustrate structure in the non-saturated hydrocarbons. *Proc. Royal Soc. Edinburgh*, 6:96, 1867.

[199] B. P. Fingerhut, T. T. Herzog, G. Ryseck, K. Haiser, F. F. Graupner, K. Heil, P. Gilch, W. J. Schreier, T. Carell, R. de Vivie-Riedle, and W. Zinth. Dynamics of ultraviolet-induced DNA lesions: Dewar formation guided by pre-tension induced by the backbone. *New Journal of Physics*, 14(6):065006, June 2012.

[200] Karin Haiser, Benjamin P Fingerhut, Korbinian Heil, Andreas Glas, Teja T Herzog, Bert M Pilles, Wolfgang J Schreier, Wolfgang Zinth, Regina de Vivie Riedle, and Thomas Carell. Mechanism of UV induced formation of dewar lesions in DNA. *Angewandte Chemie International Edition*, 51(2):408–411, 2012.

[201] Danielle G. E. Lemaire and Bela P. Ruzsicska. Quantum yields and secondary photoreactions of the photoproducts of dTpdT, dTpdc and dTpdU. *Photochemistry and Photobiology*, 57(5):755–757, May 1993.

[202] Mark Lukin and Carlos de los Santos. NMR structures of damaged DNA. *Chemical Reviews*, 106(2):607–686, February 2006.

[203] Yueqing Jing, John-Stephen Taylor, and Jeffrey F.-L. Kao. Thermodynamic and base-pairing studies of matched and mismatched DNA dodecamer duplexes containing cis-syn, (6-4) and dewar photoproducts of TT. *Nucleic Acids Research*, 26(16):3845 –3853, 1998.

[204] A. LeClerc, J. E.and Borden and C. W. Lawrence. The thymine-thymine pyrimidine-pyrimidone(6-4) ultraviolet light photoproduct is highly mutagenic and specifically induces 3' thymine-to-cytosine transitions in escherichia coli. *Proceedings of the National Academy of Sciences*, 88(21):9685 –9689, November 1991.

[205] Florian Brueckner, Ulrich Hennecke, Thomas Carell, and Patrick Cramer. CPD damage recognition by transcribing RNA polymerase II. *Science*, 315(5813):859–862, September 2007.

[206] Aziz Sancar. Structure and function of DNA photolyase and cryptochrome blue-light photoreceptors. *Chemical Reviews*, 103(6):2203–2238, June 2003.

[207] Zheyun Liu, Chuang Tan, Xunmin Guo, Ya-Ting Kao, Jiang Li, Lijuan Wang, Aziz Sancar, and Dongping Zhong. Dynamics and mechanism of cyclobutane pyrimidine dimer repair by DNA photolyase. *Proceedings of the National Academy of Sciences*, July 2011.

[208] Jiang Li, Zheyun Liu, Chuang Tan, Xunmin Guo, Lijuan Wang, Aziz Sancar, and Dongping Zhong. Dynamics and mechanism of repair of ultraviolet-induced (6-4) photoproduct by photolyase. *Nature*, 466(7308):887–890, 2010.

[209] Andrea Christa Kneuttinger, Gengo Kashiwazaki, Stefan Prill, Korbinian Heil, Markus Mueller, and Thomas Carell. Formation and direct repair of UV-induced dimeric DNA pyrimidine lesions. *Photochemistry and Photobiology*, 90(1):1–14, 2014.

[210] Shirin Faraji and Andreas Dreuw. Physicochemical mechanism of light-driven DNA repair by (6-4) photolyases. *Annual Review of Physical Chemistry*, 65(1):275–292, 2014.

[211] Richard D. Wood. DNA repair in eukaryotes. *Annual Review of Biochemistry*, 65(1):135–167, 1996.

[212] Aziz Sancar. DNA excision repair. *Annual Review of Biochemistry*, 65(1):43–81, 1996.

[213] Orlando D. Schaerer. Chemistry and biology of DNA repair. *Angewandte Chemie International Edition*, 42(26):2946–2974, July 2003.

[214] D. D. Eley and D. I. Spivey. Semiconductivity of organic substances. Part 9.-Nucleic acid in the dry state. *Transactions of the Faraday Society*, 58(0):411–415, January 1962.

[215] T. Gregory Drummond, Michael G. Hill, and Jacqueline K. Barton. Electrochemical DNA sensors. *Nature Biotechnology*, 21(10):1192–1199, October 2003.

[216] Daniel B. Hall, R. Erik Holmlin, and Jacqueline K. Barton. Oxidative DNA damage through long-range electron transfer. *Nature*, 382(6593):731–735, August 1996.

[217] Sriram Kanvah, Joshy Joseph, Gary B. Schuster, Robert N. Barnett, Charles L. Cleveland, and Uzi Landman. Oxidation of DNA: Damage to nucleobases. *Accounts of Chemical Research*, 43(2):280–287, February 2010.

[218] Wagenknecht Hans-Joachim. Principles and mechanisms of photoinduced charge injection, transport, and trapping in DNA. pages 1–26. WILEY-VCH Verlag GmbH & Co. KGaA, Weinheim, 2005.

[219] C. J. Murphy, M. R. Arkin, Y. Jenkins, N. D. Ghatlia, S. H. Bossmann, N. J. Turro, and J. K. Barton. Long-range photoinduced electron transfer through a DNA helix. *Science*, 262(5136):1025–1029, December 1993.

[220] Christoph Behrens, Lars T. Burgdorf, Anja Schwoegler, and Thomas Carell. Weak distance dependence of excess electron transfer in DNA. *Angewandte Chemie International Edition*, 41(10):1763–1766, 2002.

[221] Danila Fazio, Christian Trindler, Korbinian Heil, Chryssostomos Chatgilialoglu, and Thomas Carell. Investigation of excess-electron transfer in DNA double-duplex systems allows estimation of absolute excess-electron transfer and CPD cleavage rates. *Chemistry - A European Journal*, 17(1):206–212, 2011.

[222] Fangwei Shao, Melanie A. O'Neill, and Jacqueline K. Barton. Long-range oxidative damage to cytosines in duplex DNA. *Proceedings of the National Academy of Sciences*, 101(52):17914–17919, December 2004.

[223] Bernd Giese, Jerome Amaudrut, Anne-Kathrin Koehler, Martin Spormann, and Stephan Wessely. Direct observation of hole transfer through DNA by hopping between adenine bases and by tunnelling. *Nature*, 412(6844):318–320, July 2001.

[224] Melanie A. O'Neill, Hans-Christian Becker, Chaozhi Wan, Jacqueline K. Barton, and Ahmed H. Zewail. Ultrafast dynamics in DNA-mediated electron transfer: Base gating and the role of temperature. *Angewandte Chemie International Edition*, 42(47):5896–5900, December 2003.

[225] Frederick D. Lewis, Xiaoyang Liu, Jianqin Liu, Scott E. Miller, Ryan T. Hayes, and Michael R. Wasielewski. Direct measurement of hole transport dynamics in DNA. *Nature*, 406(6791):51–53, July 2000.

[226] Man Jae Park, Mamoru Fujitsuka, Kiyohiko Kawai, and Tetsuro Majima. Direct measurement of the dynamics of excess electron transfer through consecutive thymine sequence in DNA. *Journal of the American Chemical Society*, 133(39):15320–15323, October 2011.

[227] Claus A. M. Seidel, Andreas Schulz, and Markus H. M. Sauer. Nucleobase-specific quenching of fluorescent dyes. 1. Nucleobase one-electron redox potentials and their correlation with static and dynamic quenching efficiencies. *The Journal of Physical Chemistry*, 100(13):5541–5553, January 1996.

[228] Y. Paukku and G. Hill. Theoretical determination of one-electron redox potentials for DNA bases, base pairs, and stacks. *The Journal of Physical Chemistry A*, 115(18):4804–4810, May 2011.

[229] Mamoru Fujitsuka and Tetsuro Majima. Hole and excess electron transfer dynamics in DNA. *Physical Chemistry Chemical Physics*, 14(32):11234–11244, July 2012.

[230] Bernd Giese, Stephan Wessely, Martin Spormann, Ute Lindemann, Eric Meggers, and Maria E. Michel-Beyerle. On the mechanism of long-range electron transfer through DNA. *Angewandte Chemie International Edition*, 38(7):996–998, April 1999.

[231] R. A. Marcus and Norman Sutin. Electron transfers in chemistry and biology. *Biochimica et Biophysica Acta (BBA) - Reviews on Bioenergetics*, 811(3):265–322, August 1985.

[232] Bernd Giese. Electron transfer in DNA. *Current Opinion in Chemical Biology*, 6(5):612–618, October 2002.

[233] Khatcharin Siriwong and Alexander A. Voityuk. Electron transfer in DNA. *Wiley Interdisciplinary Reviews: Computational Molecular Science*, 2(5):780–794, 2012.

[234] Frederick D. Lewis, Robert L. Letsinger, and Michael R. Wasielewski. Dynamics of photoinduced charge transfer and hole transport in synthetic DNA hairpins. *Accounts of Chemical Research*, 34(2):159–170, February 2001.

[235] Joshua Jortner, Mordechai Bixon, Thomas Langenbacher, and Maria E. Michel-Beyerle. Charge transfer and transport in DNA. *Proceedings of the National Academy of Sciences*, 95(22):12759–12765, October 1998.

[236] Frederick D. Lewis, Taifeng Wu, Yifan Zhang, Robert L. Letsinger, Scott R. Greenfield, and Michael R. Wasielewski. Distance-dependent electron transfer in DNA hairpins. *Science*, 277(5326):673–676, January 1997.

[237] Chaozhi Wan, Torsten Fiebig, Olav Schiemann, Jacqueline K. Barton, and Ahmed H. Zewail. Femtosecond direct observation of charge transfer between bases in DNA. *Proceedings of the National Academy of Sciences*, 97(26):14052–14055, December 2000.

[238] William B. Davis, Walter A. Svec, Mark A. Ratner, and Michael R. Wasielewski. Molecular-wire behaviour in p -phenylenevinylene oligomers. *Nature*, 396(6706):60–63, November 1998.

[239] Tadao Takada, Kiyohiko Kawai, Mamoru Fujitsuka, and Tetsuro Majima. Direct observation of hole transfer through double-helical DNA over 100 a. *Proceedings of the National Academy of Sciences of the United States of America*, 101(39):14002–14006, September 2004.

[240] Megan E Nunez, Daniel B Hall, and Jacqueline K Barton. Long-range oxidative damage to DNA: Effects of distance and sequence. *Chemistry & Biology*, 6(2):85–97, February 1999.

[241] Eric Meggers, Maria E. Michel-Beyerle, and Bernd Giese. Sequence dependent long range hole transport in DNA. *Journal of the American Chemical Society*, 120(49):12950–12955, December 1998.

[242] Frederick D. Lewis. Distance-dependent electronic interactions across DNA base pairs: Charge transport, exciton coupling, and energy transfer. *Israel Journal of Chemistry*, 53(6/7):350–365, June 2013.

[243] Ravindra Venkatramani, Shahar Keinan, Alexander Balaeff, and David N. Beratan. Nucleic acid charge transfer: Black, white and gray. *Coordination Chemistry Reviews*, 255(7-8):635–648, April 2011.

[244] Frederick D. Lewis, Huihe Zhu, Pierre Daublain, Boiko Cohen, and Michael R. Wasielewski. Hole mobility in DNA a tracts. *Angewandte Chemie International Edition*, 45(47):7982–7985, 2006.

[245] Matthias Wenninger, Danila Fazio, Uwe Megerle, Christian Trindler, Stefan Schiesser, Eberhard Riedle, and Thomas Carell. Flavin-induced DNA photooxidation and charge movement probed by ultrafast transient absorption spectroscopy. *ChemBioChem*, 12(5):703–706, 2011.

[246] Melanie A. O'Neil and Jacqueline K. Barton. DNA charge transport: Conformationally gated hopping through stacked domains. *Journal of the American Chemical Society*, 126(37):11471–11483, September 2004.

[247] Fangwei Shao, Katherine Augustyn, and Jacqueline K. Barton. Sequence dependence of charge transport through DNA domains. *Journal of the American Chemical Society*, 127(49):17445–17452, December 2005.

[248] Joseph C. Genereux and Jacqueline K. Barton. Mechanisms for DNA charge transport. *Chemical reviews*, 110(3):1642–1662, March 2010.

[249] Paul T. Henderson, Denise Jones, Gregory Hampikian, Yongzhi Kan, and Gary B. Schuster. Long-distance charge transport in duplex DNA: The phonon-assisted polaron-like hopping mechanism. *Proceedings of the National Academy of Sciences*, 96(15):8353–8358, July 1999.

[250] Esther M. Conwell. Charge transport in DNA in solution: The role of polarons. *Proceedings of the National Academy of Sciences of the United States of America*, 102(25):8795–8799, June 2005.

[251] Nicolas Renaud, Yuri A. Berlin, Frederick D. Lewis, and Mark A. Ratner. Between superexchange and hopping: An intermediate charge-transfer mechanism in poly(a)-poly(t) DNA hairpins. *Journal of the American Chemical Society*, 135(10):3953–3963, February 2013.

[252] Nicolas Renaud, Yuri A. Berlin, and Mark A. Ratner. Impact of a single base pair substitution on the charge transfer rate along short DNA hairpins. *Proceedings of the National Academy of Sciences*, 110(37):14867–71, August 2013.

[253] Yuqi Zhang, Chaoren Liu, Alexander Balaeff, Spiros S. Skourtis, and David N. Beratan. Biological charge transfer via flickering resonance. *Proceedings of the National Academy of Sciences*, 111(28):10049–10054, June 2014.

[254] Karin Haiser. *Femtosekunden-Infrarotspektroskopie von UV-induzierten Photoschaeden in Nukleinsaeuren.* PhD dissertation, Ludwig-Maximilians-Universitaet, Muenchen, 2012.

[255] Benjamin Schuster. *Integration einer IR-Vielkanaldetektion in ein bestehendes Anreg-Abtast-Experiment und Femtosekundenspektroskopie an Azobenzol Dabcyl Saeure.* Master thesis, Ludwig-Maximilians Universitaet, Muenchen, 2011.

[256] Wolfgang Schreier. *UV-Strahlung und DNA-Schaeden.* PhD dissertation, Ludwig-Maximilians-Universitaet, Muenchen, 2008.

[257] Ahmed H. Zewail. Femtochemistry: Atomic-scale dynamics of the chemical bond using ultrafast lasers (nobel lecture). *Angewandte Chemie International Edition*, 39(15):2586–2631, August 2000.

[258] E. Riedle, M. Beutter, S. Lochbrunner, J. Piel, S. Schenkl, S. Spoerlein, and W. Zinth. Generation of 10 to 50 fs pulses tunable through all of the visible and the NIR. *Applied Physics B*, 71(3):457–465, September 2000.

[259] Carmen Kuebel. *Anreg-Abtast-Experiment zur Entfaltung des schaltbaren Peptids AzoTrpZip2 - Integration eines abstimmbaren ns-Lasersystems.* Master thesis, Ludwig-Maximilians-Universitaet Muenchen, 2013.

[260] H. B. Schlegel G. E. Scuseria M. A. Robb J. R. Cheeseman J. A. Montgomery Jr. T. Vreven K. N. Kudin J. C. Burant J. M. Millam S. S. Iyengar J. Tomasi V. Barone B. Mennucci M. Cossi G. Scalmani N. Rega G. A. Petersson H. Nakatsuji M. Hada M. Ehara K. Toyota R. Fukuda J. Hasegawa M. Ishida T. Nakajima Y. Honda O. Kitao H. Nakai M. Klene X. Li J. E. Knox H. P. Hratchian J. B. Cross V. Bakken C. Adamo J. Jaramillo R. Gomperts R. E. Stratmann O. Yazyev A. J. Austin R. Cammi C. Pomelli J. W. Ochterski P. Y. Ayala K. Morokuma G. A. Voth

P. Salvador J. J. Dannenberg V. G. Zakrzewski S. Dapprich A. D. Daniels M. C. Strain O. Farkas D. K. Malick A. D. Rabuck K. Raghavachari J. B. Foresman J. V. Ortiz Q. Cui A. G. Baboul S. Clifford J. Cioslowski B. B. Stefanov G. Liu A. Liashenko P. Piskorz I. Komaromi R. L. Martin D. J. Fox T. Keith M. A. Al-Laham C. Y. Peng A. Nanayakkara M. Challacombe P. M. W. Gill B. Johnson W. Chen M. W. Wong C. Gonzalez and J. A. Pople M. J. Frisch, G. W. Trucks. Gaussian 03, revision d.01, 2004.

[261] Dominik B. Bucher, Bert M. Pilles, Toni Pfaffeneder, Thomas Carell, and Wolfgang Zinth. Fingerprinting DNA oxidation processes: IR characterization of the 5-methyl-2-deoxycytidine radical cation. *ChemPhysChem*, 15(3):420–423, February 2014.

[262] Ryan Lister, Mattia Pelizzola, Robert H. Dowen, R. David Hawkins, Gary Hon, Julian Tonti-Filippini, Joseph R. Nery, Leonard Lee, Zhen Ye, Que-Minh Ngo, Lee Edsall, Jessica Antosiewicz-Bourget, Ron Stewart, Victor Ruotti, A. Harvey Millar, James A. Thomson, Bing Ren, and Joseph R. Ecker. Human DNA methylomes at base resolution show widespread epigenomic differences. *Nature*, 462(7271):315–322, November 2009.

[263] W. Rideout, G. Coetzee, A. Olumi, and P. Jones. 5-methylcytosine as an endogenous mutagen in the human LDL receptor and p53 genes. *Science*, 249(4974):1288–1290, September 1990.

[264] J. Richard Wagner and Jean Cadet. Oxidation reactions of cytosine DNA components by hydroxyl radical and one-electron oxidants in aerated aqueous solutions. *Accounts of Chemical Research*, 43(4):564–571, April 2010.

[265] Dominik B. Bucher, Bert M. Pilles, Thomas Carell, and Wolfgang Zinth. Charge separation and charge delocalization identified in long-living states of photoexcited DNA. *Proceedings of the National Academy of Sciences*, 111(12):4369–4374, March 2014.

[266] Marina K. Kuimova, Alexander J. Cowan, Pavel Matousek, Anthony W. Parker, Xue Zhong Sun, Michael Towrie, and Michael W. George. Monitoring the direct and indirect damage of DNA bases and polynucleotides by using time-resolved infrared spectroscopy. *Proceedings of the National Academy of Sciences of the United States of America*, 103(7):2150–2153, February 2006.

[267] Anthony W. Parker, Ching Yeh Lin, Michael W. George, Michael Towrie, and Marina K. Kuimova. Infrared characterization of the guanine radical cation: Finger printing DNA damage. *The Journal of Physical Chemistry B*, 114(10):3660–3667, March 2010.

[268] Dominik B. Bucher, Alexander Schlueter, Thomas Carell, and Wolfgang Zinth. Watson-crick base pairing controls excited-state decay in natural DNA. *Angewandte Chemie International Edition*, 53(42):11366–11369, October 2014.

[269] Dominik B. Bucher, Alexander Schlueter, Thomas Carell, and Wolfgang Zinth. In natuerlicher DNA wird der Zerfall des angeregten Zustands durch Watson-Crick-Basenpaarung bestimmt. *Angewandte Chemie*, 126(42):11549–11552, October 2014.

Annotation

The citations included in the published papers of this thesis are not listed in the bibliography.

Publications

Publications in Peer Reviewed Journals:

- Dominik B. Bucher, Bert M. Pilles, Toni Pfaffeneder, Thomas Carell, Wolfgang Zinth. Fingerprinting DNA Oxidation Processes: IR Characterization of the 5-Methyl-2′-Deoxycytidine Radical Cation. *ChemPhysChem*, **15**, 420-423 (2014).

- Dominik B. Bucher, Bert M. Pilles, Thomas Carell, Wolfgang Zinth. Charge separation and charge delocalization identified in long-living states of photoexcited DNA. *PNAS*, **111**, 4369–4374 (2014)

- Bert M. Pilles, Dominik B. Bucher, Lizhe Liu, Pascale Clivio, Peter Gilch, Wolfgang Zinth, Wolfgang J. Schreier. Mechanism of the Decay of Thymine Triplets in DNA Single Strands. *J. Phys. Chem. Lett.*, **5**, 1616−1622 (2014)

- Dominik B. Bucher, Alexander Schlueter, Thomas Carell, Wolfgang Zinth. Watson-Crick Base Pairing Controls Excited-State Decay in Natural DNA. *Angew. Chem. Int. Ed.*, **53**, 11366-11369 (2014), Selected as "Very Important Paper"

- Bert M. Pilles, Dominik B. Bucher, Lizhe Liu, Peter Gilch, Wolfgang Zinth, Wolfgang J. Schreier. Identification of Charge Separated States in Thymine Single Strands. *Chemical Communications.* Accepted.

Proceedings:

- Dominik B. Bucher, Bert M. Pilles, Thomas Carell, Wolfgang Zinth. Photoinduced charge transfer occurs naturally in DNA. *International Conference on Ultrafast Phenomena.* Optical Society of America. In print.

Selected Talks and Poster Presentations:

Talks:

- The 19th International Conference on Ultrafast Phenomena (Okinawa, Japan): "Photoinduced charge transfer occurs naturally in DNA" (July 2014)

- Invited Talk at Heinrich Heine-Universitaet-Duesseldorf, Prof. Peter Gilch (Duesseldorf, Germany): "What happens after light absorption in DNA? From single nucleobases to natural DNA" (June 2014)

- Annual Meeting of the Collaborative Research Center 749, Dynamics and Intermediates of Molecular Transformations (Venice, Italy): "DNA – from Photophysics to Photochemistry" (April 2014)
- Invited Talk at Riken Institute, Prof. Tahei Tahara (Tokyo, Japan): "Energy transfer in proteins and DNA investigated by ultrafast time-resolved IR-spectroscopy" (May 2013)
- Annual Meeting of the Collaborative Research Center 749, Dynamics and Intermediates of Molecular Transformations (Wildbad Kreuth, Germany): "Charge Transfer and Charge Delocalization After Light Absorption in DNA" (March 2013)

Poster Presentations:

- XVIth International Conference on Time-Resolved Vibrational Spectroscopy (Beppu, Japan, May 2013)
- Joint Meeting of the British and German Biophysical Society (Huenfeld, Germany, March 2013)
- XXIVth IUPAC Symposium on Photochemistry (Coimbra, Portugal, June 2013)

Acknowledgment

At this point I would like to express my greatest gratitude to the people who supported me during my Ph.D. thesis. Especially I would like to thank:

- **Professor Wolfgang Zinth and Professor Thomas Carell** for the possibility to work in both groups on an interdisciplinary and exciting research project. I am particularly grateful for giving me a lot of freedom to realize my own ideas and giving me support where I needed it. The inspiring atmosphere and the enthusiastic supervision has mainly contributed to the success of this thesis.

- **My former students Sabine Gerlach, Ina Guemperlein, Mara Heinlein and Alexander Schlueter** for assisting my research and performing a very diligent work.

- **My Master student Alexander Schlueter** for the successful teamwork in the "Calf Thymus" project.

- **Bert Pilles** for technical support in many IR measurements.

- **The IR-Group**: Andreas Deeg, Karin Haiser, Lizhe Liu, Bert Pilles, Michael Rampp and Wolfgang Schreier for teaching me ultrafast IR-spectroscopy and supporting me in many measurements.

- **Alexandra Michaelis and Marianne Widmann-Diermeier** for helping in organizational tasks.

- **Dr. Karl-Heinz Mantel and Florian Trommer** for their IT-support.

- **Franziska Graupner** for the time-resolved fluorescence measurements in the Dewar project.

- **My colleagues:** Pablo Dominguez, Julia Gontcharov, Teja Herzog, Stefan Hofmann, Florian Lederer, Benjamin März, Bert Pilles, Anne Reiner, Elena Samoylova, Julian Schauseil, Florian Trommer and Ilvana Turkanovic for the extraordinarily pleasant atmosphere in the research group.

- **My colleagues in the Carell Group:** Korbinian Heil for teaching me DNA photochemistry, Andrea Kneuttinger for the help with the glove-box, Toni Pfaffeneder for the UHPLC-ESI-MS/MS measurements, Korbinian Brunner and Arne Schroeder for the HPLC and spectroscopy support.

- **The machine shop:** Rudolf Schwarz, Alfons Stork, Christian Hausmann and Harald Hoppe for the very competent technical work. In addition I would like to thank Isabell Kalbe for the support in the chemistry laboratory.
- **The proofreaders:** Andreas Deeg, Greta Fackler, Julia Gontcharov, Andrea Kneuttinger, Corinna Kufner, Benjamin März, Verena Petermichl, Bert Pilles, Michael Rampp, Florian Trommer and Alexander Schlueter.
- **My family**: my parents Anna and Alfred Bucher, my sister Diana Bucher and my nephew Levin Bucher.
- **My girlfriend** Verena Petermichl.